

**THE REMOVAL OF HEAVY  
METALS FROM DILUTE  
AQUEOUS STREAMS BY THE  
USE OF ION EXCHANGE  
RESINS**

**BY**

**THEO HENRY DIETRICH**

A THESIS SUBMITTED IN PARTIAL FULFILMENT OF THE  
REQUIREMENTS FOR THE MASTERS DEGREE IN  
TECHNOLOGY (CHEMICAL ENGINEERING) AT THE CAPE  
TECHNIKON

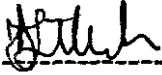
SUPERVISOR : PROF. F. W. PETERSEN

CAPE TECHNIKON

MAY 1998

# DECLARATION

I, the undersigned, hereby declare that the work contained in this thesis, is my own original work, and has not previously in it's entirety or in part, been submitted for a degree at any other institution.



-----  
T. H. DIETRICH

NOVEMBER 1998

# ABSTRACT

Ion exchange resins are widely used to remove or concentrate heavy metals from aqueous solutions or slurries. This thesis attempts to properly evaluate the interaction between ion exchange resins and heavy metals at trace metal concentrations. The durability of the resins and their effectiveness in real slurries were also investigated.

In this study, a chelating resin, as well as a cation, and anion exchange resin was contacted with aqueous solutions of heavy metals in both free and complexed form. Zinc, nickel and copper cyanide complexes were adsorbed onto the anion exchange resin, while the chelating and cation exchange resins were contacted with zinc and nickel nitrates, and cupric sulphate. All the tests were conducted in batch stirred tank reactors.

All the metal cyanide complexes behaved in a similar manner when contacted with the anion exchange resins. These tests were performed under variations in temperature, stirring speed, pH, ionic strength and initial metal concentrations. Fitting of a dual resistance model to the profiles for the uptake of the complexes, show that both film diffusion and intraparticle diffusion rates were improved with an increase in temperature, and that film diffusion rates improved with an increase in stirring speed. A high ionic strength negatively affected equilibrium loading as well as diffusional rates. It was found that at these low concentrations, the diffusional rates improves with a decrease in the external metal concentration.

A comparative study involving the chelating and cation exchange resins were performed, during which the resins were contacted with the metals in free form. It was found that at high metal concentrations, the chelating resin induced a rate limiting effect, but at trace concentrations, this effect is virtually negated. Whereas the cation exchange resin exhibited little selectivity in adsorbing the metals, it was found that the chelating resin prefers the metals in the  $Cu > Ni > Zn$ . The chelating resin proved to be no less durable than the cation exchange resin, and both slightly lost their ability to adsorb the metal cations as a result of the effects of an inert coarse sand

slurry. Tests performed with a real ore leachate, showed the cation exchange resin to be efficient at a low pH , but also relatively non selective, since the adsorption of copper from the leachate was greatly reduced due to the presence of other heavy metals.

## ACKNOWLEDGEMENTS

The work carried out in this thesis was carried out at the Department of Mechanical and Process Engineering at the Cape Technikon between January 1996 and December 1997.

I owe much gratitude to Prof. Francis Petersen for his guidance and encouragement during the course of this work. In addition, I would like to thank Ms. Cynthia Sivambu for her assistance with the experimental work, as well as with the typing of the thesis.

I also wish to thank my family and friends for their encouragement during the last two years.

The Foundation for Research and Development are gratefully acknowledged for their financial assistance.

# CONTENTS

	<b>PAGE</b>
ABSTRACT	i
ACKNOWLEDGEMENTS	iii
CONTENTS	iv
LIST OF FIGURES	viii
LIST OF TABLES	xi
<b>CHAPTER 1</b>	
<b>INTRODUCTION</b>	<b>1</b>
1.1 Heavy metals in the environment	1
1.2 South African Standards	2
1.3 Conventional treatment	2
1.4 Waste treatment	3
1.5 Ion exchange for waste recovery	4
1.6 Objectives of the study	5
<b>CHAPTER 2</b>	
<b>LITERATURE REVIEW</b>	<b>9</b>
2.1 Ion exchange resins	9
2.1.1 Chemical and physical properties	9
2.1.2 Preparation	11

2.2	<b>Mechanism of ion exchange</b>	12
2.2.1	<b>Anion exchange</b>	13
2.2.2	<b>Cation exchange</b>	14
2.2.3	<b>Ion exchange with chelation</b>	15
2.3	<b>Ion exchange in dilute heavy metal solutions</b>	16
2.4	<b>Kinetic parameters</b>	18
2.4.1	<b>External film diffusion</b>	19
2.4.2	<b>Intraparticle diffusion</b>	20
2.4.3	<b>Chemical reaction control</b>	20
2.5	<b>Factors influencing the ion exchange process</b>	21
2.6	<b>Formation of metal complexes</b>	22
2.7	<b>Speciation</b>	23
2.8	<b>Ion exchange equilibria</b>	23
2.9	<b>Significance of the literature review</b>	25
<b>CHAPTER 3</b>	<b>ADSORPTION KINETICS</b>	<b>28</b>
3.1	<b>Assumptions</b>	28
3.2	<b>Material balance equations</b>	29
3.2.1	<b>Batch stirred tank reactor</b>	29
3.2.2	<b>Numerical solution</b>	33
3.3	<b>Estimation of kinetic parameters</b>	33
3.3.1	<b>External mass transfer coefficient</b>	33
3.3.2	<b>Intraparticle diffusion</b>	34

<b>CHAPTER 4</b>	<b>EXPERIMENTAL</b>	<b>35</b>
4.1	Experimental materials	35
4.2	Preparation and pre-treatment	36
4.3	Batch experiments	37
4.4	Durability tests	38
4.5	Leaching and adsorption	39
4.6	Equilibrium experiments	39
4.7	Analytical methods	40
<b>CHAPTER 5</b>	<b>ION EXCHANGE ISOTHERM</b>	<b>44</b>
5.1	Anion exchange equilibria	44
5.2	Cation exchange equilibria	45
5.3	Chelating exchange equilibria	45
<b>CHAPTER 6</b>	<b>FACTORS INFLUENCING THE ADSORPTION PROCESS</b>	<b>56</b>
6.1	Agitation	56
6.2	Initial metal concentration	57
6.3	pH levels	58
6.4	Temperature	59
6.5	Ionic strength	60
6.6	Effect of competing ions	61
6.7	Summary	62

<b>CHAPTER 7</b>	<b>COMPARATIVE PERFORMANCE OF CHELATING AND CATION EXCHANGE RESINS</b>	<b>85</b>
7.1	Monometallic curves	85
7.2	Multimetallic curves	88
7.2.1	Competitive ion exchange on AMBERLITE 252H	88
7.2.2	Competitive ion exchange on AMBERLITE IRC 718	89
7.3	Durability tests	90
7.4	Application of the kinetic model	91
7.5	Real mining leachate	92
<b>CHAPTER 8</b>	<b>CONCLUSIONS AND RECOMMENDATIONS</b>	<b>112</b>
8.1	Conclusion	112
8.2	Recommendations	113
<b>REFERENCES</b>		<b>115</b>
<b>APPENDIX A</b>	<b>COMPUTER PROGRAM FOR THE ADSORPTION OF A SINGLE METAL SPECIES ONTO ION EXCHANGE RESIN IN A BATCH REACTOR</b>	<b>121</b>
<b>APPENDIX B</b>	<b>TABULATION OF EXPERIMENTAL RESULTS</b>	<b>128</b>
<b>NOMENCLATURE</b>		<b>166</b>

# LIST OF FIGURES

	<b>PAGE</b>
<b>Figure 1.1</b> Typical flowsheet of a metal / cyanide bearing waste water treatment plant	<b>7</b>
<b>Figure 1.2</b> Typical flowsheet of an ion exchange system.	<b>8</b>
<b>Figure 4.1</b> Diagram of the batch adsorber experimental apparatus.	<b>42</b>
<b>Figure 5.1</b> Equilibrium adsorption of zinc cyanide on AMBERLITE IRA 900.	<b>47</b>
<b>Figure 5.2</b> Equilibrium adsorption of nickel cyanide on AMBERLITE IRA 900.	<b>48</b>
<b>Figure 5.3</b> Equilibrium adsorption of copper cyanide on AMBERLITE IRA 900.	<b>49</b>
<b>Figure 5.4</b> Equilibrium adsorption of zinc on AMBERLITE 252H.	<b>50</b>
<b>Figure 5.5</b> Equilibrium adsorption of nickel on AMBERLITE 252H.	<b>51</b>
<b>Figure 5.6</b> Equilibrium adsorption of copper on AMBERLITE 252H.	<b>52</b>
<b>Figure 5.7</b> Equilibrium adsorption of copper on AMBERLITE IRC 718.	<b>53</b>
<b>Figure 5.8</b> Equilibrium adsorption of nickel on AMBERLITE IRC 718.	<b>54</b>
<b>Figure 5.9</b> Equilibrium adsorption of zinc on AMBERLITE IRC 718.	<b>55</b>
<b>Figure 6.1</b> The effect of agitation on the adsorption of zinc cyanide onto AMBERLITE IRA 900.	<b>69</b>
<b>Figure 6.2</b> The effect of agitation on the adsorption of nickel cyanide onto AMBERLITE IRA 900.	<b>70</b>
<b>Figure 6.3</b> The effect of agitation on the adsorption of copper cyanide onto AMBERLITE IRA 900.	<b>71</b>

<b>Figure 6.4</b>	<b>The effect of initial metal concentration on the adsorption of zinc cyanide onto AMBERLITE IRA 900.</b>	<b>72</b>
<b>Figure 6.5</b>	<b>The effect of initial metal concentration on the adsorption of nickel cyanide onto AMBERLITE IRA 900.</b>	<b>73</b>
<b>Figure 6.6</b>	<b>The effect of initial metal concentration on the adsorption of copper cyanide onto AMBERLITE IRA 900.</b>	<b>74</b>
<b>Figure 6.7</b>	<b>The effect of solution pH on the adsorption of zinc cyanide onto AMBERLITE IRA 900.</b>	<b>75</b>
<b>Figure 6.8</b>	<b>The effect of solution pH on the adsorption of nickel cyanide onto AMBERLITE IRA 900.</b>	<b>76</b>
<b>Figure 6.9</b>	<b>The effect of solution pH on the adsorption of copper cyanide onto AMBERLITE IRA 900.</b>	<b>77</b>
<b>Figure 6.10</b>	<b>The effect of solution temperature on the adsorption of zinc cyanide onto AMBERLITE IRA 900.</b>	<b>78</b>
<b>Figure 6.11</b>	<b>The effect of solution temperature on the adsorption of nickel cyanide onto AMBERLITE IRA 900.</b>	<b>79</b>
<b>Figure 6.12</b>	<b>The effect of solution temperature on the adsorption of copper cyanide onto AMBERLITE IRA 900.</b>	<b>80</b>
<b>Figure 6.13</b>	<b>The effect of ionic strength on the adsorption of zinc cyanide onto AMBERLITE IRA 900.</b>	<b>81</b>
<b>Figure 6.14</b>	<b>The effect of ionic strength on the adsorption of nickel cyanide onto AMBERLITE IRA 900.</b>	<b>82</b>
<b>Figure 6.15</b>	<b>The effect of ionic strength on the adsorption of copper cyanide onto AMBERLITE IRA 900.</b>	<b>83</b>
<b>Figure 6.16</b>	<b>The uptake curves of zinc, nickel and copper cyanide as competing anions, on AMBERLITE IRA 900.</b>	<b>84</b>
<b>Figure 7.1</b>	<b>Monometallic curves of nickel, copper and zinc adsorption onto AMBERLITE 252H.</b>	<b>97</b>
<b>Figure 7.2</b>	<b>Monometallic curves of nickel, zinc and copper adsorption onto AMBERLITE IRC 718.</b>	<b>98</b>

<b>Figure 7.3</b>	<b>Multimetallic curves of nickel, zinc and copper adsorption onto AMBERLITE 252H.</b>	<b>99</b>
<b>Figure 7.4</b>	<b>Comparison of the monometallic and multimetallic curves of zinc adsorption onto AMBERLITE 252H.</b>	<b>100</b>
<b>Figure 7.5</b>	<b>Comparison of the monometallic and multimetallic curves of nickel adsorption onto AMBERLITE 252H.</b>	<b>101</b>
<b>Figure 7.6</b>	<b>Comparison of the monometallic and multimetallic curves of copper adsorption onto AMBERLITE 252H.</b>	<b>102</b>
<b>Figure 7.7</b>	<b>Multimetallic curves of nickel, copper and zinc adsorption onto AMBERLITE IRC 718.</b>	<b>103</b>
<b>Figure 7.8</b>	<b>Comparison of the monometallic and multimetallic curves of copper adsorption onto AMBERLITE IRC 718.</b>	<b>104</b>
<b>Figure 7.9</b>	<b>Comparison of the monometallic and multimetallic curves of nickel adsorption onto AMBERLITE IRC 718.</b>	<b>105</b>
<b>Figure 7.10</b>	<b>Comparison of the monometallic and multimetallic curves of zinc adsorption onto AMBERLITE IRC 718.</b>	<b>106</b>
<b>Figure 7.11</b>	<b>Comparison of the uptake curves for copper adsorption onto the treated and untreated resin (AMBERLITE IRC 718).</b>	<b>107</b>
<b>Figure 7.12</b>	<b>Electron micrograph of AMBERLITE IRC 718 before treatment with a slurry.</b>	<b>108</b>
<b>Figure 7.13</b>	<b>Electron micrograph of AMBERLITE IRC 718 after treatment with a slurry.</b>	<b>109</b>
<b>Figure 7.14</b>	<b>Comparison of the uptake curves for copper adsorption onto treated and untreated resin (AMBERLITE 252H).</b>	<b>110</b>
<b>Figure 7.15</b>	<b>Comparison of the uptake curves of the adsorption of the synthetic copper solution and the ore leachate onto AMBERLITE 252H.</b>	<b>111</b>

# LIST OF TABLES

	<b>PAGES</b>	
<b>Table 2.1</b>	<b>Cumulative formation constants for metal cyanides.</b>	<b>27</b>
<b>Table 4.1</b>	<b>Wavelengths used for atomic absorption spectrophotometric analysis.</b>	<b>43</b>
<b>Table 6.1</b>	<b>Standard conditions for experiments.</b>	<b>63</b>
<b>Table 6.2</b>	<b>The effect of agitation on the adsorption of nickel , copper and zinc cyanide onto AMBERLITE IRA 900.</b>	<b>64</b>
<b>Table 6.3</b>	<b>The effect of initial metal concentration on the adsorption of zinc , nickel and copper cyanide onto AMBERLITE IRA 900.</b>	<b>65</b>
<b>Table 6.4</b>	<b>The effect of pH levels on the adsorption of zinc , nickel and copper cyanide onto AMBERLITE IRA 900.</b>	<b>66</b>
<b>Table 6.5</b>	<b>The effect of temperature on the adsorption of zinc , nickel and copper cyanide onto AMBERLITE IRA 900.</b>	<b>67</b>
<b>Table 6.6</b>	<b>The effect of ionic strength on the adsorption of zinc , nickel and copper cyanide onto AMBERLITE IRA 900.</b>	<b>68</b>
<b>Table 7.1</b>	<b>The adsorption of zinc , nickel and copper onto AMBERLITE 252 H.</b>	<b>94</b>

<b>Table 7.2</b>	<b>Comparison of monometallic and multimetallic loading.</b>	<b>95</b>
<b>Table 7.3</b>	<b>The effect of the inert sand slurry on AMBERLITE 252 H and AMBERLITE IRC 718.</b>	<b>96</b>

# CHAPTER 1

## INTRODUCTION

### 1.1 HEAVY METALS IN THE ENVIRONMENT

The occurrence of hazardous wastes in the environment is unavoidable due to a vast array of industrial activities. Unfortunately, the disposal of nonbiodegradable inorganic wastes, such as heavy metals to aqueous streams is a direct result of these activities. Due to its toxicity, the presence of heavy metals in rivers and catchment areas is of major concern. These metals are virtually indestructible and even in dilute form, metals such as zinc and copper are toxic to humans. If they are ingested by aquatic life in contaminated water, they will continue up the food chain to human beings. (Valenti, 1992).

Raw industrial effluents are likely to contain these anthropogenic pollutants, and its removal prior to effluent discharge is imperative. The sources of these effluents cover a wide range of industrial wastewaters, including hydrometallurgical liquors, spent electroplating baths and metal finishing wastewaters. (Loureiro, *et al* 1988).

Recently, environmental pressures has lead to the search for methods for removing toxic metal wastes from aqueous streams, even when they are

present in very dilute concentrations. This is in line with the current regulatory trend, which is for heavy metal discharge limits approaching those of drinking water standards, (Reed *et al*, 1994).

Due to the nature of wastewater treatment processes, accumulation of mineral content is inherent in water reuse, thus considerable environmental concern has focused on these toxins, especially in areas where water reuse is practised. Although the heavy metals are of relatively low value, economic interest in the recovery of these metals has increased, especially as a result of more effective processing of low grade ores. In addition, the non-compliance to governmental standards for discharge limits may lead to stiff penalties.

## 1.2 SOUTH AFRICAN STANDARDS

In terms of governmental legislation set in 1984, the requirements to which wastewater resulting from industrial operations should conform, after purification, are indeed stringent.

According to these standards, the maximum concentration in parts per million for copper is from 0.02 - 1 ppm, depending on the receiving environment. For zinc, the limits are from 0.3 - 5 ppm. (Murray, 1987).

## 1.3 CONVENTIONAL TREATMENT

Traditional approaches used to treat aqueous metal bearing wastes, other than land disposal include, (Grosse, 1986) :

\* Precipitation : alkali, sulphide, magnesium oxide ,

- \* Reduction : chromate, selenites, selenates and oximium tetroxide ,
- \* Stabilization or solidification ,
- \* Cyanide destruction , and
- \* Biological treatment.

Most of these methods are ideal for treatment of waste streams containing high levels of dissolved heavy metals. However, at trace metal concentrations, these methods become either impractical or ineffective. Furthermore, the preferred method of precipitation is severely limited by complex formation due to the presence of complexing agents such as cyanide in wastewaters, (Grosse, 1986).

In view of these restraints, ion exchange technology offers an alternative to treating dilute and complexed metal containing wastes. A typical metal / cyanide bearing wastewater treatment plant is shown in Figure 1.1.

#### 1.4 WASTE RECOVERY

The economic feasibility of metals recovery operations are primarily dependent upon three factors, (Grosse, 1986) :

1. Metal type and concentration.
2. Availability of material quantity within close proximity, and
3. Economical (profitable) recovery process.

However, justification for recovery processes such as ion exchange is not exclusive to raw materials savings. Reduced operating costs for "end - of - pipe" pollution control can be a significant factor.

## 1.5 ION EXCHANGE FOR WASTE RECOVERY

Ion exchange and resin adsorption systems offer a versatile separation process with wide application to the metal finishing industry. Ion exchange has all the advantages of evaporative processes for recovery. In addition, it can serve as a polishing step after conventional wastewater treatment and purification of liquids wastes. By definition, ion exchange is a separation technology which removes various ionic species from solution via interchanging reversible ions between the solution (aqueous waste) and the exchanger (e.g. resin).

Many applications for ion exchange systems have been demonstrated. The development of reciprocating flow and countercurrent exchange systems have enhanced the potential application of ion exchange for plating "drag out" recovery by (1) providing reduced equipment costs (due to small resin sizes), (2) automatic regeneration of resin, and (3) their compact size.

These systems are currently being used for dragout recovery from chromium, copper and nickel plating rinses, purification of spent process acids (e.g. chromium acid) and mixed wastewater deionization. Figure 1.2 shows a schematic representation of an ion exchange system utilized for polishing wastewaters, following conventional treatment, (Grosse, 1986).

Although other adsorbents, such as activated carbon can be utilized in recovery processes, ion exchange technology is an ideal alternative, since it is based on the development of more specific ligands with matrices of considerable strength and mechanical resistance, (Diaz and Mijangos, 1987). Hence, ion exchange resins are more selective than activated carbon and are also more durable.

Also, since the resins are available as cation exchange, anion exchange and chelating resins, metals in ionic and complexed form can be removed by this method. Moreover, the development of chelating resins, which offer extremely high selectivity toward toxic heavy metals over competing alkali and alkali - earth metals, (Zhu *et al*, 1990), provides an excellent method for removal of heavy metals complex waste solutions.

## 1.6 OBJECTIVES OF THIS STUDY

Ion exchange processes are mainly employed as tertiary processes whereby aqueous effluent is "polished" prior to effluent discharge. However, these processes have the potential to be primary metal removal processes for waste streams having low concentrations of metals. (Reed *et al*, 1994). Moreover, the ability of ion exchange resins to concentrate trace levels of metals creates the possibility of recovering metals from low grade ores.

Although the removal of heavy metals by ion exchange has been investigated by numerous authors, (Young *et al*, 1991; Loureiro *et al*, 1988; Green 1988) little work has been done on the removal of heavy metals at low concentrations. Notable exceptions have been publications investigating

removal of trace metals by the use of chelating resins, (Pesavento *et al*, 1993). Moreover, removal of heavy metals at trace quantities in the presence of complex forming ligands has received no attention at all.

The main purpose of this study was to investigate the removal of three heavy metals, i.e. nickel, copper and zinc at trace concentrations in ionic and complexed form, by the use of ion exchange resins. The metals in ionic form were contacted with a cation exchange and chelating resin, and the complexed metals were removed by an anion exchange resin. The specific objectives were:

- \* To investigate possible factors influencing the anion exchange process, emphasising the effect of initial metal concentration, pH, stirring speed, temperature and ionic strength.
- \* To perform a comparative study between the cation and chelating resins, focusing on adsorptive performance in synthetic heavy metal solutions and on selectivity in a competitive environment.
- \* To develop a kinetic model which can predict metal adsorption onto the ion exchange resins.
- \* To conduct durability tests on the resins by exposure to a coarse sand slurry.
- \* To test ion exchange performance with a real mining slurry.

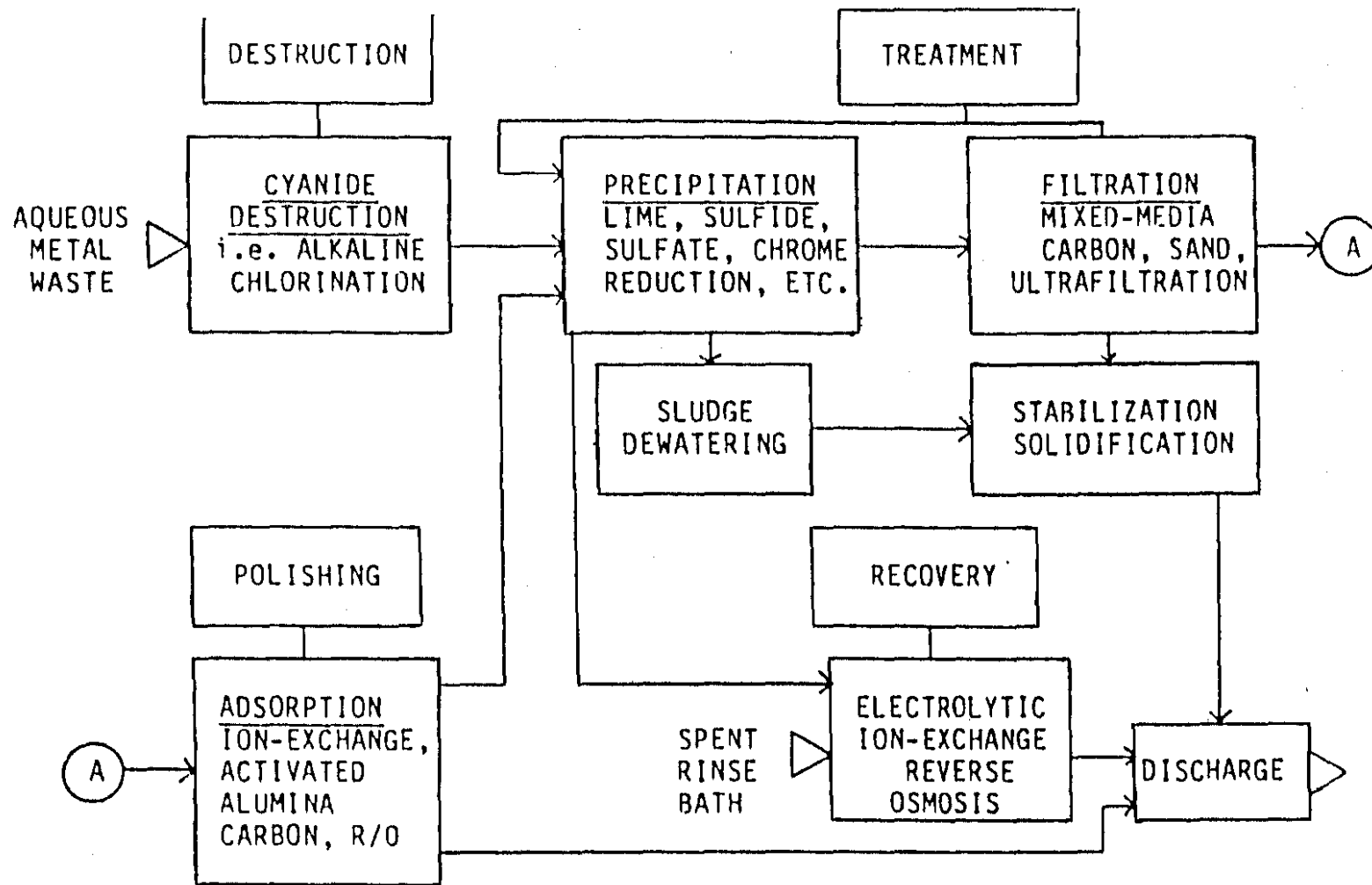


FIGURE 1.1 Typical metal / cyanide bearing wastewater treatment plant.

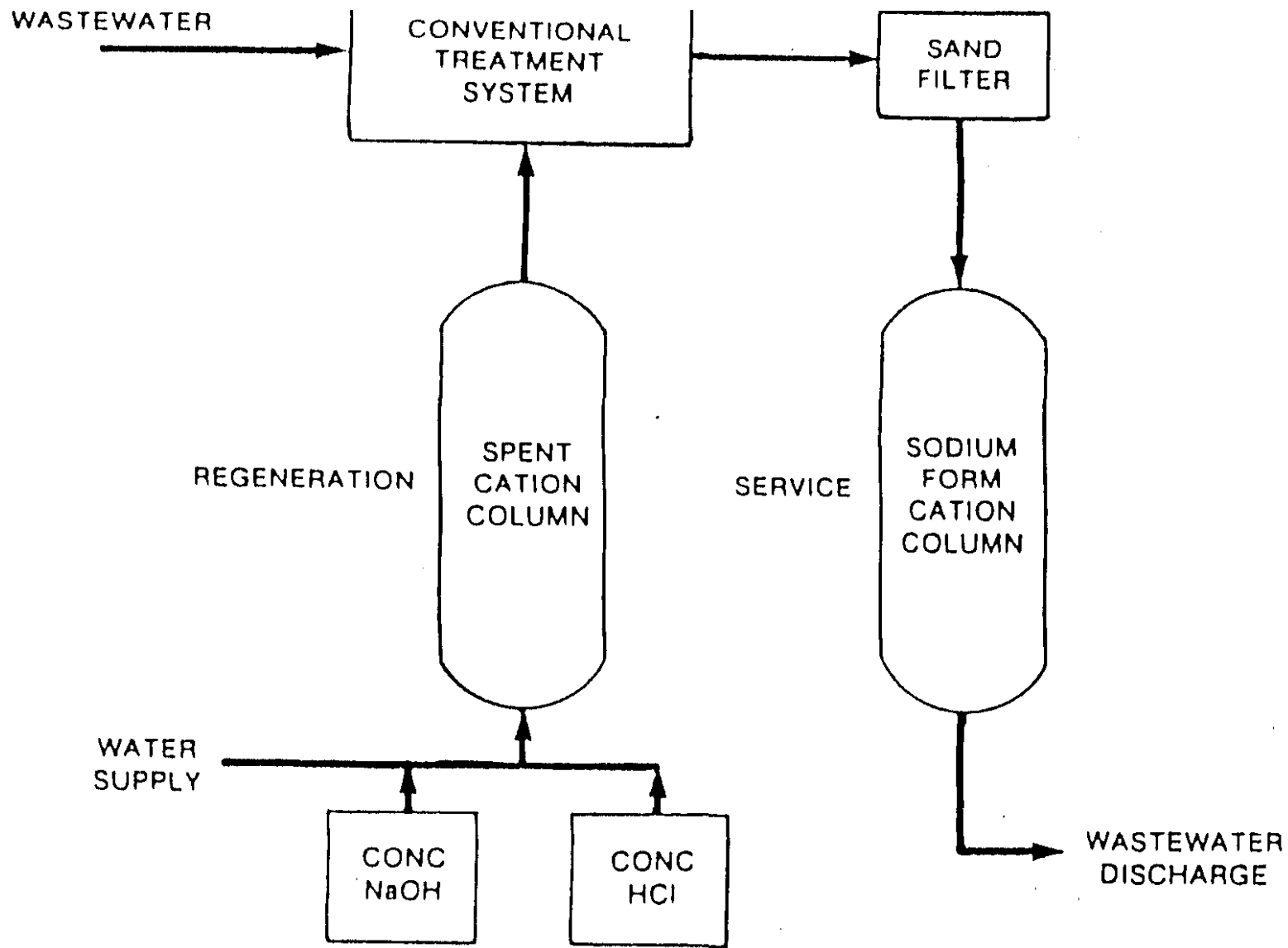


FIGURE 1.2 Ion exchange system utilised for polishing wastewaters.

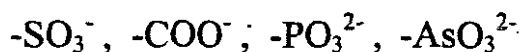
# CHAPTER 2

## LITERATURE REVIEW

### 2.1 ION EXCHANGE RESINS

#### 2.1.1 CHEMICAL AND PHYSICAL PROPERTIES

The most important class of ion exchangers are the organic ion-exchange resins. Their framework, the so-called matrix, consists of an irregular, macromolecular, three dimensional network of hydrocarbon chains. The matrix carries ionic groups such as :



in cation exchangers, and



in anion exchangers.

The resins are made insoluble by the introduction of crosslinking agents, usually divinylbenzene which interconnect the various hydrocarbon chains. An ion exchange resin particle is practically one single macromolecule. Its dissolution would require rupture of carbon-carbon bonds. Thus, the resins are insoluble in all solvents by which they are not destroyed.

The chemical, thermal and mechanical stability and the ion exchange behaviour of the resins, depend chiefly on the structure and the degree of crosslinking of the matrix and on the nature and number of the fixed ionic groups. The degree of crosslinking determines the mesh width of the matrix and thus the swelling ability of the resin and the mobilities of the counter ions in the resin. The latter, in turn, determine the rates of ion exchange and other processes.

The mesh width of very highly crosslinked resins is of the order of only a few Angstrom units. The mesh width of very weakly crosslinked and fully swollen resins may exceed 100 Angstrom units. Highly crosslinked resins are harder and more resistant to mechanical breakdown and attrition.

The chemical and thermal stability of the resins is not unlimited. The most frequent causes for resin deterioration are chemical and thermal degradation of the matrix, for example, by oxidation and loss of fixed ionic groups, for example by thermal hydrolysis. Most of the present commercial resins are stable in all solvents except strong oxidising or reducing agents and withstand temperatures of up to 100°C. However, strong-base anion exchange resins, begin to deteriorate above 60°C.

The chemical nature of the fixed ionic groups greatly affects ion exchange equilibrium. An important factor is the acid or base strength of the groups. Weak acid groups such as  $\text{-COO}^-$  are ionized only at high pH. At low pH, they combine with  $\text{H}^+$  ions, forming undissociated  $\text{-COOH}$ , and thus no longer act as fixed charges. In contrast, strong acid groups such as  $\text{-SO}_3^-$  remain ionized even at low pH. Similarly, weak base groups such as  $\text{-NH}_3^+$

lose a proton forming uncharged  $\text{-NH}_2$ , when the pH is high and strong base groups such as  $\text{-N}^+(\text{CH}_3)_3$  remain ionized even at high pH.

The nature of the fixed ionic groups also affects the selectivity of the resins. Counter ions which tend to associate with the fixed groups by say, forming ion pairs or complexes are preferred by the resin. For example resins with sulphonic acid groups prefer  $\text{Ag}^+$ , resins with carboxylic acid groups prefer alkaline earth cations, and resins with chelating groups prefer certain heavy metal cations. (Helfferich, 1995).

### 2.1.2 PREPARATION

Most of the present ion exchange resins are addition copolymers prepared from vinyl monomers. The copolymer beads are prepared by the pearl polymerization technique. The monomers are mixed and a polymerization catalyst such as benzoyl peroxide is added. The mixture is then added to a thoroughly agitated aqueous solution which is kept at the temperature required for polymerization (usually 85 to 100°C).

The mixture forms small droplets which remain suspended. A suspension stabilizer in the aqueous phase prevents agglomeration of the droplets. The size of the droplets then depends on the nature of the suspension stabilizer, the viscosity of the solution and the agitation, and can be varied within wide limits. The polymer is then obtained in the form of fairly uniform spherical beads. (Helfferich, 1995).

As long as solvents which expand the resin are used in this process, an open, but heterogeneous structure is formed. Such resins are generally called

macroporous or macroreticular resin. The macroreticular structure embodies fixed large pores, presenting a sponge-like matrix which imparts superior resistance to mechanical and osmotic shock.

## 2.2 MECHANISM OF ION EXCHANGE

Ion exchange operations are essentially metathetical chemical reactions between an electrolyte in solution and an insoluble electrolyte with which the solution is contacted. The mechanism by which ion exchange take place in resinous beads is well understood. Ion exchange is, as a rule purely a diffusion phenomenon, and the following individual processes take place , (Treybal, 1968) :

1. Diffusion of ions from the bulk of the liquid to the external surface of an exchanger particle.
2. Inward diffusion of ions through the solid to the site of exchange.
3. Exchange of the ions.
4. Outward diffusion of the released ions to the surface of the solid.
5. Diffusion of the released ions from the surface of the solid to the bulk of the liquid.

However, depending on the application, the exchanging ions may be either cationic or anionic of nature and the exchange of ions may be accompanied by other processes, such as chelation or complex formation.

### 2.2.1 ANION EXCHANGE

Strong base anion exchange resins are commonly employed to remove anions like  $\text{Ni}(\text{CN})_4^{2-}$ ,  $\text{Cu}(\text{CN})_4^{2-}$  and  $\text{Zn}(\text{CN})_4^{2-}$  from cyanide leach liquors. The functional group of a strong base resin normally is a quaternary ammonium group possessing a permanent positive charge. Metal cyanides are therefore extracted by an ion - exchange reaction as shown here for zinc cyanide :



where the symbol 1- denotes the inert backbone or matrix of the resin, and  $\text{X}^-$  denotes a monovalent anion such as  $\text{OH}^-$ .

The complex metal cyanides on the resin can be eluted from the resin by ion exchange in which the equilibrium depicted in equation 2.1 can be forced to the left-hand side by an increase in the concentration of  $\text{X}^-$ . However, unlike weak - base resins, which can be eluted by an adjustment in pH, the elution of strong base resin is not easy due to the affinity the metal cyanides have for the strong base resins. The results of the equilibrium loading of gold, silver and several base metals from pregnant cyanide solutions from two South African gold mines onto two strong base resins indicate that the heavy metals, copper, nickel, and zinc are more strongly absorbed than the gold, silver and lead. (Fleming and Cromberge, 1984).

In addition to the exchange, a metal cyanide anion can displace the counter ion associated with a positively charged group and become attached to the

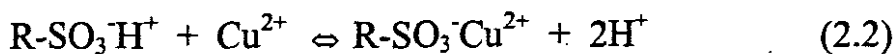
strong base resin by the formation of an ion pair. This reaction is not dependent on pH and therefore loading at the high pH values of leach liquors poses no problem.

## 2.2.2 CATION EXCHANGE

Cation exchange occurs when a positively charged ion (cation) in solution penetrates the polymeric resin and exchanges with a similarly charged ion already attached to the fixed ionic group. These resins can be classified in two groups.

- a) Strong acid exchange resin.
- b) Weak acid exchange resin.

Strong acid exchange resins contain functional groups, derived from a strong acid (normally sulphuric acid). The degree of ionization is analogous to that of a strong acid (low  $pK_a$ ) which permits the hydrogen to be dissociated and ready for exchange over a wide pH range. These resins can remove metals by the following ion exchange reaction :



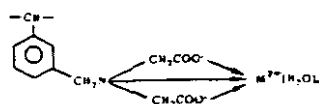
Weak acid exchange resin, on the other hand, contain functional groups derived from a weak acid commonly of the carboxylic or phenolic group. Such resins are useful only within a fairly narrow pH range.

### 2.2.3 ION EXCHANGE WITH CHELATION

Chelate ion exchangers are widely used not only in waste-water treatment, but also because of their high selectivity, for the recovery of valuable metals. These exchangers, are in general, co-ordinating copolymers with covalent bound side atoms (Lewis bases) that can form co-ordinate bonds with most of the toxic metal ions (Lewis acids). Due to co-ordination type interactions all such chelating exchangers offer extremely high selectivity towards commonly encountered toxic  $M^{2+}$  cations, namely  $Cu^{2+}$ ,  $Pb^{2+}$ ,  $Ni^{2+}$ ,  $Cd^{2+}$  and  $Zn^{2+}$  over competing alkaline ( $Na^+$ ,  $K^+$ ) and alkaline-earth ( $Ca^{2+}$ ,  $Mg^{2+}$ ) metal cations, (Sengupta *et al*, 1991).

Chelating resins are ion exchangers in which chelating agents, such as iminodiacetic acid has been incorporated. The chelating agents are usually introduced into the matrix of a styrene-divinylbenzene polymer, (Schmuckler 1965). The sorption mechanism of these resins is through chelation, instead of simple ion exchange, and the following illustration represents the nature of metal ion binding for iminodiacetate functionalities, (Sengupta and Zhu, 1992).

Iminodiacetate:



where there are one N and two O donor atoms per functional group. The chelating ion exchangers are distinguished from the ordinary type of ion exchanger by two main properties, (Schmuckler, 1965) :

(1) High selectivity. The affinity of particular metal ions to a certain chelating ion exchanger depends mainly on the chelating group and not on the size of the ion, its charge, or other physical properties, which determine the order of preference in the case of the ordinary ion exchanger.

(2) Bond strength. In ordinary ion exchangers, the bonding is electrostatic with a strength of the order 2 - 3 Kcal / mole, while in chelating resins the binding energy is of the order 15 - 25 Kcal / mole, (Schmuckler 1964).

### 2.3 ION EXCHANGE IN DILUTE HEAVY METAL SOLUTIONS

The first attempts to apply ion exchange for metal recovery were in connection with recovery of copper from waste liquors of the cuprammonium rayon and brass industry, silver from photographic film manufacturing wastes, and chromium from electroplating wastes. Uranium was the first metal to be recovered from leach solutions by ion exchange on a large scale, and the great amount of research done in this field opened the doors to the wide possibilities of using ion exchange for recovering other metals from leach solution. The exchange process is especially useful in the treatment of very dilute solutions with heavy metal concentrations in the order of 10 ppm or less. (Habashi, 1980).

The effect that certain process parameters have on the adsorption of heavy metals at trace concentrations have not been properly investigated. Fleming and Cromberge (1984), reported on the effects of pH, temperature, agitation and the presence of competing ions on the adsorption of gold cyanide onto anion exchange resins. However, the effect of these parameters on heavy metal adsorption - whether in the ionic or complexed state - needs attention.

Diaz and Mijangos, (1987), have successfully applied the ion exchange process to an industrial wastewater containing significant quantities of iron and base metals, including copper, nickel, cobalt and zinc. A chelating resin containing iminodiacetic acid groups, was utilised because of its selectivity for heavy metals over other minerals present in the waste solution. Significant metal loading was achieved, but the exchange / chelation reaction was shown to be highly pH dependent and copper retention was shown to be most efficient at low pH values.

Shallcross *et al* (1988), indicated the selective behaviour of a strong acid cation exchange resin for divalent alkali-earth metal ions over monovalent alkali ions. However, this is to be expected because the selectivity exhibited by cation exchangers depend mainly on the properties of the exchanging ions.

Activated carbon has also been shown to have the ability to adsorb heavy metal ions and complexes. Reed *et al*, (1994), treated metal-bearing wastewaters with granular activated carbon. However, the presence of the complexing agent EDTA adversely affected adsorptive performance. (Tan and Teo 1987), used four different powdered activated carbons to adsorb chromium and lead ions from solution.

The uptake rates of the metal ions were rapid and equilibrium was attained in less than one hour. However, the adsorptive process was found to be overly sensitive to the effects of parameters such as pH, carbon dosage and initial adsorbate concentration.

The durability of resin beads is of importance in any industrial application. Researchers do not yet fully understand the greater damage to resin beads in

mechanical agitators, but think it may be related to the power concentrated around the impeller. In order to quantify resin breakdown due to agitation and mechanical manipulation it is necessary to rely on empirical data. In this study the resin beads were contacted with a coarse sand slurry at a high stirring speed in batch reactors. Any decrease in adsorptive capacity or kinetics due to the abrasive action of the slurry was then compensated for by a mathematical model. In this respect a comparative study was done between the chelating and cation exchange resin, to see if the lower degree of crosslinking of the chelating resin would influence its durability.

Gupta *et al* (1987), made up synthetic waste solution to simulate real waste water properties during their investigation into the ion exchange of metal cyanide complexes. However, very little work has been done on real waste waters or low grade ore leachates. In this study, resin performance was also tested with a real mining slurry.

## 2.4 KINETIC PARAMETERS

The diffusional phenomenon characterising adsorptive process can be divided into two mechanisms :

- (a) Interdiffusion of counter ions in the adherent films (film diffusion).
- (b) Interdiffusion of counter ions within the ion exchanger itself (intraparticle diffusion).

The slower of these two processes would control the rate of exchange of ions within an ion exchanger. (Helfferich, 1995).

### 2.4.1 EXTERNAL FILM DIFFUSION

The film diffusion mass transfer model assumes that the overall exchange phenomenon is controlled by the liquid-phase mass transfer resistance to ionic interdiffusion in the stationary liquid film around the exchanger particle, (Petruzzelli *et al*, 1995).

All factors which tend to increase the rate of interdiffusion in the beads and to reduce the rate in the films favour film diffusion. This film diffusion control may prevail in systems with ion exchangers of high concentration of fixed ionic groups, low degree of crosslinking and small particle size, with dilute solutions and with inefficient agitation, (Helfferich, 1995). The flux equation for mass transfer in the liquid boundary layer is usually given by a linear driving force, (Petersen, 1991).

$$n_1 = k_f (C - C_s) \quad (2.3)$$

where  $k_f$  is the external film mass transfer coefficient.

### 2.4.2 INTRAPARTICLE DIFFUSION

Intraparticle diffusion takes place via surface diffusion along the pore walls of the adsorbent and pore diffusion in the liquid phase down the adsorbent pores. The effect of pore diffusion is negligible since surface diffusion has been shown to be the determining transport mechanism in most cases, (Neretnieks, 1976).

Van Lier (1983), concluded that it is adequate to model the intraparticle diffusion by a single effective diffusion coefficient. According to Helfferich, (1995), the exchange flux is proportional to the concentration of fixed charges and to interdiffusion coefficients in the beads and is inversely proportional to the bead radius ; on the other hand, the flux is independent of the film thickness, solution concentration and diffusion coefficients in the film.

During intraparticle diffusion control, film diffusion takes place so much faster, that the concentration differences in the film are instantaneously levelled out, thus concentration gradients exist only in the beads.

#### 2.4.3 CHEMICAL REACTION CONTROL

There are many known ion exchange processes which are accompanied by true chemical reactions. However, whether these reactions are rate controlling has been an issue of great contention.

Yoshida *et al* (1986), proved that for ion exchange with chelation, the chelation reaction may be rate controlling for very small particle sizes (radius of less than  $10^{-4}$  m).

Although particle diffusion control prevails at larger particle sizes, the chelation reaction does influence the uptake rates due to the binding of ions on whose diffusion, ion exchange depends, (Liberti and Helfferich, 1983). With few exceptions, such as complexing of some trivalent transition-metal ions, reactions of ions in solution are known to be fast, thus rendering

reaction-retarded diffusion control as a more likely situation than reaction control.

## 2.5 FACTORS INFLUENCING THE ION EXCHANGE PROCESS

In order to properly characterise the process of adsorption of heavy metals onto ion exchange resins, it is necessary to study the factors that might influence the ion exchange process. Towards this end, a sensitivity analysis was performed on the parameters that might influence the adsorption of the metal cyanides onto an anion exchange resin.

Tan and Teo (1987), showed that the adsorption of heavy metal ions on activated carbon depends significantly on the pH, carbon dosage and initial adsorbate concentration. However, due to their vastly differing physico-chemical properties a parallel between activated carbon and polymeric resins cannot be drawn. Unfortunately, the majority of work performed on anion exchange resins, has been for the extraction of precious metals from cyanide solutions. Fleming and Cromberge (1984), found that solution pH had little effect on the rate of loading or on the equilibrium loading of gold cyanide onto a strong base resin. However, increasing temperature improved uptake rates, and an increase in ionic strength negatively affected equilibrium loading.

Sengupta and Zhu (1992), found that the adsorption of metal ions onto chelating resins is highly pH dependent. Under acidic conditions ( $\text{pH} \leq 2.0$ ) the metal removal capacities of chelating polymers are essentially lost, due to the formidable competition from hydrogen ions.

## 2.6 FORMATION OF METAL COMPLEXES

The mining industry uses cyanide, a complexing agent in the recovery of gold and silver. As cyanide is not a selective complexant, heavy metals that occur in the ore also gets dissolved and is present in the leached pulp. At equilibrium, the formation of these complexes may be described by the following equations and constants :



where M and L represents the metal and cyanide ions respectively. The formation constant K is an indication of the stability of the complex. A large value for the formation constants, indicate that the concentrations of the complex formed is much greater than the species from which it is formed . Table 2.1 indicates cumulative formation constants for metal-cyanide complexes.

## 2.7 SPECIATION

Copper exists as  $Cu(CN)_2^-$  ;  $Cu(CN)_3^{2-}$  ; and  $Cu(CN)_4^{3-}$  in a strong cyanide solution. However, as to which species adsorbs onto the anion exchange resin is not solely dependent on the amount of excess cyanide. Gupta *et al*,

(1987) found that although all the species existed in their waste solution, it was mainly the  $\text{Cu}(\text{CN})_2^-$  species that adsorbed onto the resin. It was inferred that the interaction between the resin sites and the anions is dependent on the chemical nature, the shape, and the polarizability of the anion. For ions of the same polarizabilities, the univalent anions are preferred to the multivalent anions because a univalent anion needs only one resin site and so it can sit very close to the resin backbone.

Zinc is most stable in the zinc-tetracyano ( $\text{Zn}(\text{CN})_4^{2-}$ ) complex. This was also found to be the adsorbing species by (Gupta *et al*, 1987).

Similarly, the  $\text{Ni}(\text{CN})_4^{2-}$  complex would be expected to be the dominant adsorbing species on a anion exchange resin.

## 2.8 ION EXCHANGE EQUILIBRIA

Ion exchange equilibrium is attained when an ion exchanger is placed in an electrolyte solution containing a counter ion which is different from that in the ion exchanger. Suppose that the ion exchanger is initially in the A form and that the counter ion in the solution is B. Counter - ion exchange occurs, and the ion A in the ion exchanger is partially replaced by B:



The concentration ratio of the two competing counter-ion species in the ion exchanger is usually different from that in the solution; as a rule, the ion exchanger selects one species in preference to the other.

Ion exchange equilibrium can be characterised by the ion - exchange isotherm. This isotherm is a graphical representation which, in principle, covers all possible experimental conditions at a given temperature. Any specific set of experimental conditions (solution concentration, relative amounts of counter ions, etc.) corresponds to one point on the isotherm surface. (Helfferich 1995)

A popular model for ion exchange is the linear absorption model (LAM), which is based on the assumption that the concentration  $C_b$  of bound molecules in a sorbent material is proportional to the concentration  $C$  of the unbound sorbate in the same material. (Nestle and Kimmich 1996)

$$C_b = kC \quad (2.5)$$

where  $k$  is a constant.

However this model does not consider saturation effects. This deficiency can be overcome by using a Langmuir sorption isotherm.

According to (Zheng *et al*, 1995), the Langmuir isotherm can be expressed as

$$q_i = q_0 K_L C_i / 1 + K_L C_i \quad (2.6)$$

where  $q_i$  and  $C_i$  are concentrations of the cations,  $i$ , in the solid and liquid phases, respectively,  $K_L$  is the Langmuir isotherm constant, and  $q_0$  is the ion exchange capacity.

The Langmuir isotherm ( Equation 2.6) is based on the assumption that the maximum adsorption occurs when a single layer of molecules cover the adsorbent surface and that the adsorption energy is constant ( Morris and

Weber 1962). At very low concentrations, the Langmuir isotherm reduces to a linear form.

## 2.9 SIGNIFICANCE OF THE LITERATURE REVIEW

The recovery of precious metals from aqueous solutions, has received much attention. Unfortunately, due to its relatively low value the recovery of heavy metals - especially in dilute form - has not received as much attention. Thus, a need exists for a proper evaluation of the interaction between dilute heavy metals solution and ion exchange resins. This can only be achieved by testing the sensitivity of the ion exchange process to the variations in the conditions that might influence it. It also clear that a need exists to investigate the removal of heavy metals form solutions containing complexing agents such as cyanide, especially with low metal to cyanide ratios.

Although there has been publications dealing with the removal of trace metals by the use of chelating resins, this has to be placed in perspective by comparison with a normal cation exchange resin.

The majority of authors dealing with the heavy metal - ion exchange employ synthetic waste solution for their experimental work. However, the practicality of these interactions in an industrial sense, should be tested by

the use of a real waste solution and by testing the durability of the ion exchange resin in an aggressive environment , i.e. a mining slurry.

TABLE 2.1 Cumulative formation constants for metal cyanides

	Log $K_1$	Log $K_2$	Log $K_3$	Log $K_4$
Copper (I) cyanide	*N/A	24.0	28.59	30.30
Nickel cyanide	N/A	N/A	N/A	31.30
Zinc cyanide	N/A	N/A	N/A	16.70

\* NOT AVAILABLE

# CHAPTER 3

## ADSORPTION KINETICS

In this chapter a dual resistance model is described which involves both external film diffusion and intraparticle diffusion, and which is similar to the model used by (Petersen, 1991). Although this model was developed mainly for adsorption onto activated carbon, the macroporous structure of the resin used in this study allows it to be applicable (Hall *et al*, 1966).

### 3.1 ASSUMPTIONS

It is necessary to state the following main assumptions, before the development of the model.

- The resin particles can be treated as equivalent spheres.
- The radial transport of metal ions and complexes into the pores of the resin can be described by a surface diffusion mechanism.
- Pore diffusion is assumed to be negligible.
- Accumulation of metal ions and complexes in the liquid phase within the pores of the resin is negligible.
- It is assumed that the ion exchange reaction on the resin occur instantaneously, so that equilibrium exists at the solid - liquid interface.

- The diffusivity of metal ions and complexes remains constant during a run, and is independent of the position inside the resin particle.

This model has been extended to accommodate the exposure of resin to a slurry environment. For this purpose the parameters *beta* ( $\beta$ ) and *delta* ( $\delta$ ) have been defined as follows :

$\beta$  - The change in the rate of adsorption due to the contact of the slurry with the resin external surface.

$\delta$  - The change in capacity for solute to the resin due to contact of the slurry with the resin external surface.

If  $\beta = \delta = 1$ , there will be no change in the adsorption profile.

If  $\beta < 1$ , there will be a negative change in the rate of adsorption.

Similarly if  $\delta < 1$ , there will be a negative change in the capacity of the resin.

## 3.2 MATERIAL BALANCE EQUATIONS.

This model accounts for the accumulations of adsorbate in the macropores of the resin and was applied to the cation - exchange, anion exchange and chelating resins.

### 3.2.1 BATCH STIRRED TANK REACTOR

The rate controlling step in an ion exchange operation is greatly dependent on the structure and properties of the resin beads. However, it can safely be

assumed that film diffusion is rate controlling in the initial stages of a batch adsorption experiment. Diffusion through the liquid film can be described by Fick's first law :

$$n = -D \frac{\partial C}{\partial r} \quad (3.1)$$

Assuming spherical geometry and integrating Equation (3.1) over the film thickness leads to:

$$n = k_f (C - C_s) \quad (3.2)$$

where  $k_f = \frac{D}{\alpha}$

When Fick's law is used to describe the flux of adsorbate through the differential element of the spherical adsorbent particle, (Equation 3.1) becomes :

$$n = D\rho_R \frac{\partial Q}{\partial r} \quad (3.3)$$

A mass balance over a differential element for spherical bead with a radial thickness  $\Delta r$  yields :

Accumulation in macropores = mass flow into macropores at  $(r + \Delta r)$  - mass flow in macropores at  $r$ .

$$4\pi r^2 \rho_R \frac{\partial Q}{\partial t} = D\rho_R \frac{\partial}{\partial r} \left[ r^2 \frac{\partial Q}{\partial r} \right] 4\pi \quad (3.4)$$

Equation (3.4) can be simplified to the following partial differential equation:

$$\frac{\partial Q}{\partial t} = D \frac{\partial^2 Q}{\partial r^2} + \frac{2D}{r} \frac{\partial Q}{\partial r} \quad (3.5 a)$$

According to Vermeulen (1958), the surface diffusion model may be approximated by a quadratic driving force. They showed that the following expression :

$$D \rho_R \frac{\partial}{\partial r} \left[ r^2 \frac{\partial Q}{\partial r} \right]$$

may be replaced by :

$$\frac{60 \bar{D}}{dp^2} \left[ \frac{Q_s^2 - Q^2}{2Q} \right]$$

where  $\bar{D} = \psi D$

equation (3.5 a) can thus also be written as :

$$\frac{dQ}{dt} = \frac{60 \bar{D}}{dp^2} \left[ \frac{Q_s^2 - Q^2}{2Q} \right] \quad (3.5 b)$$

which is an ordinary differential equation, and represents the material balance for the macropores.

The mass balance over the batch reactor yields :

$$-V \frac{dC}{dt} = n A \quad (3.6)$$

The surface area  $A$  of the resin beads can be described as follows :

$$A = \frac{6M}{\rho_R dp} \quad (3.7)$$

A combination of Equations (3.6) ; (3.7) and (3.2) leads to the liquid phase material balance :

$$\frac{dC}{dt} = \frac{6k_f M}{\rho_R dp V \epsilon} (C_s - C) \quad (3.8)$$

The assumption of no accumulation of metals at the external surface of the adsorbent, yields the following equation :

$$\left. \frac{dQ}{dr} \right|_{r=R} = \frac{k_f \beta}{\alpha \phi D} (C - C_s) \quad (3.9)$$

where  $\beta$  is the parameter that accounts for the reduction in the uptake rates due to effects of the slurry.

The phase conversion factor  $\phi = \frac{1}{\epsilon}$  for the resin.

The distribution of the adsorbate between the solution and adsorbed phase is defined by the Langmuir isotherm :

$$Q = \frac{\delta q K_L C_e}{1 + K_L} = \frac{\delta P C_e}{1 + K_L} \quad (3.10)$$

where P is combination of the maximum capacity of the resin q and the isotherm constant  $K_L$ .

$\delta$  is the parameter that accounts for the reduction in exchange capacity due to the loss in external surface as a result of contact with the synthetic slurry.

## 3.2.2 NUMERICAL SOLUTION

### 3.2.2.1 BATCH STIRRED TANK REACTOR

The parabolic partial differential equations derived in this section can be solved by substituting finite divided differences for the partial derivatives (Chapra and Canale 1989). Thus, the Equations ( 3.5 a ), (3.8) and (3.9) were solved by means of discretization with finite differences. In order to achieve this, the interval  $0 < r < R$  is divided into n conveniently equal sections.

## 3.3 ESTIMATION OF KINETIC PARAMETERS

### 3.3.1 EXTERNAL MASS TRANSFER COEFFICIENT

It is necessary to estimate the film transfer coefficient to provide an input into the model. The initial stages of adsorption is dominated by film transfer, and a linear concentration gradient from the bulk liquid to the resin particle is postulated. Furthermore, it is assumed that the adsorbate concentration at

the particle surface  $C_s$  is negligible in the early stages, compared to the bulk liquid concentration  $C$ .

This means that the Equation (3.8) will simplify to :

$$\frac{dC}{dt} = \frac{6K_f M}{\rho_R dpV \epsilon} C \quad (3.11)$$

Integrating equation (3.11) results in :

$$\ln \left[ \frac{C_0}{C} \right] = \frac{6k_f M}{\rho_R dpV \epsilon} t \quad t \rightarrow 0 \quad (3.12)$$

### 3.3.2 INTRAPARTICLE DIFFUSION

In the homogeneous surface diffusion model, the surface diffusion coefficient  $D$  is actually a lumped intraparticle diffusion coefficient. The intraparticle diffusivity can be estimated by using the Runge-Kutta solution for the batch kinetics of a single solute in a Powell least squares regression routine (Van Deventer, 1984).

# CHAPTER 4

## EXPERIMENTAL

This chapter describes the experimental techniques and materials used in contacting the ion exchange resin with the heavy metal ions and complexes.

### 4.1 EXPERIMENTAL MATERIALS

Experiments were performed whereby the anion exchange resin was contacted with synthetic metal cyanide solutions. The adsorbates used were zinc cyanide, copper(I)cyanide and potassium tetracyanonickelate(II) hydrate. The  $K_2 Ni(CN)_4$  was obtained from Sigma Aldrich as a crystalline salt and the  $Zn(CN)_2$  and  $CuCN$  from Merck as insoluble precipitates. The latter two complexes were dissolved in an excess of potassium cyanide at a temperature of  $50^\circ C$ . All reagents were of analytical grade and distilled deionised water was used throughout.

The cation and chelating resins were contacted with the synthetic metal salts : zinc nitrate, nickel nitrate and cupric sulphate. The  $Ni(NO_3)_2 \cdot 6H_2O$  and  $CuSO_4 \cdot 5H_2O$  were obtained from Saarchem and the  $Zn(NO_3)_2 \cdot 6H_2O$  from Merck.

The ion exchange resins employed in this study are all styrene divinylbenzene co-polymers with a macroreticular structure that embodies fixed large pores, presenting a sponge-like matrix. The resins were obtained as spherical beads from A.C.I.X., a division of National Chemical Products Ltd. (South Africa). The different resins may be divided as follows :

\* AMBERLITE IRC 718 is a chelating, weakly acidic cation exchange resin, incorporating iminodiacetic acid functional groups in its matrix. It has a mean bead diameter of 600 - 800  $\mu\text{m}$  , total exchange capacity of  $\geq 1,0$  eq/L ( $\text{Na}^+$  form), and a bulk density of 630 - 700 g/L ( $\text{Na}^+$  form).

\* AMBERLITE 252H is a strong acid cation exchange resin, containing sulphonic, functional groups. It has a mean bead diameter of 600 - 800  $\mu\text{m}$  , total exchange capacity of  $\geq 1.7$  eq/L ( $\text{H}^+$  form), and a bulk density of 720 - 790 g/L ( $\text{H}^+$  form).

\* AMBERLITE IRA 900 CL is a strong base anion exchange resin containing quaternary ammonium functional groups. It has a mean bead diameter of 600 - 800  $\mu\text{m}$  , total exchange capacity of  $\geq 1.0$  eq/L ( $\text{Cl}^-$  form), and a bulk density of 640 - 710 g/L ( $\text{Cl}^-$  form).

#### 4.2 PREPARATION AND PRE-TREATMENT

Due to the low initial concentrations ( $\leq 10$  ppm) of metals in solution, and the subsequent small amounts of resin, an accurate method of quantifying the amount of resin used in each experiment had to be developed. To this effect,

a method similar to the one used by (Van Vliet *et al*, 1980) was used. This method involves centrifugation of the resin to a touch dry state and then accurately weighing of small portions. The reliability of this method was then tested by comparing the results of several adsorption tests, which were performed under the same experimental conditions, such as pH and initial concentration. In order to avoid discrepancies in uptake rates, most of the fine resin beads were removed to obtain a more uniform particle size distributions.

The amount of water removed due to centrifugation was calculated and the necessary corrections were made when using the free settled volume method of measurement.

The chelating resin AMBERLITE IRC 718, which was obtained in sodium form was washed with distilled water and converted to the hydrogen form by a column procedure, by passing a 4% solution of HCl through it. Then the column was washed with distilled water to neutrality. By the same method, the AMBERLITE 252H, was converted to the hydrogen form through contact with a 4% solution of H<sub>2</sub>SO<sub>4</sub>. The anion exchange resin which was received in Cl<sup>-</sup> form was converted to SO<sub>4</sub><sup>2-</sup> form by contact with 4% H<sub>2</sub>SO<sub>4</sub>.

### 4.3 BATCH EXPERIMENTS

All experiments were performed in batch stirred tank reactors made of perspex and of diameter 10cm, height 15cm and three evenly spaced baffles of 1cm width. The solutions were agitated by a perforated flat blade impeller of width 6cm and height 5cm. The stainless steel impeller was driven by a Heidolph variable speed overhead stirrer. A sketch of the apparatus is given

in Figure 4.1. Unless otherwise stated, solutions of 1L volume were used, and a stirring speed of about 300 rpm was maintained.

Experiments were performed to evaluate the factors that might influence the adsorption of the metal cyanides on the anion exchange resin. This called for variations in stirring speed, pH, temperature, initial concentrations and ionic strength. Variation in pH was achieved by the addition of dilute HCl or KOH, and the ionic strength was adjusted by the addition KCl. An initial metal concentration of 10 ppm was maintained throughout except when the effect of a variation in initial concentration was studied.

During the comparative study between the cation and chelating resins, an initial metal concentration of 2 ppm was used throughout. Standard curves were set up by contacting each metal with 0.046g of the resin. Experiments were then done whereby zinc, copper and nickel were then adsorbed simultaneously on both the cation and chelating resins. Solutions in contact with the chelating resin was kept at an optimum pH, due to the ineffectiveness of this resin at a very low pH.

#### 4.4 DURABILITY TESTS

Tests were performed whereby the cation exchange and chelating resins were exposed to a slurry of coarse sand particles ( 1 - 2 mm diameter) for 72 hours at a stirring speed of 520 rpm, in a baffled tank reactor. The concentration of sand used in each reactor varied from 40 to 160 g/l of sand.

After careful separation of the resin and slurry, the resin was used in adsorption tests with a dilute solution of cupric sulphate. The results of these

tests were then compared to the results of tests performed with an equal amount of untreated resin and copper concentration. Any deviation from the normal uptake rates or equilibrium loading would then indicate that the mechanical action of the sand particles has led to a reduction in sorption capacity and kinetics.

#### 4.5 LEACHING AND ADSORPTION

A real mineral ore was obtained from the Black Mountain mine in Aggeneys, in the Northern Cape in South Africa. This oxidized ore contains mostly copper oxide, but other heavy metals such as zinc and lead were found to be present in the ore. The ore was received as oxidised rocks and had to be crushed and ground to a very small particle size.

Leaching experiments were conducted in a baffled tank reactor with 2% sulphuric acid being the leaching agent, for 100g of the finely milled ore. These tests produced an acidic leachate consisting mainly of cupric sulphate.

After carefully separating the leachate from the residual solid matter, adsorptive tests were performed on the cation exchange resin AMBERLITE 252H. The results of these tests were then compared to results of tests performed with a synthetic solution of cupric sulphate.

#### 4.6 EQUILIBRIUM EXPERIMENTS

The kinetic model used in this study incorporates an equilibrium model which accounts for the distribution of metals between the resin phase and the

liquid phase. To this effect equilibrium tests were performed in 1L stirred tank reactors.

According to (Gupta *et al*, 1987), most metal cyanide complexes reach their equilibrium sorption capacity onto anion exchange resins at metal concentrations of below 1 mg/L. Preliminary tests confirmed this, and consequently only 0.02 g of the anion exchange resin was used with different initial metal concentrations. This was done to obtain accurate loading values at very low metal concentrations.

These tests were conducted over a period of two days with samples being taken periodically and analysed for zinc, nickel and copper, so as to monitor the approach to equilibrium. Once the concentration of the metal in the liquid phase remained constant, the loading of the metal in the resin could be calculated. Single component isotherms were drawn up to characterise the equilibrium distribution of zinc, nickel and copper between the liquid phase and the anion exchange resin.

Similar tests were performed on the chelating and cation exchange resins. Only 1 ml and 0.5 ml of these resins were used respectively.

#### 4.7 ANALYTICAL METHODS

The determination of metal concentration in solution was achieved by the use of a Varian Techtron AA - 1275 atomic absorption spectrophotometer, with an air-acetylene flame. Table 4.1 details the absorbance peaks used for each metal at different concentration ranges. The pH of all solutions was

measured with a Beckmann Ø 71 pH meter coupled to a Beckmann electrode.

Scanning electron micrographs of the resin external surface was taken at the CSIR facility in Pretoria.

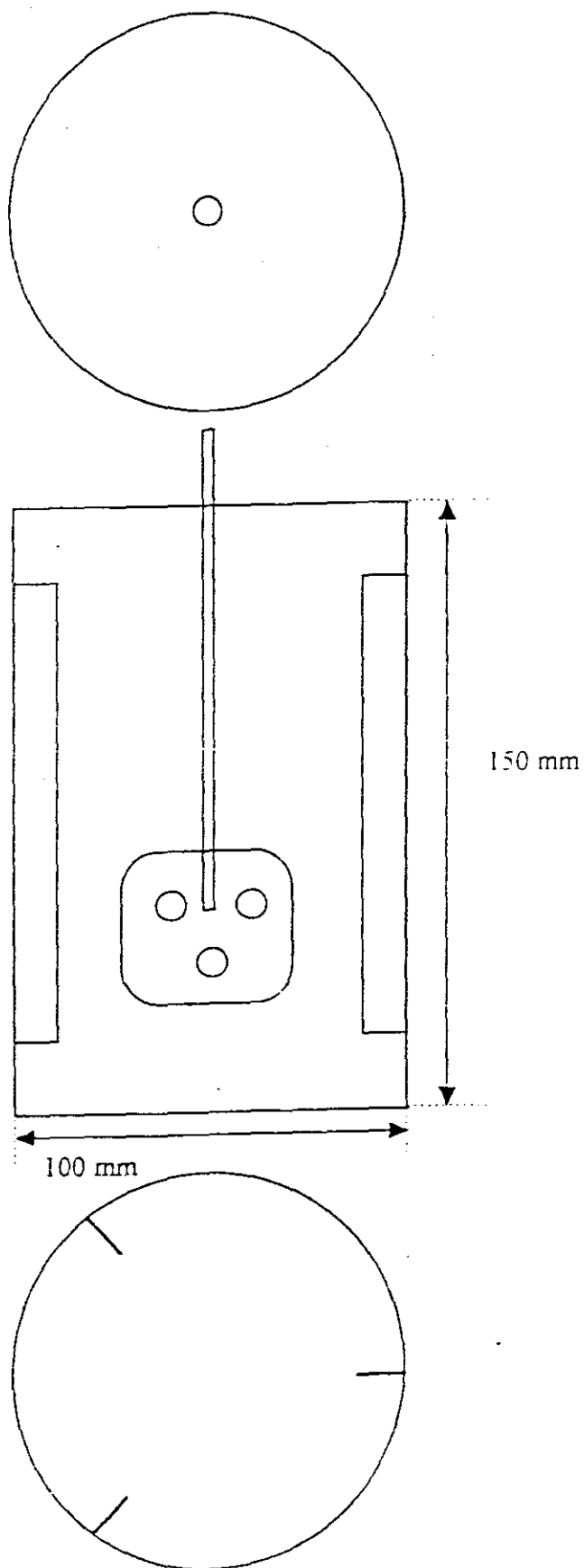


**FIGURE 4.1 : Diagram of the batch reactor and impeller**

Table 4.1 Wavelengths used for atomic absorption spectrophotometric analysis

Element	Concentration (ppm)	Wavelength nm
<b>Cu</b>	2	324.7
	100	218.2
	alternative	327.4
<b>Ni</b>	2	232.0
	alternative	341.5
<b>Zn</b>	2	213.9
	alternative	307.6

# CHAPTER 5

## ION EXCHANGE ISOTHERMS

In ion exchange equilibrium, the concentration ratios of the competing counter - ion species in the ion-exchanger and in the solution are not the same. As a rule, the ion exchanger prefers one species to the other. Each species is thus distributed differently between the aqueous solution and the ion exchange resin, (Helfferich 1995).

The distribution of the heavy metals between the ion exchanger and the aqueous solution can be quantitatively explained by an equilibrium isotherm. In this study, single component isotherms were set up for each of the heavy metal and ion exchange resins. The Langmuir isotherm was found to fit all of the experimental data. Predictive equilibrium loading values were obtained by reducing the Langmuir expression to a linear form, evaluating the slope and intercept from the regression and obtaining values for the maximum capacity  $q$  and Langmuir constant  $K_L$ .

### 5.1 ANION EXCHANGE EQUILIBRIA

Lopez *et al* (1992), applied a variety of isotherms to the binary exchange of anions on two strong base anion exchange resins. They found the Langmuir isotherm to be most suitable for both data prediction and correlation.

The Langmuir isotherm provided a reasonably good fit to the metalcyanide / sulphate exchange on AMBERLITE IRA 900. It can be seen from Figures 5.1 to 5.3 that the exchange equilibrium is characterised by a sharply negative curve which is an indication of the resin's selectivity for the metal complexes over the divalent sulphate anions. All three complexes reach their maximum sorption capacity at very low metal concentrations in solutions.

## 5.2 CATION EXCHANGE EQUILIBRIA

The cation exchange resin used in this study, AMBERLITE 252H was used by Shallcross *et al.*, (1988) for the Na - Ca exchange system. Their isotherms showed extreme selectivity for the  $\text{Ca}^{2+}$  over  $\text{Na}^+$  ions. In this study the resin was converted to the hydrogen form and equilibrated with solutions of cupric sulphate and nickel and zinc nitrate. The highly negative curvature of Figures 5.4 to 5.6 is an indication of the resin's selectivity for the divalent metal ions over protons and due to the high capacity of the resin, a loading of up to 80 kg/tonne is achieved. However, it is clear from the loading values that there is little preference given to any of the metals by the cation exchange resin.

## 5.3 CHELATING EXCHANGE EQUILIBRIA

The chelating resin, AMBERLITE IRC 718 contains iminodiacetic acid functional groups  $-\text{N}(\text{CH}_2\text{COOH})_2$  that behaves as a weak acid and it thus has a strong affinity for protons. Mijangos and Diaz (1992), studied metal-proton equilibrium relations with a similar chelating resin, at different solution pH values. It is clear from their monometallic isotherms, that at a pH value of 4.2, equilibrium loading is at an optimum for copper and nickel and at pH 4.6

for zinc. At lower pH values, the loading is significantly reduced for nickel and zinc while copper loading was still significant at a pH value as low as 4.3.

It was thus decided to equilibrate the metals with the proton loaded resin at an optimum pH value of 4.3. The isotherm given in Figure 5.7 indicate the high selectivity the resin has for copper over the hydrogen ions, as shown by the sharply negative curve. However, the isotherms given in Figures 5.8 and 5.9, show that nickel and zinc do not exhibit the same behaviour.

According to Pesavento *et al* (1993), the loading of metals on the chelating resins is dependent on the nature and strength of the bond formed between the metal and chelating group. They found that the bond formation constant is highest for copper, followed by nickel and zinc. The nature of the isotherm in this study seems to be in agreement with these conclusions and it can be seen that the equilibrium loading values are in the order  $Cu > Ni > Zn$ .

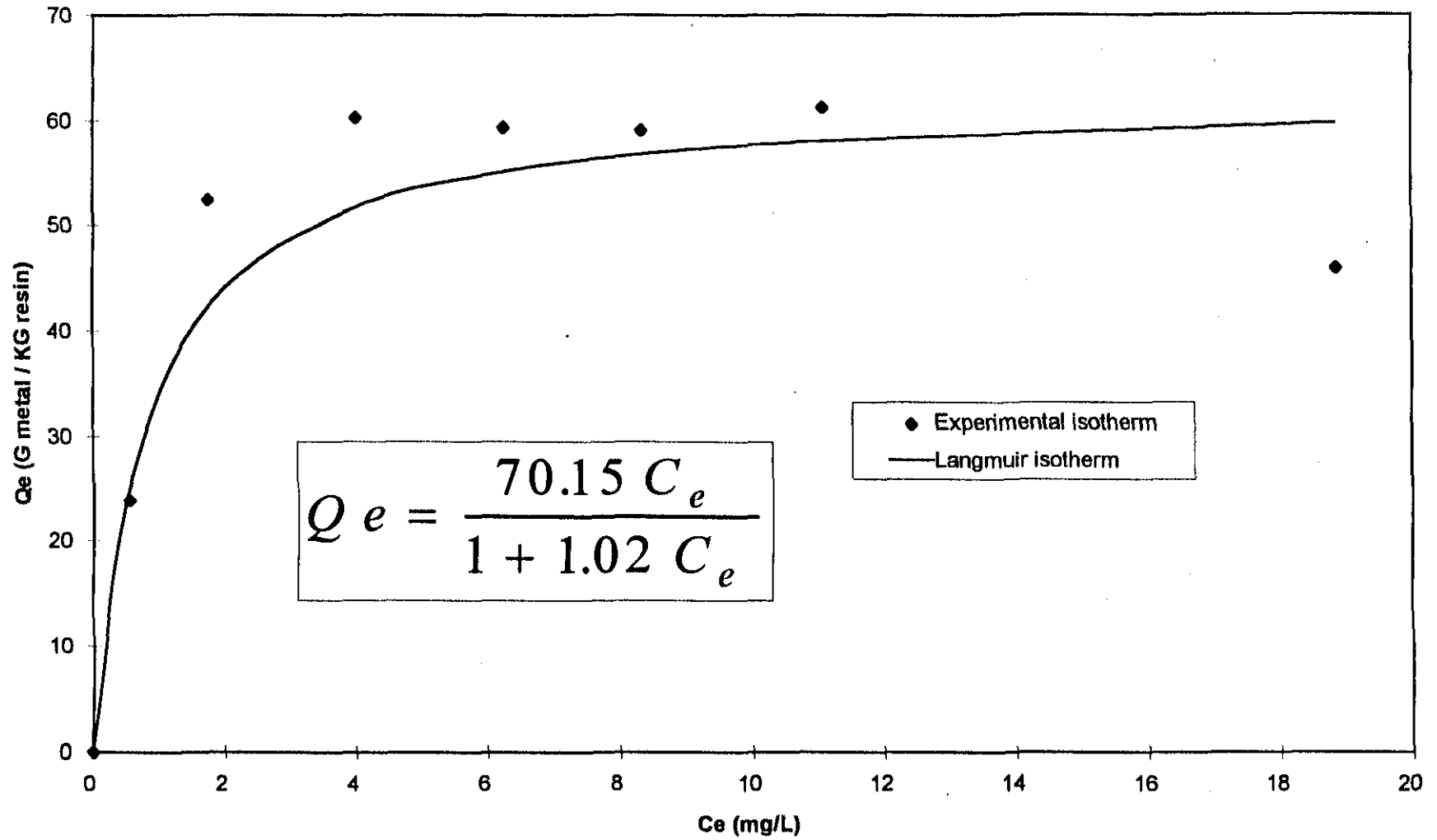


Figure 5.1 Equilibrium adsorption of zinc cyanide on AMBERLITE IRA 900.

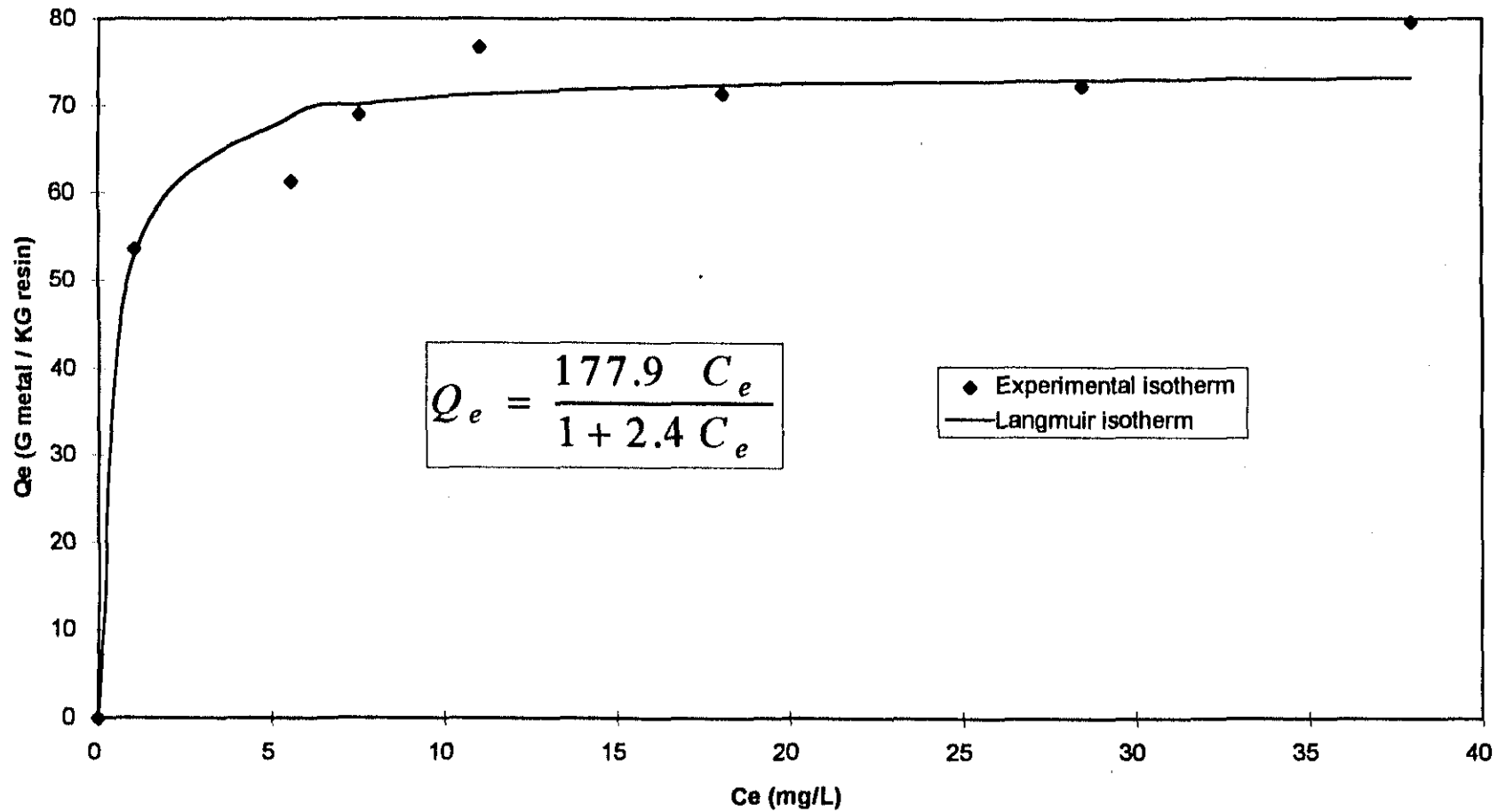


Figure 5.2 Equilibrium adsorption of nickel cyanide on AMBERLITE IRA 900.

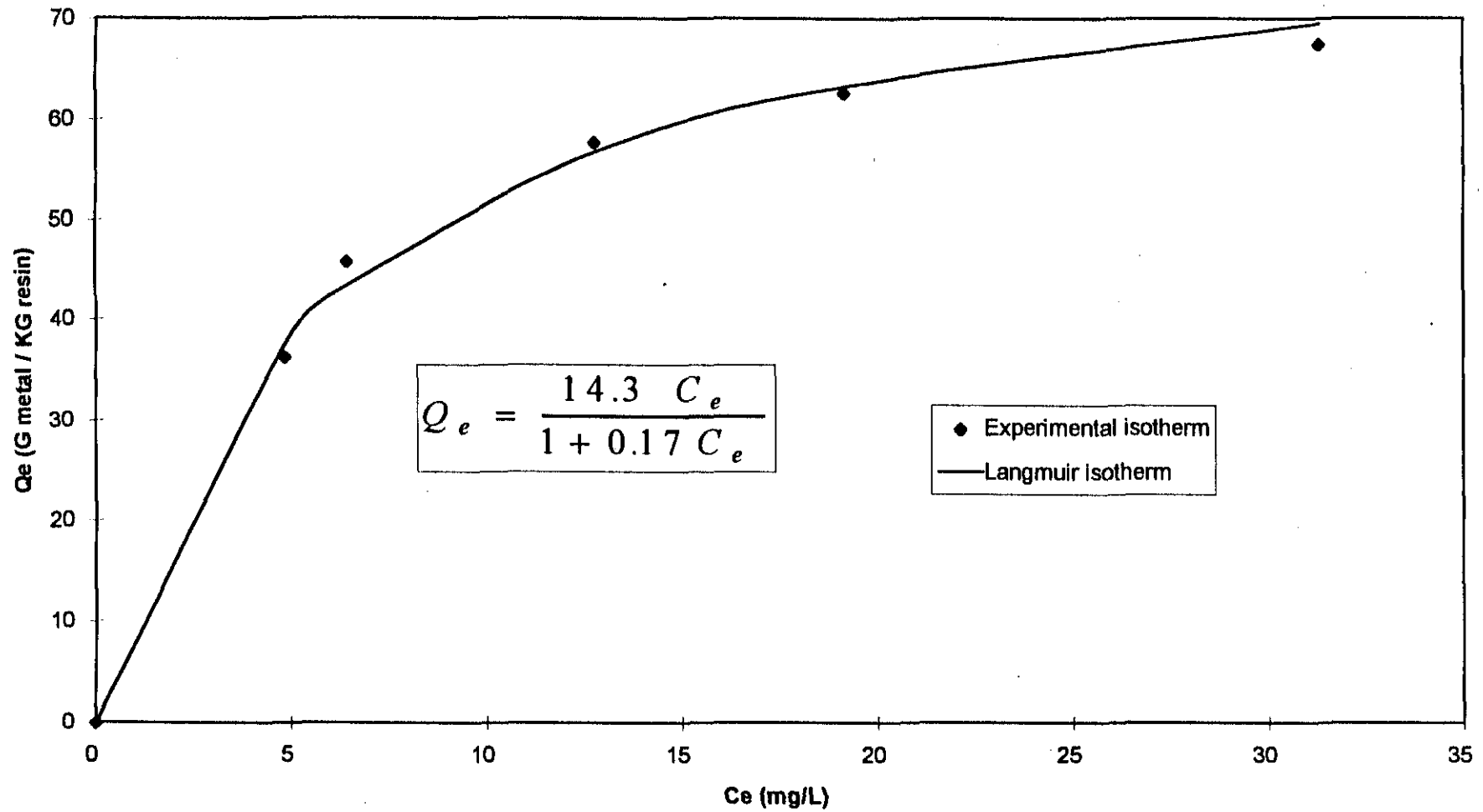


Figure 5.3 Equilibrium adsorption of copper cyanide on AMBERLITE IRA 900.

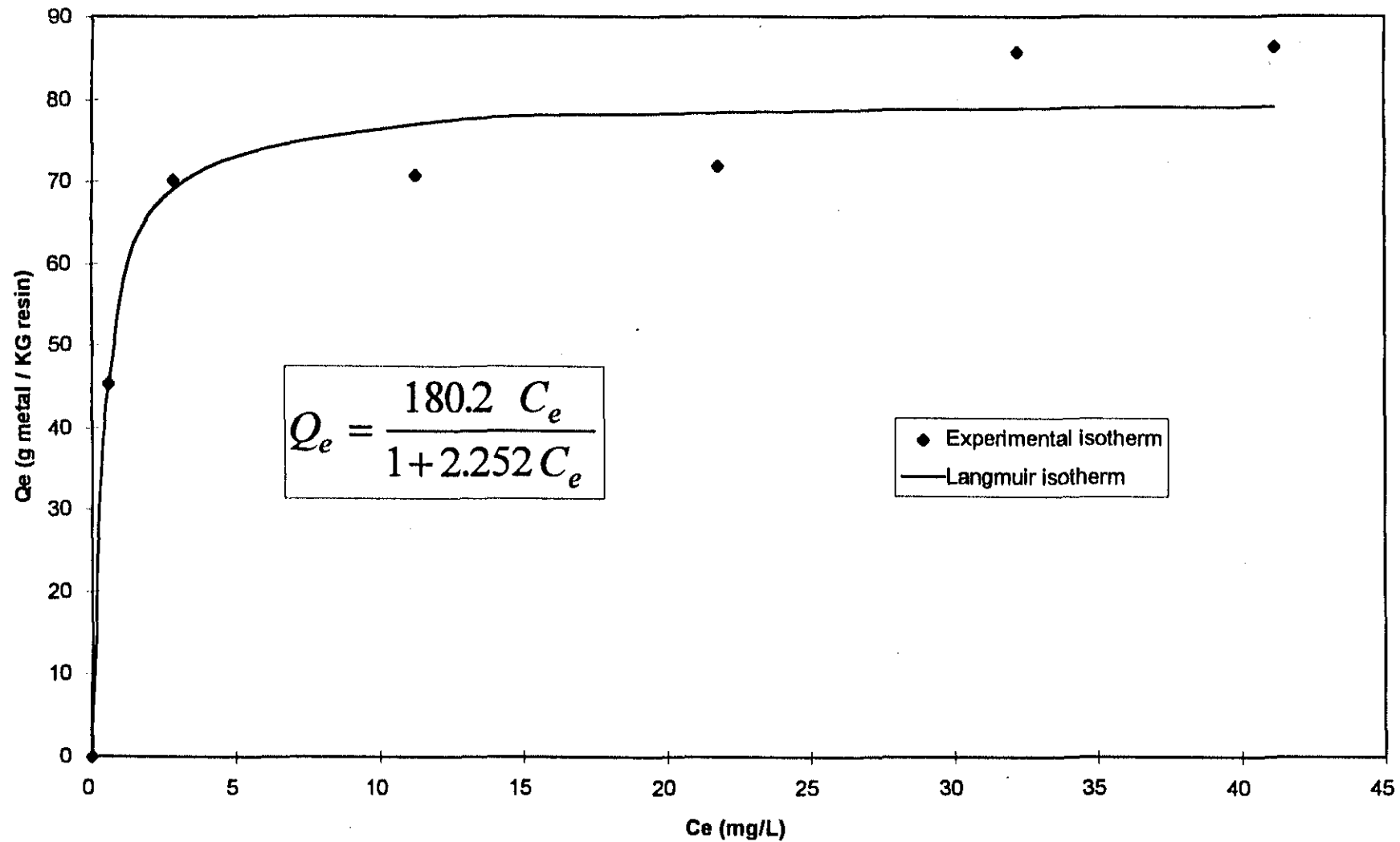


Figure 5.4 Equilibrium adsorption of zinc on AMBERLITE 252H.

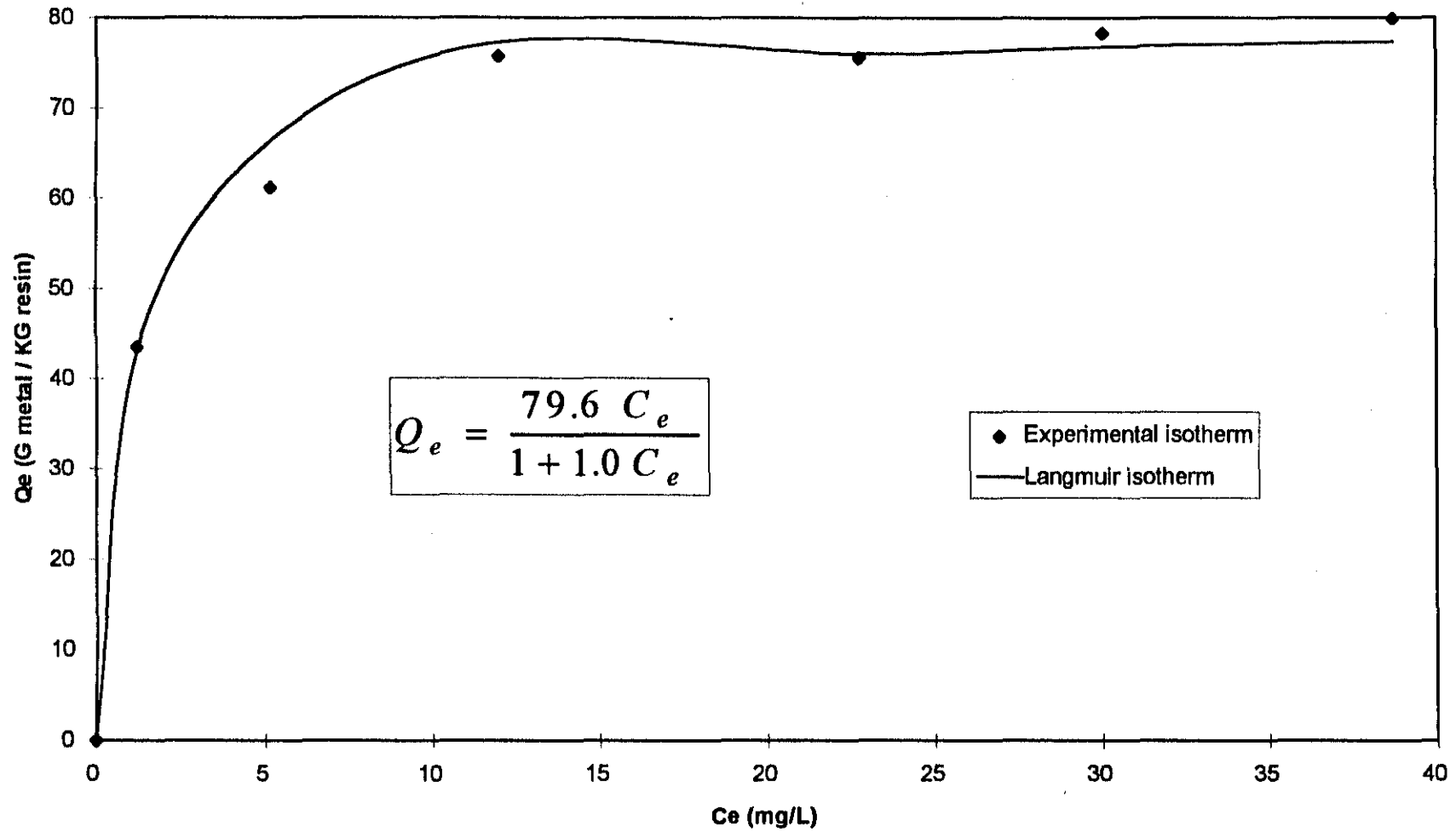


Figure 5.5 Equilibrium adsorption of nickel on AMBERLITE 252H

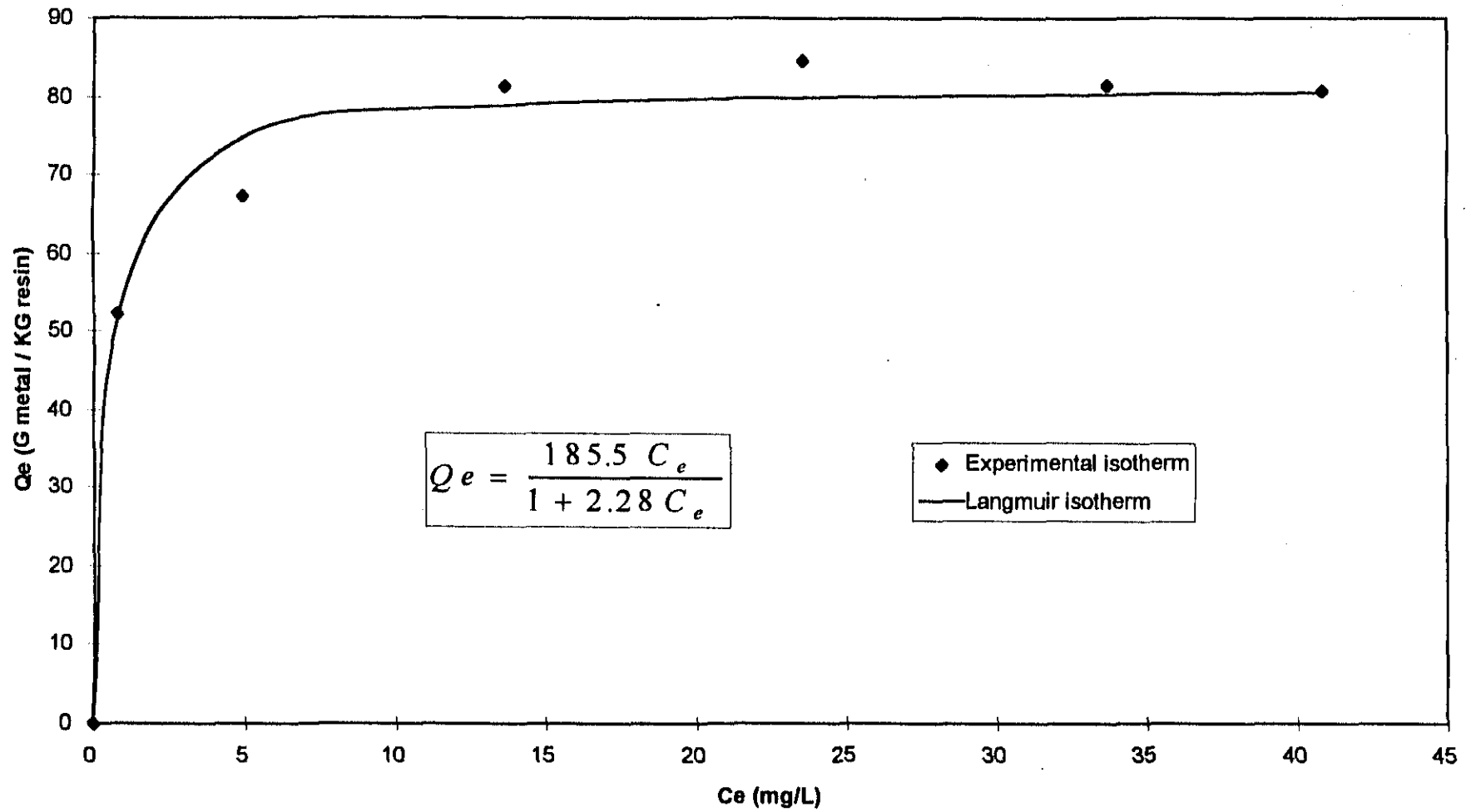


Figure 5.6 Equilibrium adsorption of copper on AMBERLITE 252H

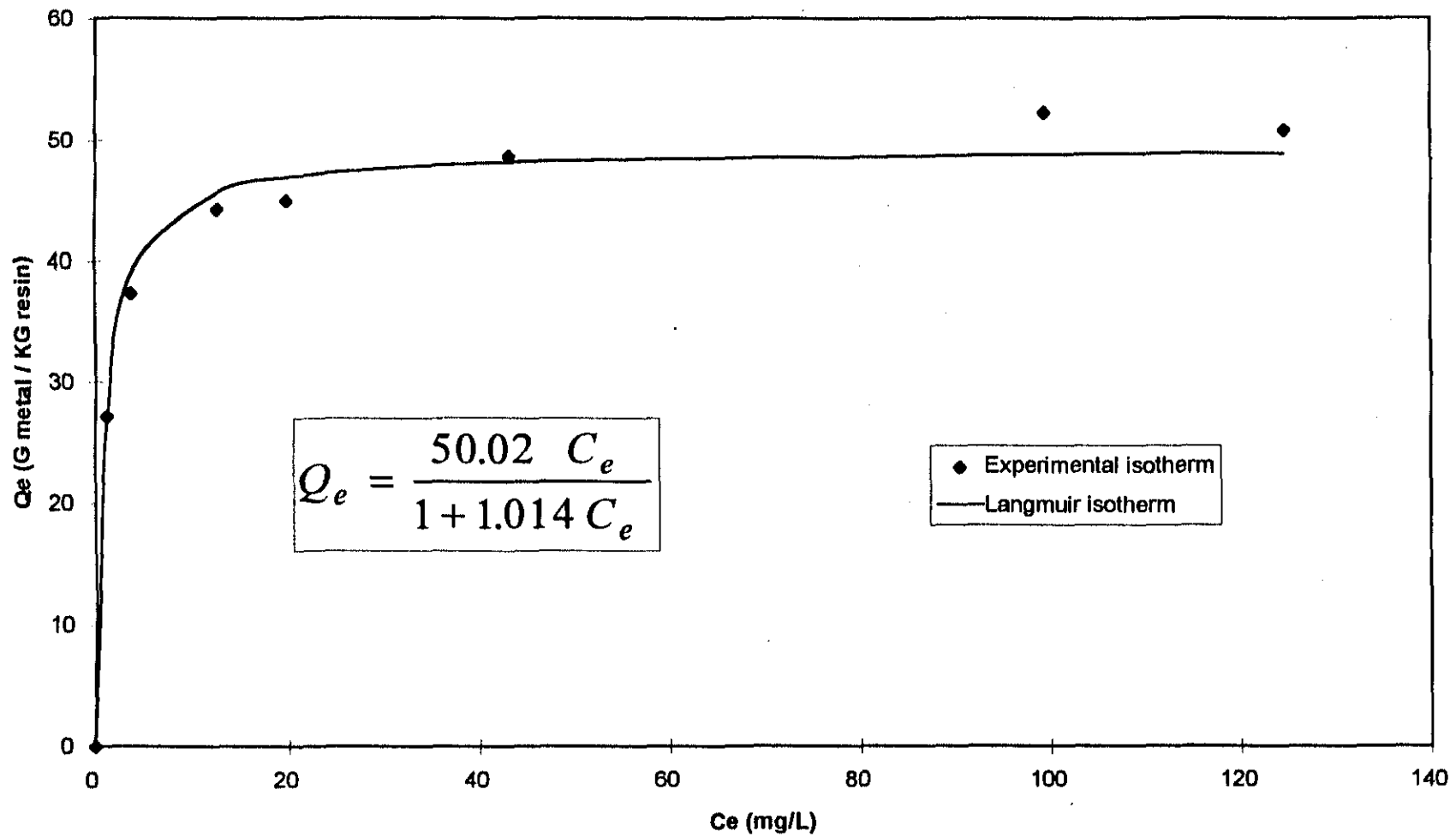


Figure 5.7 Equilibrium adsorption of copper on AMBERLITE IRC 718.

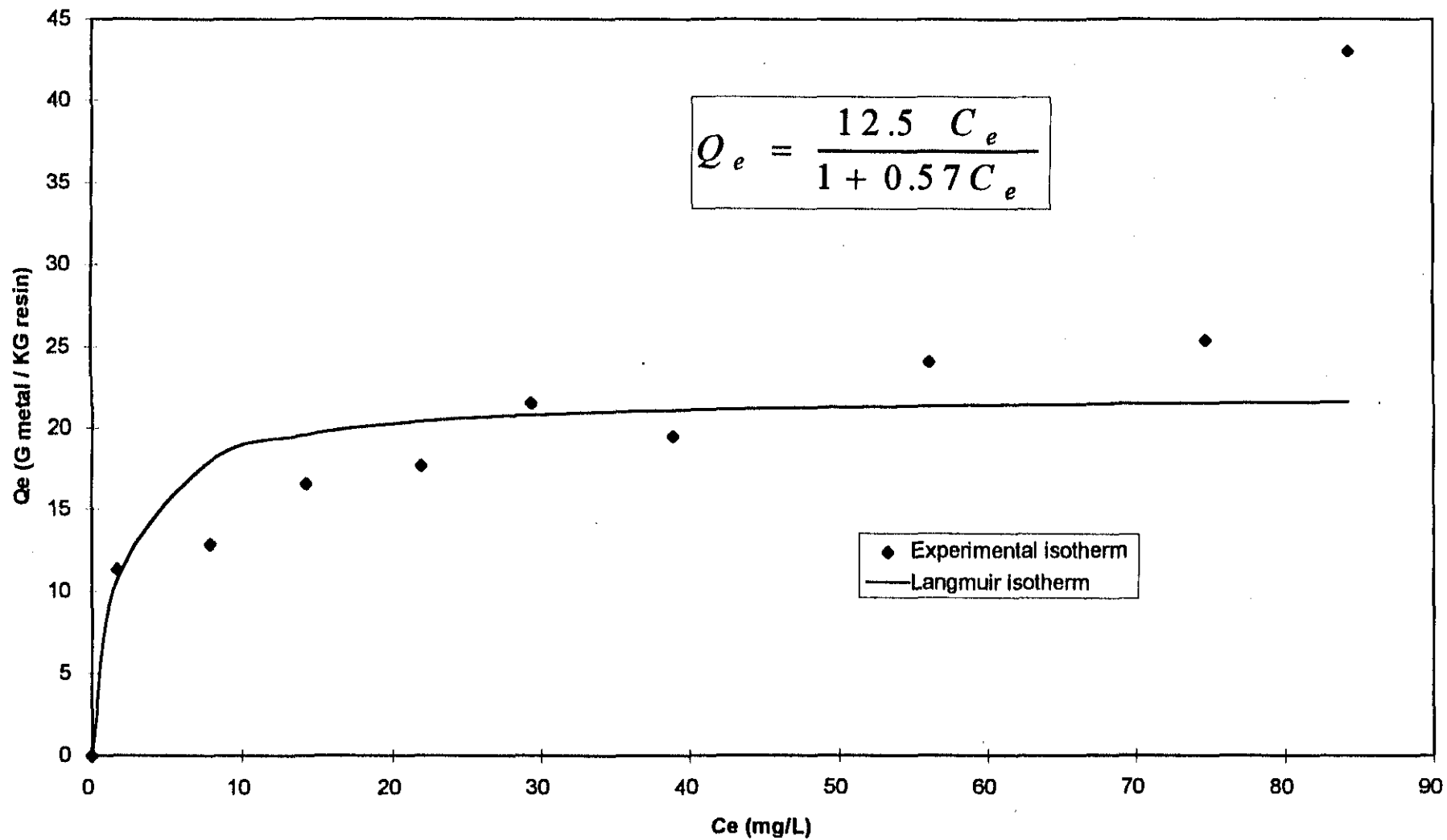


Figure 5.8 Equilibrium adsorption of nickel on AMBERLITE IRC 718.

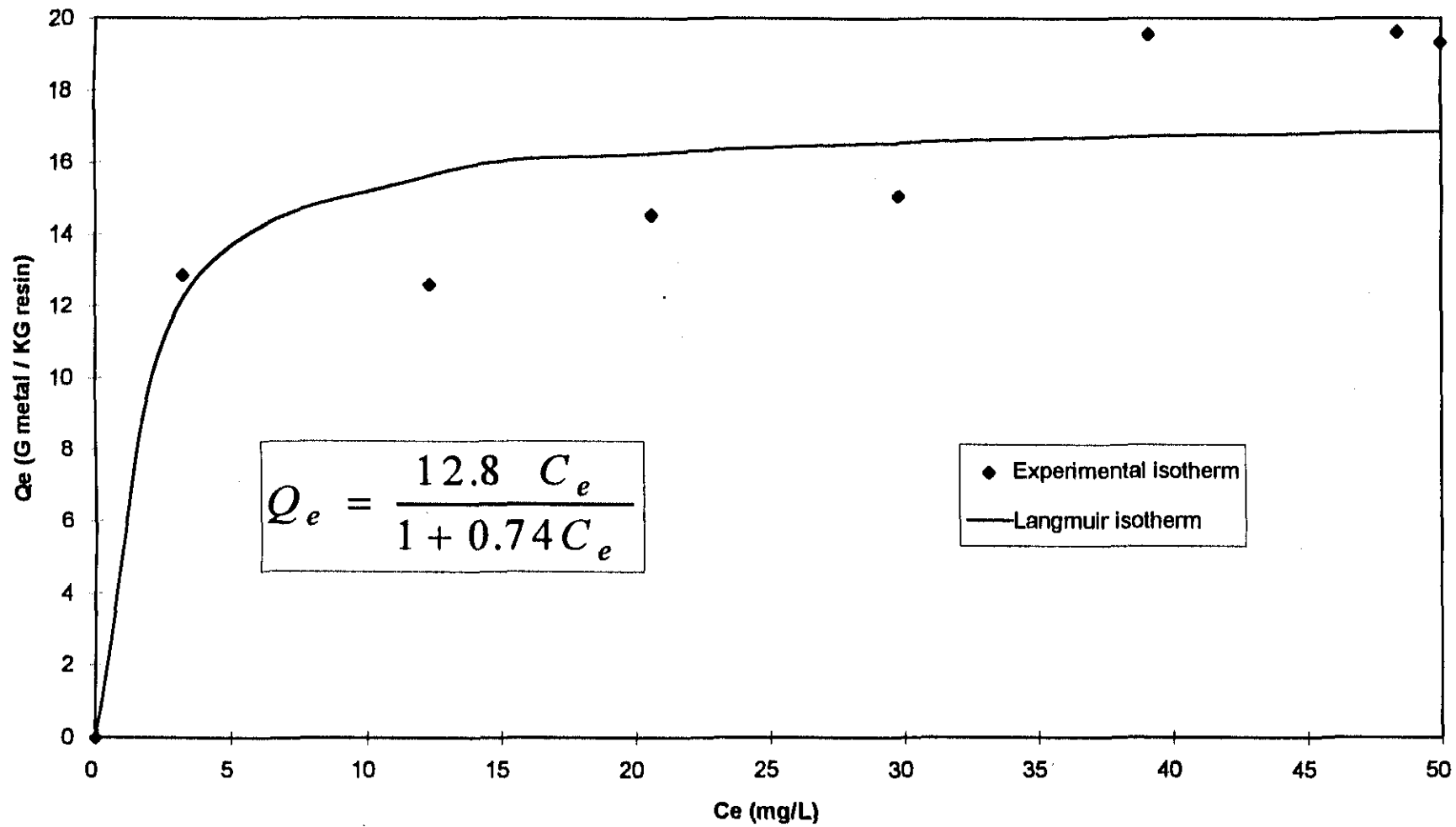


Figure 5.9 Equilibrium adsorption of zinc on AMBERLITE IRC 718.

# CHAPTER 6

## FACTORS INFLUENCING THE ADSORPTION PROCESS

In this chapter, the extent to which the adsorption of the metal cyanides onto the strong base anion exchange resin is influenced by variations in experimental conditions, were investigated. The parameters pH, temperature, initial metal concentration, ionic strength and stirring speed were varied and the effects on ion exchange kinetics and equilibrium loading were monitored.

In each figure containing the metal uptake curves, a reference “standard” adsorption curve is included as to highlight changes in the mass transfer parameters. The experimental conditions used for the tests to obtain the reference curves are given in Table 6.1. The results given in Table 6.2 quantitatively explains the observed changes in the uptake curves.

### 6.1 AGITATION

It is postulated that ion exchangers are surrounded by a “film” through which diffusion of the counter ions take place. In order to ascertain if this diffusion mechanism is significantly rate controlling, experiments were conducted at different impeller speeds.

Fleming and Cromberge (1984), tested the influence of stirring speed at different pH values, ionic strength and gold concentration on a strong base resin. They found that for each of the experimental conditions, the loading rate increased with increasing stirring speed, pointing to at least a partial contribution from film diffusion.

The results of experiments performed at a 10 ppm initial metal concentration at different stirring speeds for nickel, zinc and copper are given in Figure 6.1 to 6.3. It is clear that the stirring rate indeed has a marked influence on the rate of exchange. Table 6.2 indicates the dependence of the mass transfer coefficient ( $k_f$ ) on the stirring rates for the metal cyanide-resin interaction. This is an indication that external film transfer is indeed rate controlling to a certain extent. The values for the intraparticle diffusion coefficient ( $D$ ) remain fairly constant for all the metal extractions at the different stirring speeds.

## 6.2 INITIAL METAL CONCENTRATION

Tests were conducted by contacting the same mass of resin under similar conditions to solutions with different initial metal concentrations. The results are depicted in Figure 6.4 to 6.6. Gupta *et al*, (1987) indicated that metal cyanides reach their equilibrium sorption capacity onto most strong base anion exchange resins at a concentration of below 1 mg/L. It is thus clear that this interaction is governed by a very strong driving force, even at trace concentrations.

The zinc, copper and nickel cyanide complexes exhibited similar loading profiles for a concentration variation of 5 - 10 mg/L. It can be seen from

Table 6.3 , that both  $k_f$  and  $D$  decreases with increasing metal concentrations. These trends seem to indicate that the ion exchange rate increases as the external metal concentration decreases. A possible explanation for this phenomenon could be that at these low concentrations, the effect of the diffusional driving force is negligible, compared to other factors such as swelling of the resin beads and the effect of osmotic pressure. According to Helfferich (1995), the amount of swelling decreases with an increase in solution concentration. At higher solution concentrations the resin beads will swell to a lesser extent and this would have an influence on the uptake of solutes on the resin. However, the diffusional driving force is lower at 5 ppm than at 10 ppm, and hence the equilibrium parameter  $P$  had to be slightly adjusted to account for the slight decrease in equilibrium capacity at the lower solution concentration.

### 6.3 pH LEVELS

The metal cyanides were contacted with the resin at different pH values. The results indicated by Figures 6.7 - 6.9 show that over the pH range 8 - 12, the pH value has a negligible effect on the rate of loading and on the loading at equilibrium. The strong base resin used in this study ; AMBERLITE IRA 900, posses functional groups with fixed ion positive charges (quaternary ammonium groups).

The metal cyanide anion can displace the counter ion associated with the positively charged group and become attached to the resin by the formation of an ion pair. This reaction is not dependent on solution pH and therefore, optimum loading can be achieved at a wide pH band.

Due to the formation of the deadly HCN gas at low pH values, no effort was made to evaluate the ion exchange process at pH values below 8. However,

Fleming and Cromberge (1984), showed that the strong base resin-metal cyanide interaction is unaffected at pH values as low as 3. However, from Table 6.4, it can be seen that for zinc cyanide there is a slight increase in  $k_f$  and  $D$  as the pH increases. This trend is not repeated by the other metals.

#### 6.4 TEMPERATURE

By the use of thermally controlled waterbaths, the temperature of the metal cyanide solutions were varied from 20°C to 60°C.

The results shown in Figures 6.10 to 6.12 indicate that the rate of loading of copper, nickel and zinc cyanide increases with increasing temperature, but that equilibrium loading is only slightly affected.

As in ordinary solutions, diffusion coefficients in ion exchangers increase with increasing temperature. Thus, the mobility of the counter ions are all improved, causing a reduction in the time needed for each ion to reach an exchange site and for the displaced ion to reach the bulk liquid. Furthermore, as the temperature increases, the retarding specific or electrostatic interactions become weaker and the resin matrix relaxes, facilitating the to and fro movement of the ions, (Helfferich 1995). Table 6.5 shows that the film transfer coefficient and the intraparticle diffusional coefficient ( $D$ ) improved markedly with an increase in temperature.

## 6.5 IONIC STRENGTH

The ionic strength of the metal cyanide solutions were varied from between 0.001M to 0.1M, by the addition of a KCl solution. The results shown in Figures 6.13 to 6.15, indicate that for an ionic strength of up to 0.01M, the ion exchange process is not significantly affected. However, at 0.01M ionic strength, there is a significant decrease in equilibrium loading of all the metal complexes, with the effect on nickel cyanide, being most pronounced.

According to Fleming and Cromberge (1984), who conducted similar tests with gold cyanide, the reduction in loading capacity may be attributed to the increased competition between the metal cyanides and chlorine anions for active sites on the resin. However, since the loading capacity remained reasonably unaffected at 0.01M ionic strength, when the chlorine ions are already present in significant quantities, it can be concluded that the strong base resin remain fairly selective for the metal cyanide complexes over monovalent anions such as chlorine ions.

However, the competitive effect of the  $\text{Cl}^-$  ions also had an effect on the exchange rates. The values for  $k_f$  at a molar strength of 0.1M, are markedly lower than at 0.001M and 0.01M. As can be seen from Table 6.6, this effect was significant for all three metal complexes.

As only single component isotherms were incorporated into the kinetic model, it was necessary to adjust the equilibrium parameter  $P$  to account for the decrease in equilibrium loading of the metal cyanides due to the competitive effect of the chlorine ions.

## 6.6 EFFECT OF COMPETING IONS

Experiments were performed whereby the zinc, nickel and copper cyanides were simultaneously contacted with the strong base resin AMBERLITE IRA 900, to illustrate the competitive behaviour of these complexes. All the metals were present at a 10 mg/L initial concentration, and 0.1 grams of the resin was used.

Figure 6.16 shows the uptake curves of the different metal species and illustrates clearly that zinc cyanide is adsorbed fairly strongly onto the resin followed by nickel cyanide and copper cyanide respectively. It can be seen that all three metals reach an apparent equilibrium after 5 hours, but then deviates from this state.

The copper and nickel cyanide seem to desorb, while the zinc cyanide seem to continue to adsorb onto the resin. After about 25 hours a true equilibrium is reached. A likely explanation for this phenomenon is that the zinc cyanide displaces the adsorbed nickel and copper complexes, due to its strong affinity for the anion exchange resin.

It has been shown that small amounts of zinc cyanide in solution cause a large drop in equilibrium loading of gold cyanide. It is thus to be expected that the zinc cyanide would have a similar effect when in competition with other heavy metal complexes.

## 6.7 SUMMARY

The experimental results produced in this study coupled with the kinetic model provides a relatively good idea of how sensitive the metal cyanide-strong base resin interaction is to fluctuations in experimental conditions at dilute metal concentrations. The zinc, copper and nickel cyanides all behaved in a similar way and the following conclusions may be drawn :

- At trace concentrations, all the metal complexes exhibit a strong affinity towards the ion exchange resin.
- The ion exchange process is independent of solution pH.
- Competing ions such as  $\text{Cl}^-$  have a notable influence on equilibrium loading and ion exchange kinetics, only if present in significant quantities.
- The anion exchange resin is strongly selective towards zinc cyanide over copper and nickel cyanide, when these complexes are brought into competition with each other.

Table 6.1 Standard Conditions

	NiCN	CuCN	ZnCN
pH	8.72	11.0	11.10
Temperature	20°C	20°C	20°C
Stirring speed	300 rpm	300 rpm	300 rpm
Initial concentration	10 ppm	10 ppm	10 ppm

Table 6.2 The effect of agitation on the adsorption of nickel, copper and zinc cyanide on AMBERLITE IRA 900.

No	Adsorbate	Conditions	$k_f \times 10^5$ (m/s)	$D \times 10^{12}$ (m <sup>2</sup> /s)	P	$K_L$
A	ZnCN	180 rpm	3.3	3.4	75.5	1.21
B		300 rpm	4.7	3.9	75.5	1.21
C		440 rpm	6.5	4.2	75.5	1.21
D		standard	4.6	3.9	75.5	1.21
E	NiCN	180 rpm	3.3	4.5	177.9	2.41
F		300 rpm	4.8	4.5	177.9	2.41
G		400 rpm	6.2	4.5	177.9	2.41
H		standard	4.8	4.5	177.9	2.41
I	CuCN	170 rpm	3.7	9.8	14.3	0.17
J		310 rpm	5.8	9.0	14.3	0.17
K		440 rpm	6.0	9.0	14.3	0.17
L		standard	4.4	5.0	14.3	0.17

Table 6.3 The effect of initial metal concentration on the adsorption of zinc, nickel and copper cyanide on AMBERLITE IRA 900.

No	Adsorbate	Conditions	$k_f \times 10^5$ (m/s)	$D \times 10^{12}$ (m <sup>2</sup> /s)	P	$K_L$
A	ZnCN	5 ppm	3.8	20	72	1.21
B		8 ppm	2.6	0.28	72	1.21
C		10 ppm	2.6	0.15	72	1.21
D		standard	4.6	3.9	72	1.21
E	NiCN	5 ppm	4.6	5.0	170	2.41
F		8 ppm	4.4	1.02	170	2.41
G		10 ppm	4.4	1.0	170	2.41
H		standard	4.8	4.5	170	2.41
I	CuCN	5 ppm	6.8	90	13.0	0.17
J		8 ppm	4.2	80	13.0	0.17
K		10 ppm	3.4	90	13.0	0.17
L		standard	4.4	5.0	13.0	0.17

Table 6.4 The effect of pH levels on the adsorption of zinc, nickel and copper on AMBERLITE IRA 900.

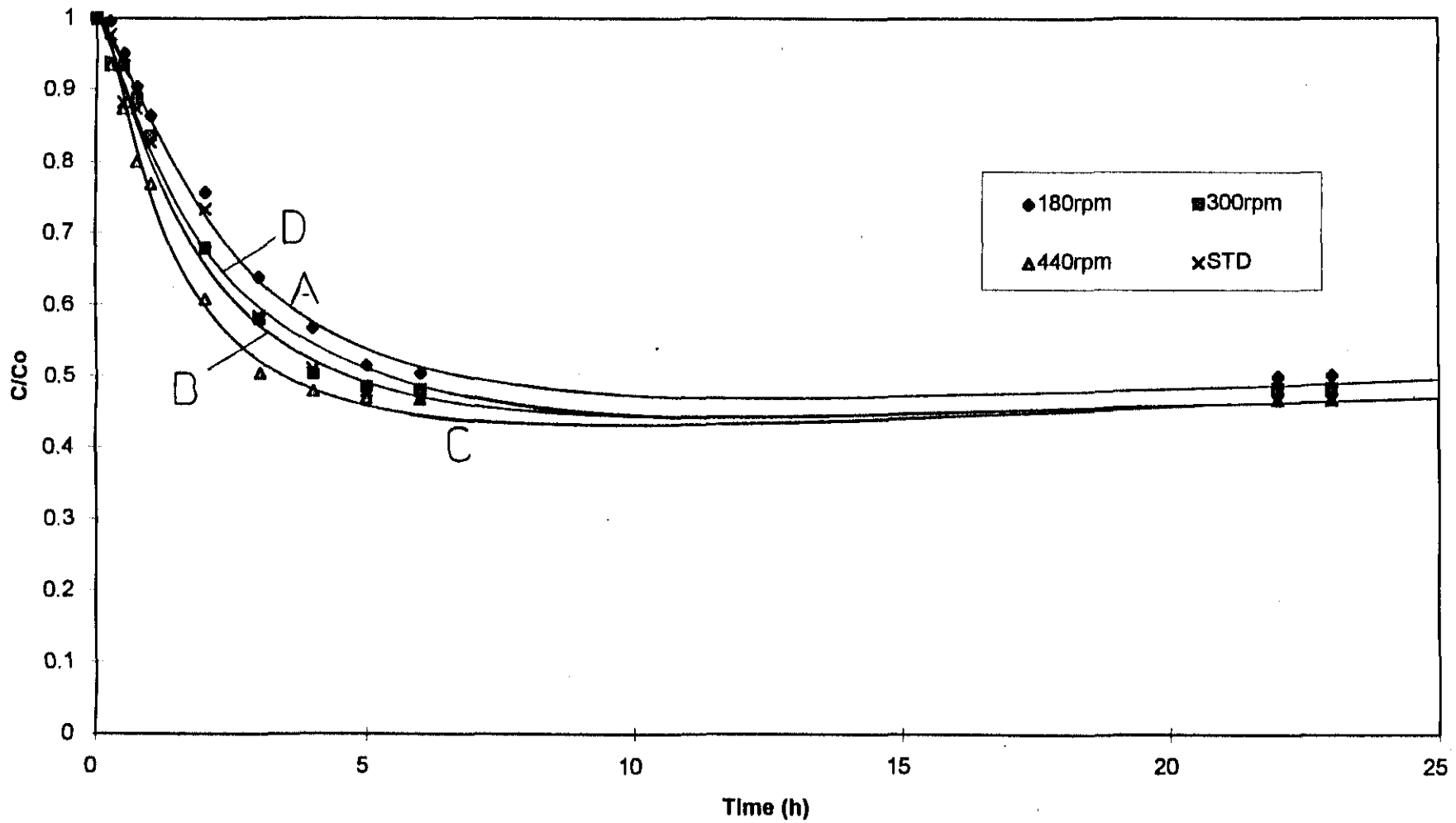
No	Adsorbate	Conditions	$k_f \times 10^5$ (m/s)	$D \times 10^{12}$ (m <sup>2</sup> /s)	P	$K_L$
A	ZnCN	pH 8	4.3	1.2	75.45	1.21
B		pH 10	4.8	2.3	75.45	1.21
C		pH 12	5.2	3.9	75.45	1.21
D		standard	4.6	3.9	75.45	1.21
E	NiCN	pH 8	4.5	5.0	177.96	2.41
F		pH 10	4.0	5.0	177.96	2.41
G		pH 12	4.0	5.2	177.96	2.41
H		standard	4.8	4.5	177.96	2.41
I	CuCN	pH 8	3.8	8.0	14.3	0.17
J		pH 10	3.8	8.0	14.3	0.17
K		pH 12	3.8	8.0	14.3	0.17
L		standard	4.4	5.0	14.3	0.17

Table 6.5 The effect of temperature on the adsorption of zinc, nickel and copper cyanide on AMBERLITE IRA 900.

No	Adsorbate	Conditions	$k_f \times 10^5$ (m/s)	$D \times 10^{12}$ (m <sup>2</sup> /s)	P	$K_L$
A	ZnCN	20°C	4.6	3.9	75.45	1.21
B		40°C	6.8	5.0	75.45	1.21
C		60°C	8.5	8.0	75.45	1.21
D		standard	4.6	3.9	75.45	1.21
E	NiCN	20°C	4.4	1.0	177.96	2.41
F		40°C	6.9	2.5	177.96	2.41
G		60°C	8.2	2.8	177.96	2.41
H		standard	4.8	4.5	177.96	2.41
I	CuCN	20°C	4.4	5.0	14.3	0.17
J		40°C	8.3	9.8	14.3	0.17
K		60°C	9.9	20	14.3	0.17
L		standard	4.4	5.0	14.3	0.17

Table 6.6 The effect of ionic strength on the adsorption of zinc, nickel and copper on AMBERLITE IRA 900.

No	Adsorbate	Conditions	$k_f \times 10^5$ (m/s)	$D \times 10^{12}$ (m <sup>2</sup> /s)	P	$K_L$
A	ZnCN	0.001 M	5.3	6.8	60	1.21
B		0.01 M	5.2	6.8	60	1.21
C		0.1 M	4.0	4.2	60	1.21
D		standard	4.5	3.9	60	1.21
E	NiCN	0.001 M	5.6	7.0	140	2.41
F		0.01 M	5.6	7.5	140	2.41
G		0.1 M	4.3	2.3	140	2.41
H		standard	4.8	4.5	140	2.41
I	CuCN	0.001 M	4.9	8.0	11	0.17
J		0.01 M	4.8	8.0	11	0.17
K		0.1 M	3.8	7.0	11	0.17
L		standard	4.4	5.0	11	0.17



**FIGURE 6.1** Adsorption profile of zinc cyanide onto AMBERLITE IRA 900 at different stirring speeds.  
 ( $C_0 = 10 \text{ ppm}$  ;  $m = 0.101 \text{ g}$  ;  $V = 1.0 \text{ L}$  )

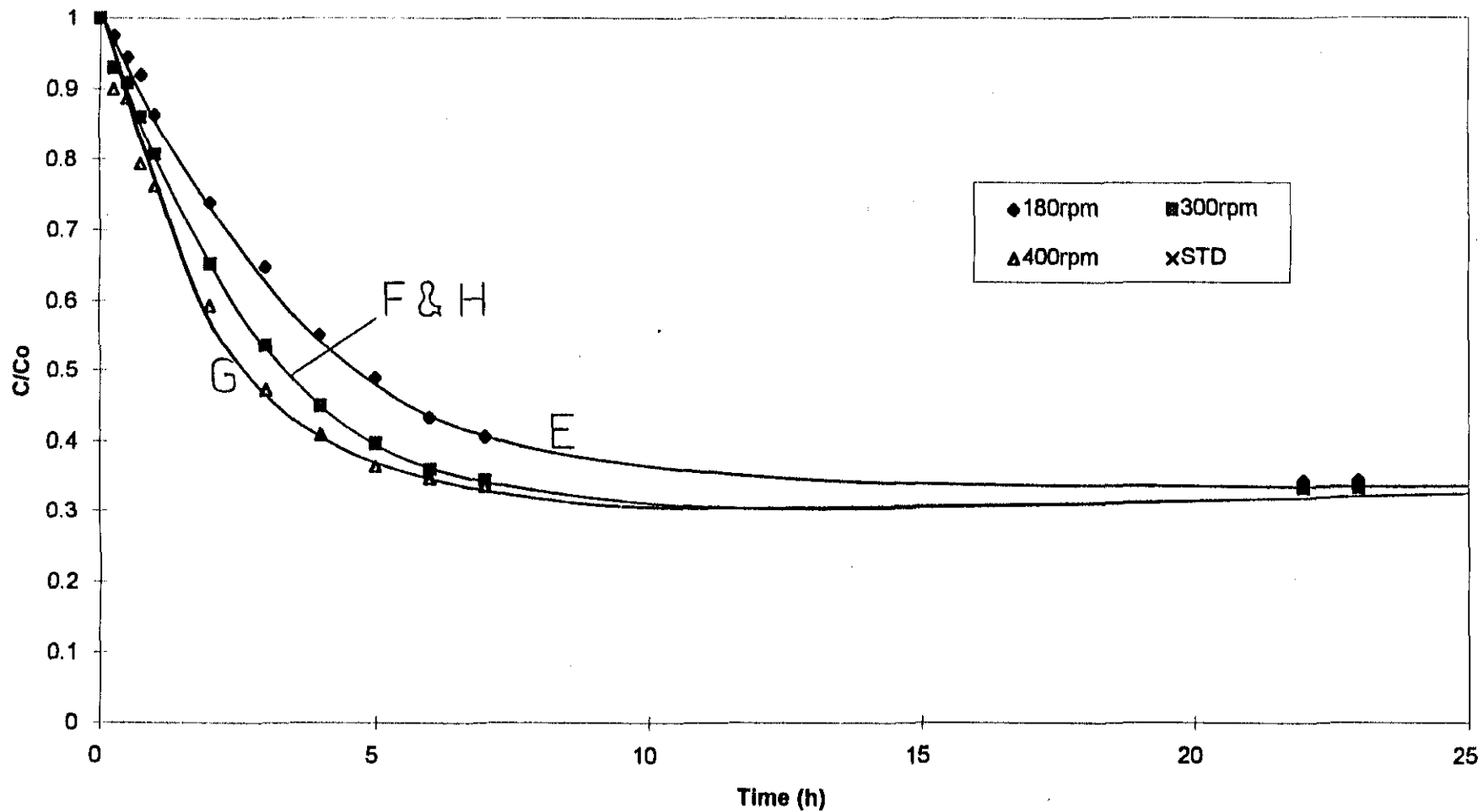
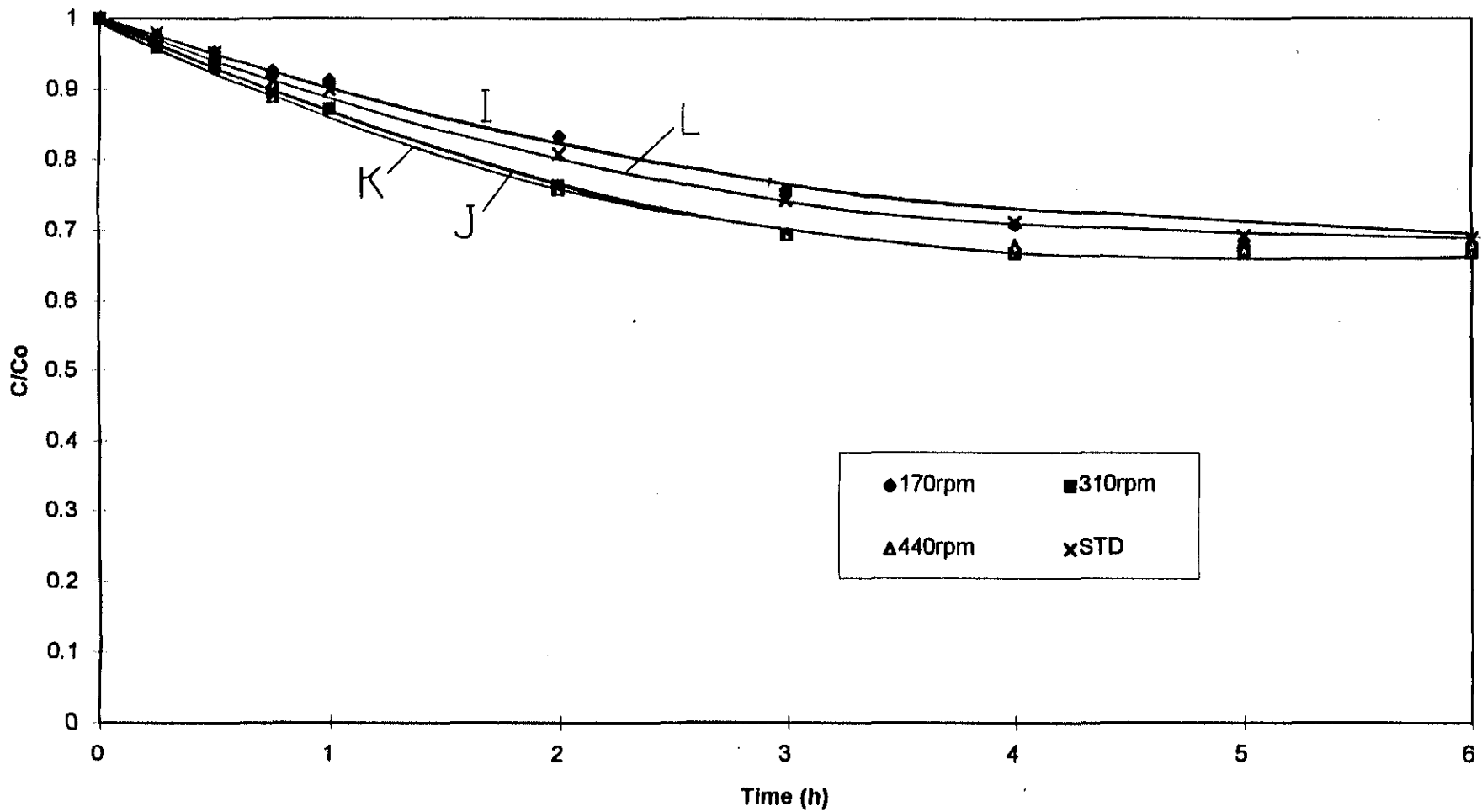
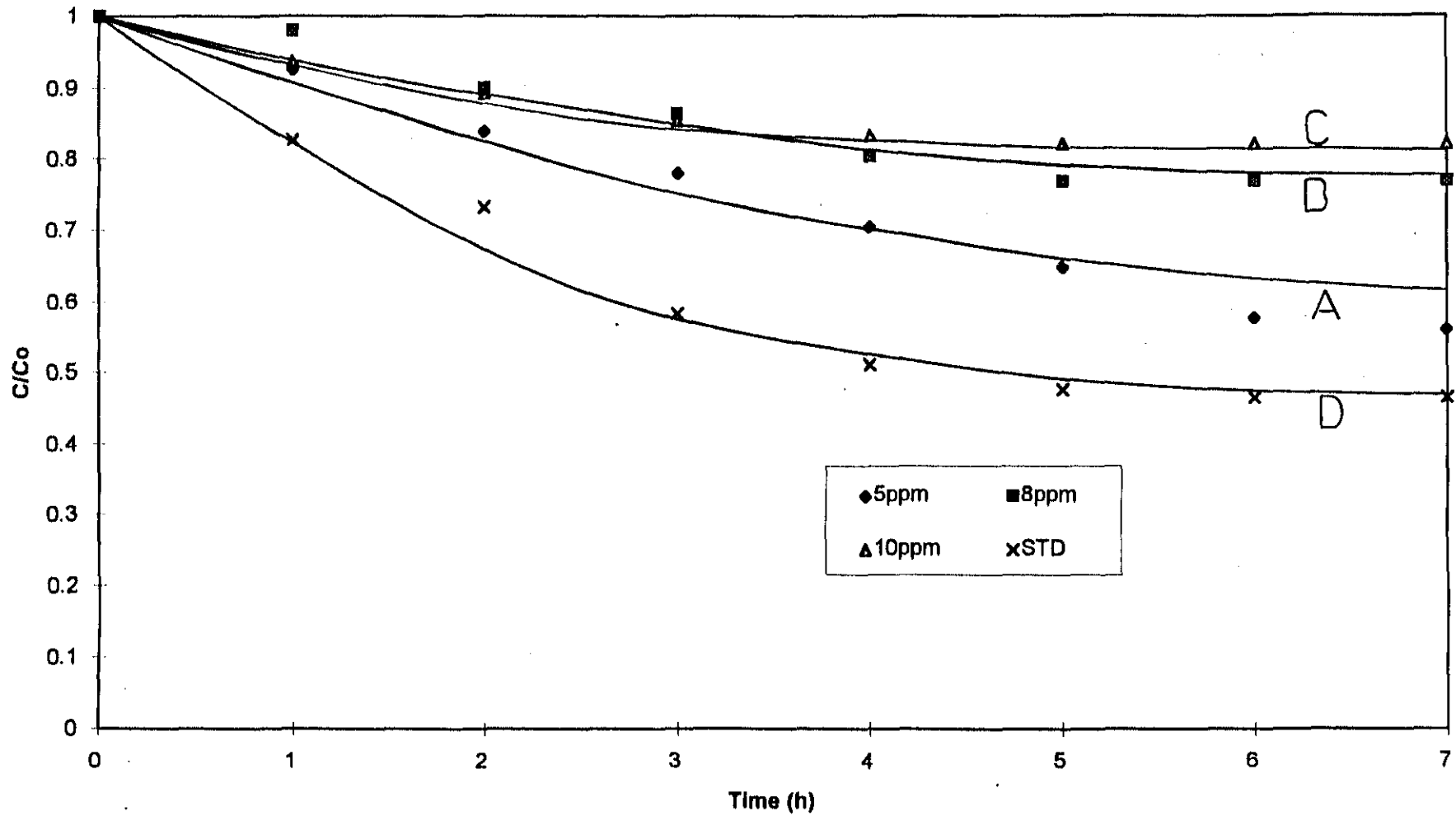


FIGURE 6.2 Adsorption profile of nickel cyanide onto AMBERLITE IRA 900 at different stirring speeds. ( $C_o = 10$  ppm ;  $m = 0.10$  g ;  $V = 1.0$  L )



**FIGURE 6.3 Adsorption profile of copper cyanide onto AMBERLITE IRA 900 at different stirring speeds. ( $C_0 = 10$  ppm ;  $m = 0.07$ g ;  $V = 1.0$  L )**



**FIGURE 6.4 Adsorption profile of zinc cyanide onto AMBERLITE IRA 900 at different initial metal concentrations. (  $V = 1.0$  L ;  $m = 0.054$ g ;  $N = 300$ rpm )**

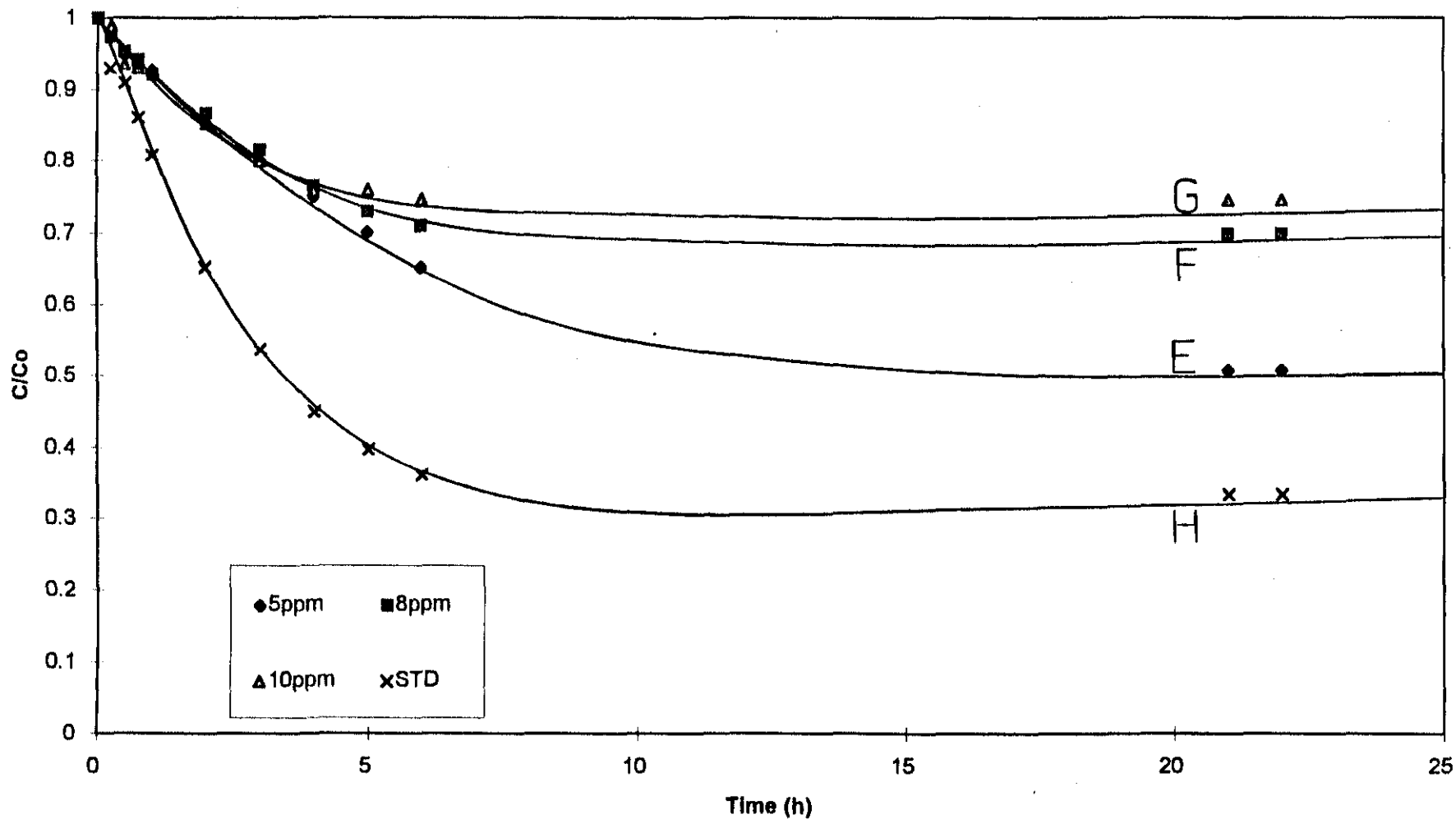


**FIGURE 6.5** Adsorption profile of nickel cyanide onto AMBERLITE IRA 900 at different initial metal concentrations. (V = 1.0 L ; m = 0.04g ; N = 300 rpm )

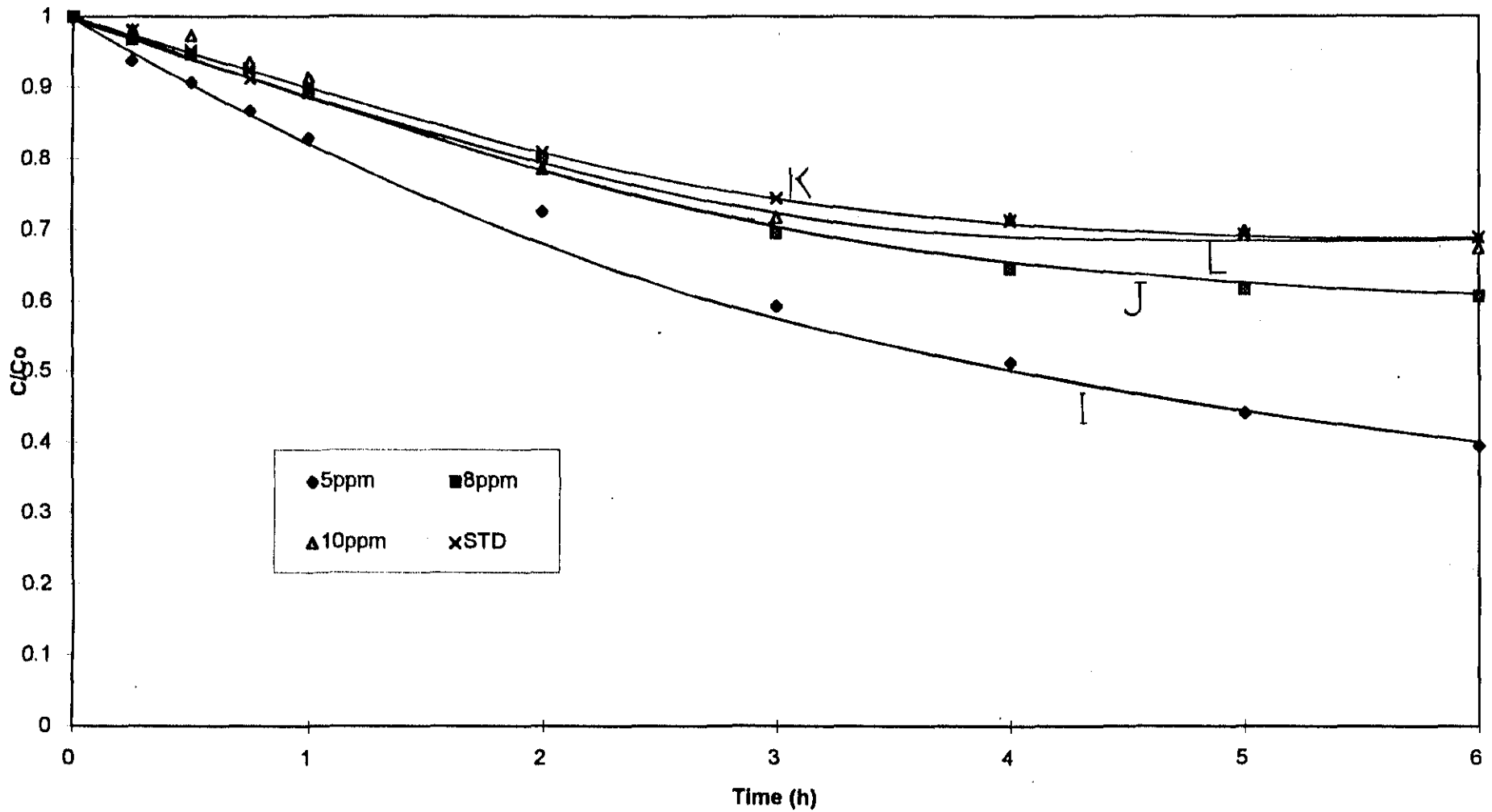


**FIGURE 6.6 Adsorption profile of copper cyanide onto AMBERLITE IRA 900 at different initial metal concentrations. (  $V = 1.0 \text{ L}$  ;  $m = 0.045\text{g}$  ;  $N = 300\text{rpm}$  )**

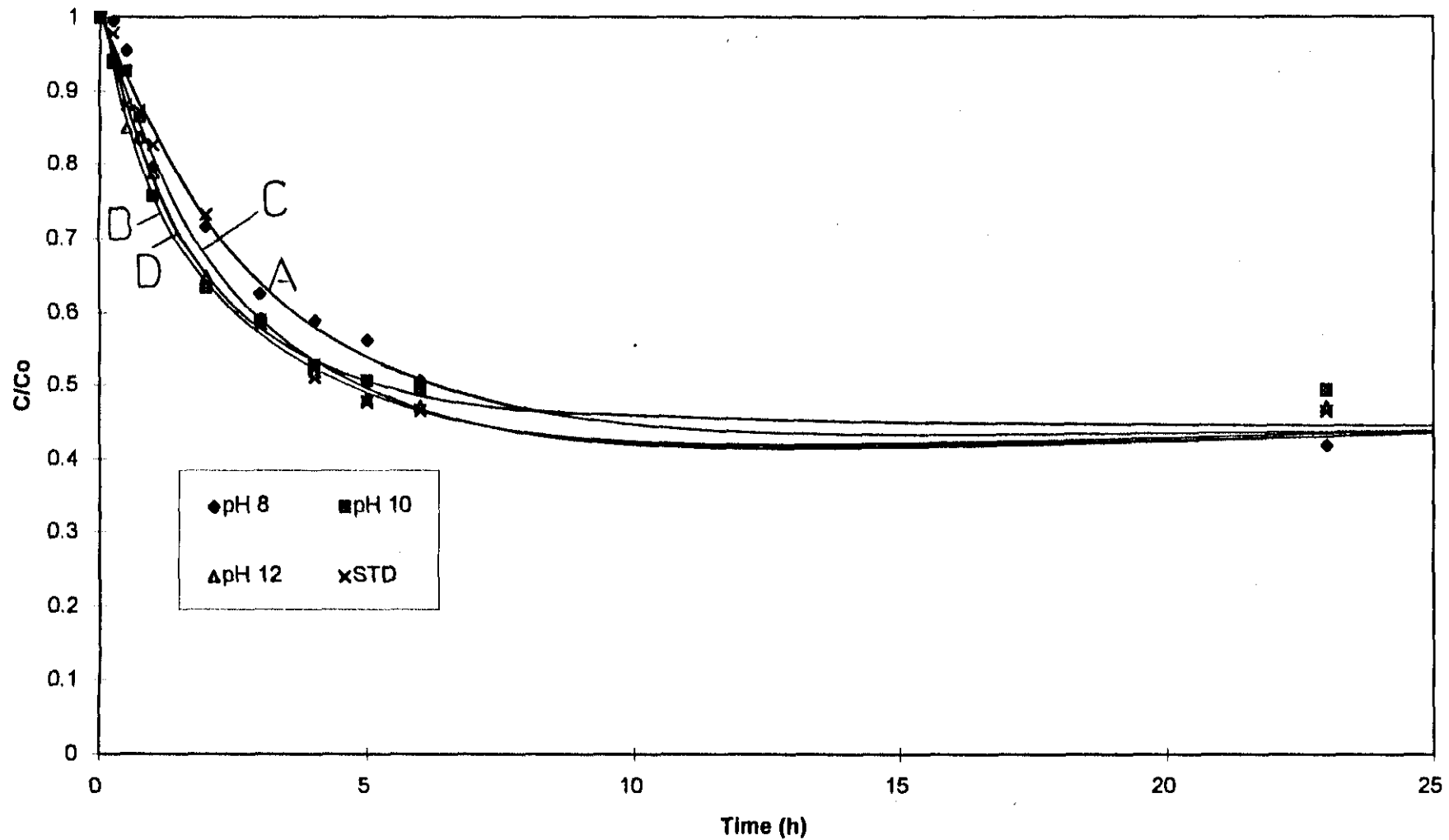
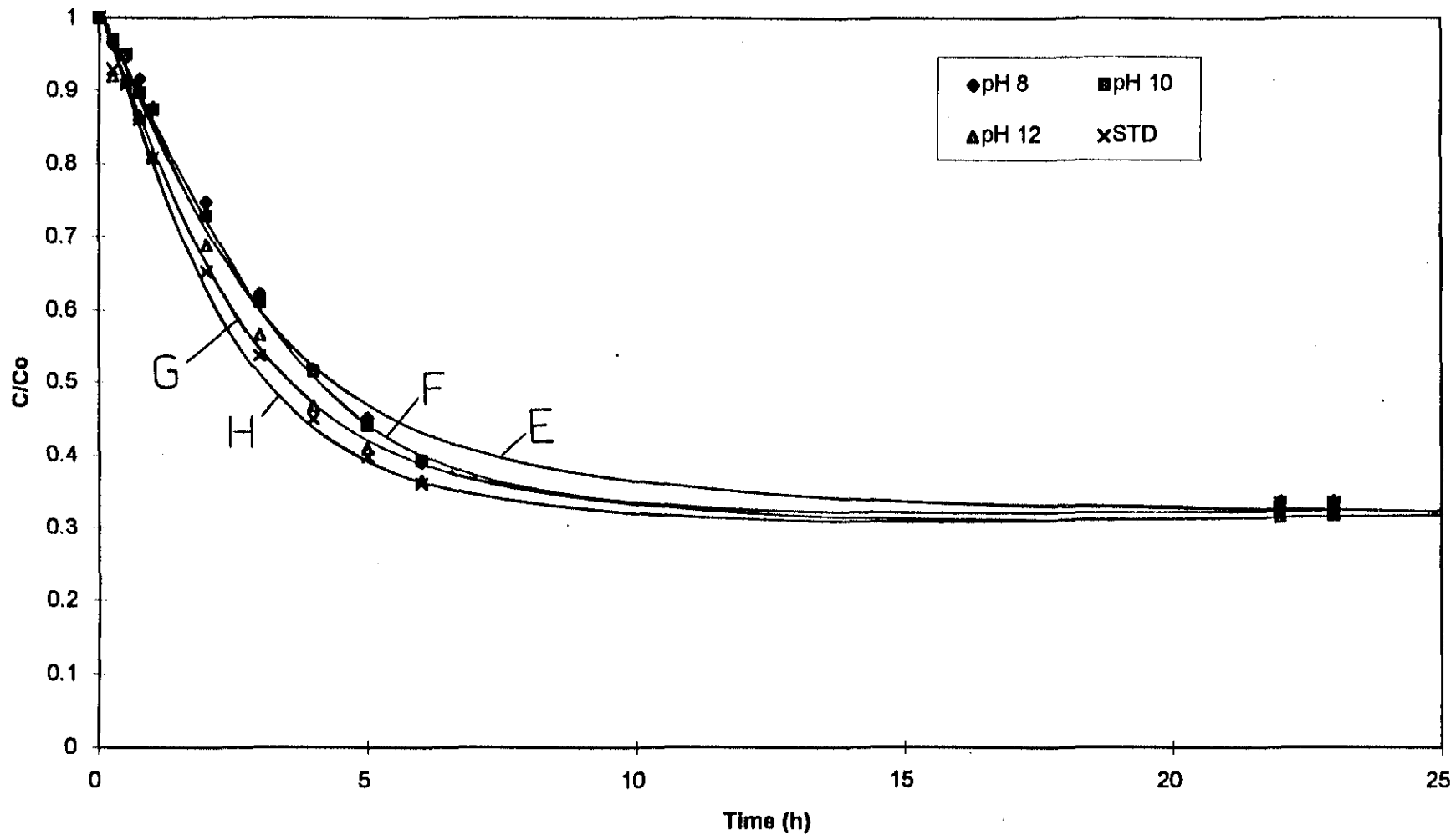
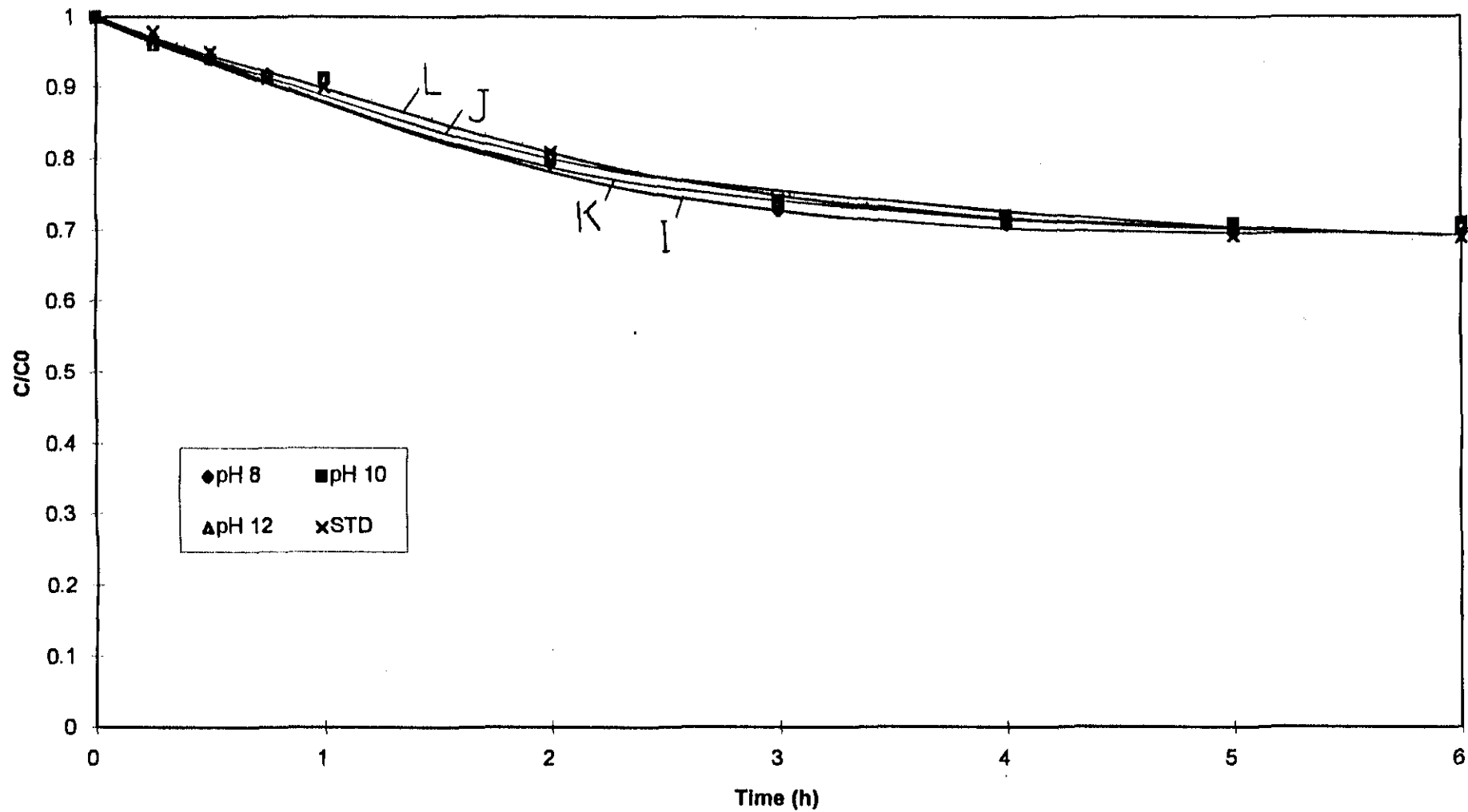


FIGURE 6.7 Adsorption profile of zinc cyanide onto AMBERLITE IRA 900 at different pH values. (  $V = 1.0 \text{ L}$  ;  $m = 0.101 \text{ g}$  ;  $N = 300 \text{ rpm}$  )



**FIGURE 6.8** Adsorption profile of nickel cyanide onto AMBERLITE IRA 900 at different pH values.  
 (  $V = 1.0 \text{ L}$  ;  $m = 0.101\text{g}$  ;  $N = 300\text{rpm}$  )



**FIGURE 6.9** Adsorption profile of copper cyanide onto AMBERLITE IRA 900 at different pH values.  
 (  $V = 1.0 \text{ L}$  ;  $m = 0.07 \text{ g}$  ;  $N = 300 \text{ rpm}$  )

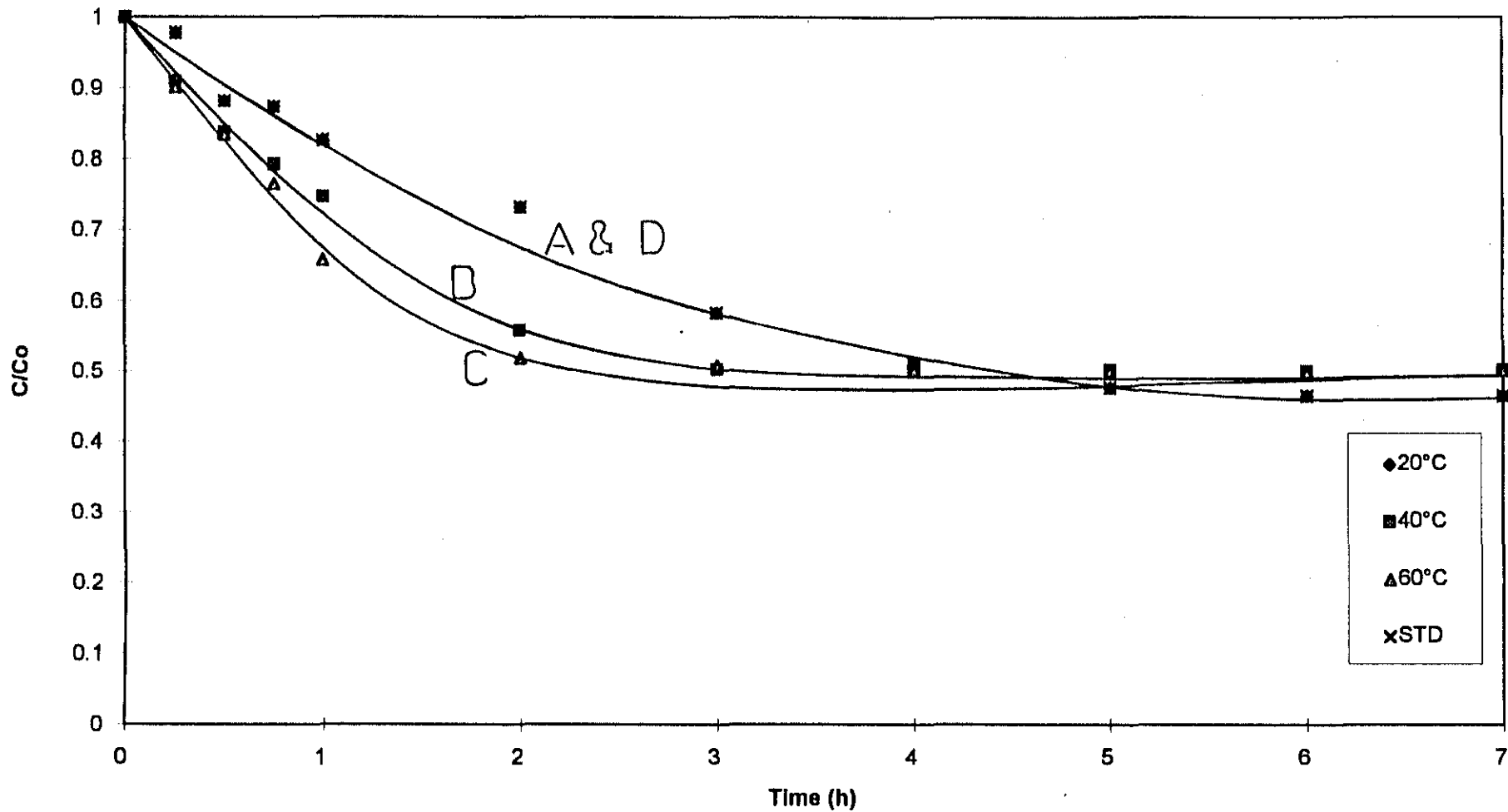


FIGURE 6.10 Adsorption profile of zinc cyanide onto AMBERLITE IRA 900 at different solution temperatures. (  $C_0 = 10$  ppm ;  $V=1.0$  L ;  $m = 0.1$ g ;  $N = 300$ rpm )

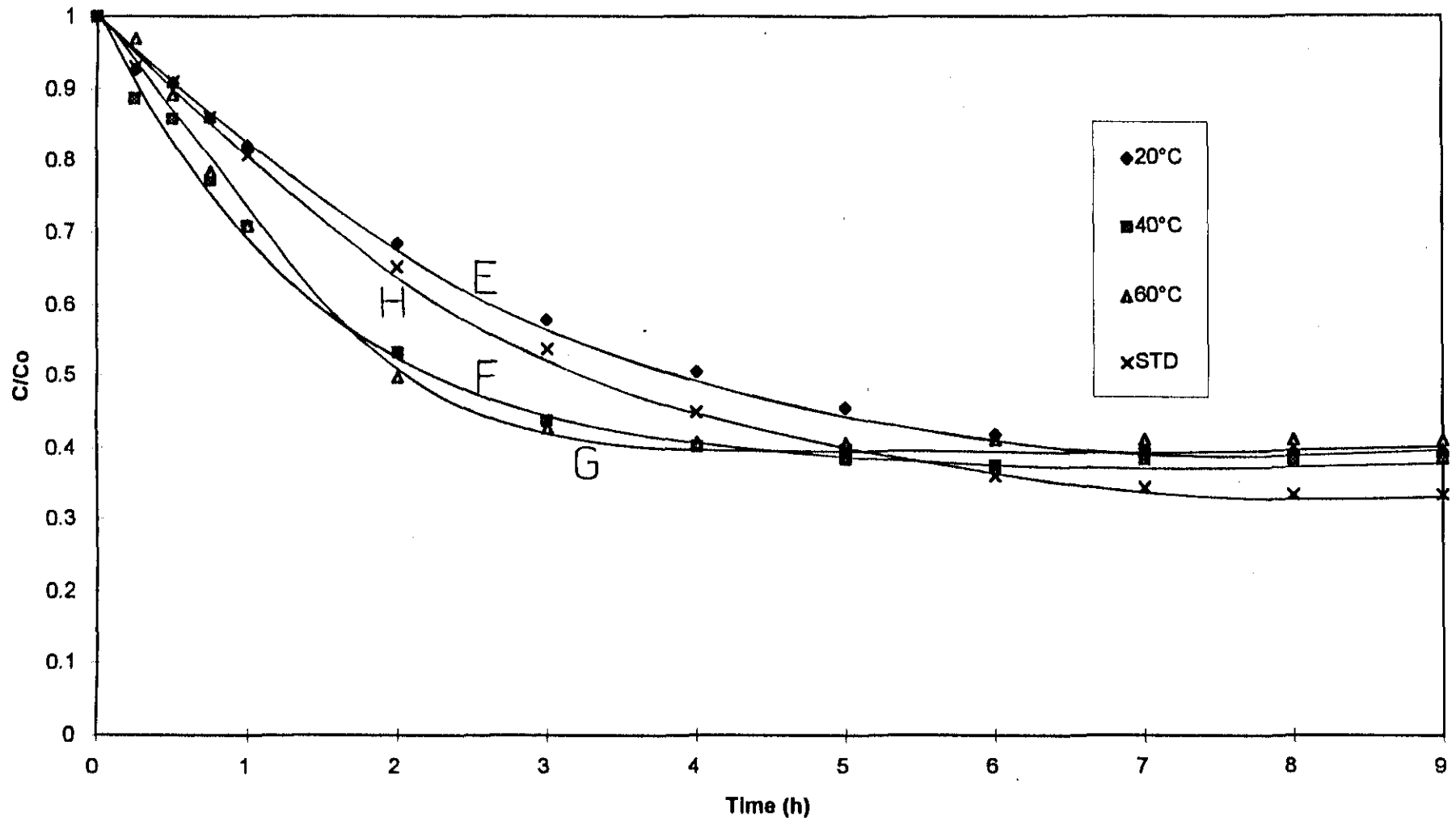


FIGURE 6.11 Adsorption profile of nickel cyanide onto AMBERLITE IRA 900 at different solution temperatures. (  $C_o = 10$  ppm ;  $V = 1.0$  L ;  $m = 0.1$ g ;  $N = 300$ rpm )

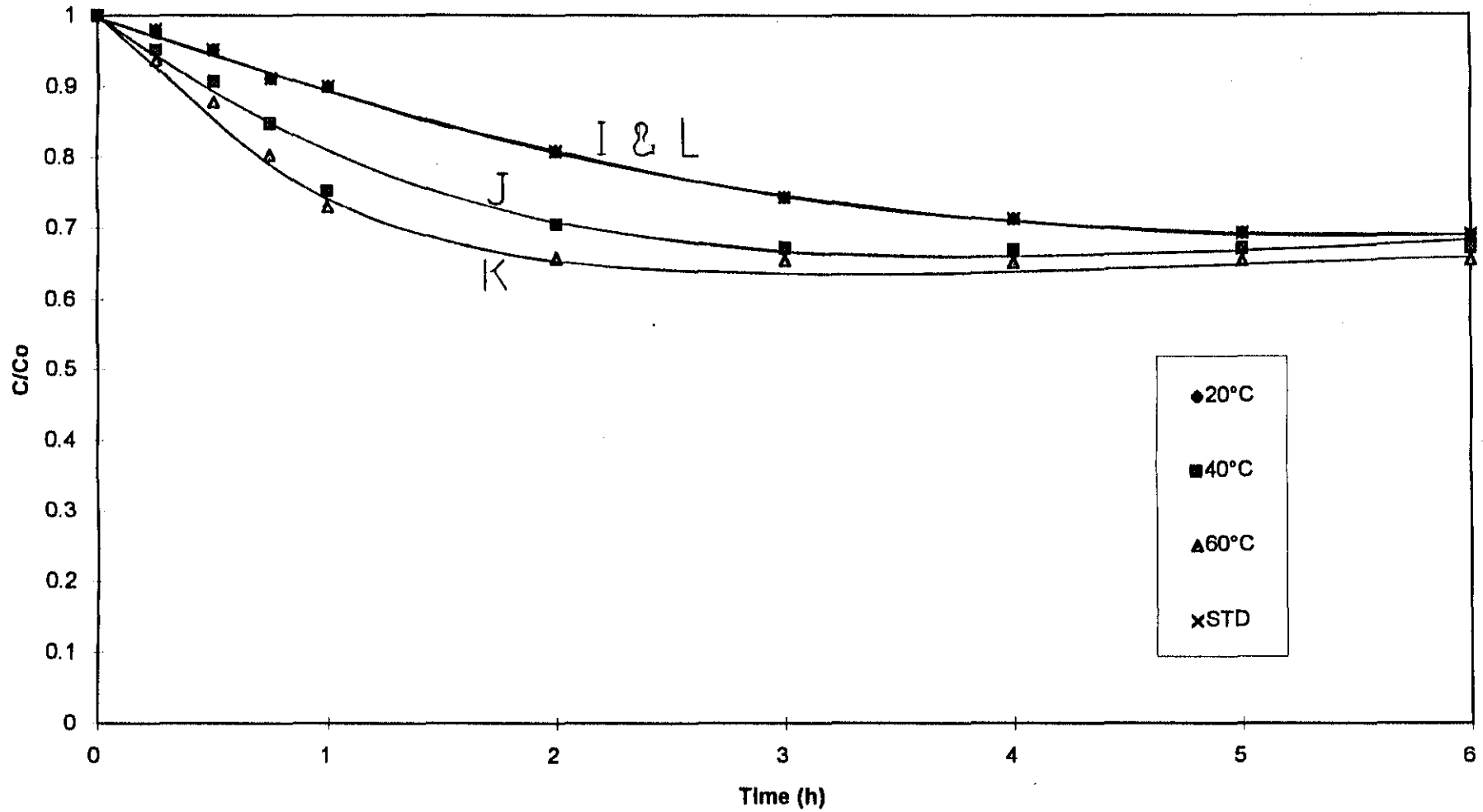


FIGURE 6.12 Adsorption profile of copper cyanide onto AMBERLITE IRA 900 at different solution temperatures. ( $C_0 = 10$  ppm ;  $V = 1.0$  L ;  $m = 0.07$ g ;  $N = 300$ rpm )

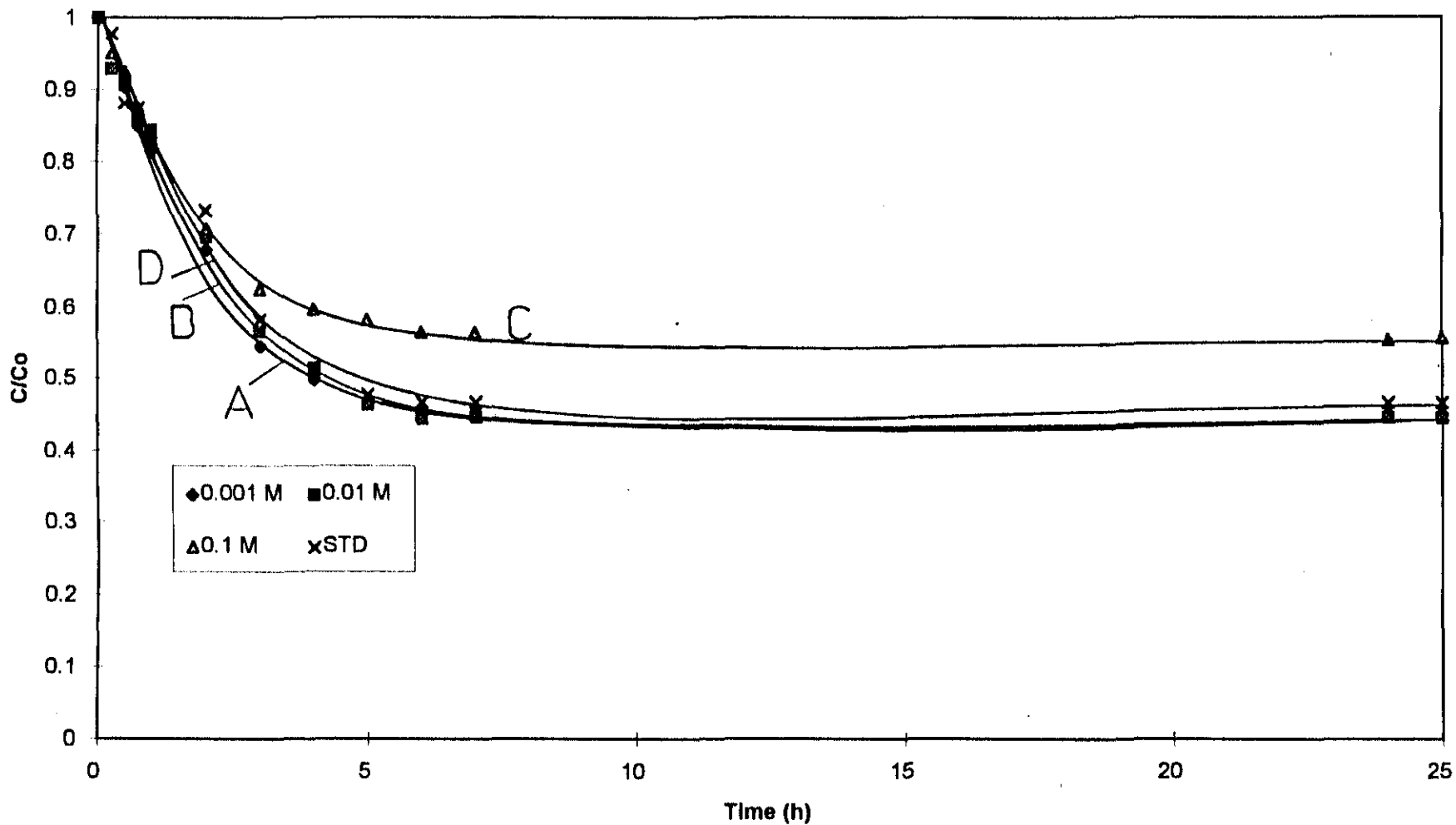


FIGURE 6.13 Adsorption profile of zinc cyanide onto AMBERLITE IRA 900 under various ionic strengths. (  $V = 1.0 \text{ L}$  ;  $m = 0.101 \text{ g}$  ;  $N = 300 \text{ rpm}$  )

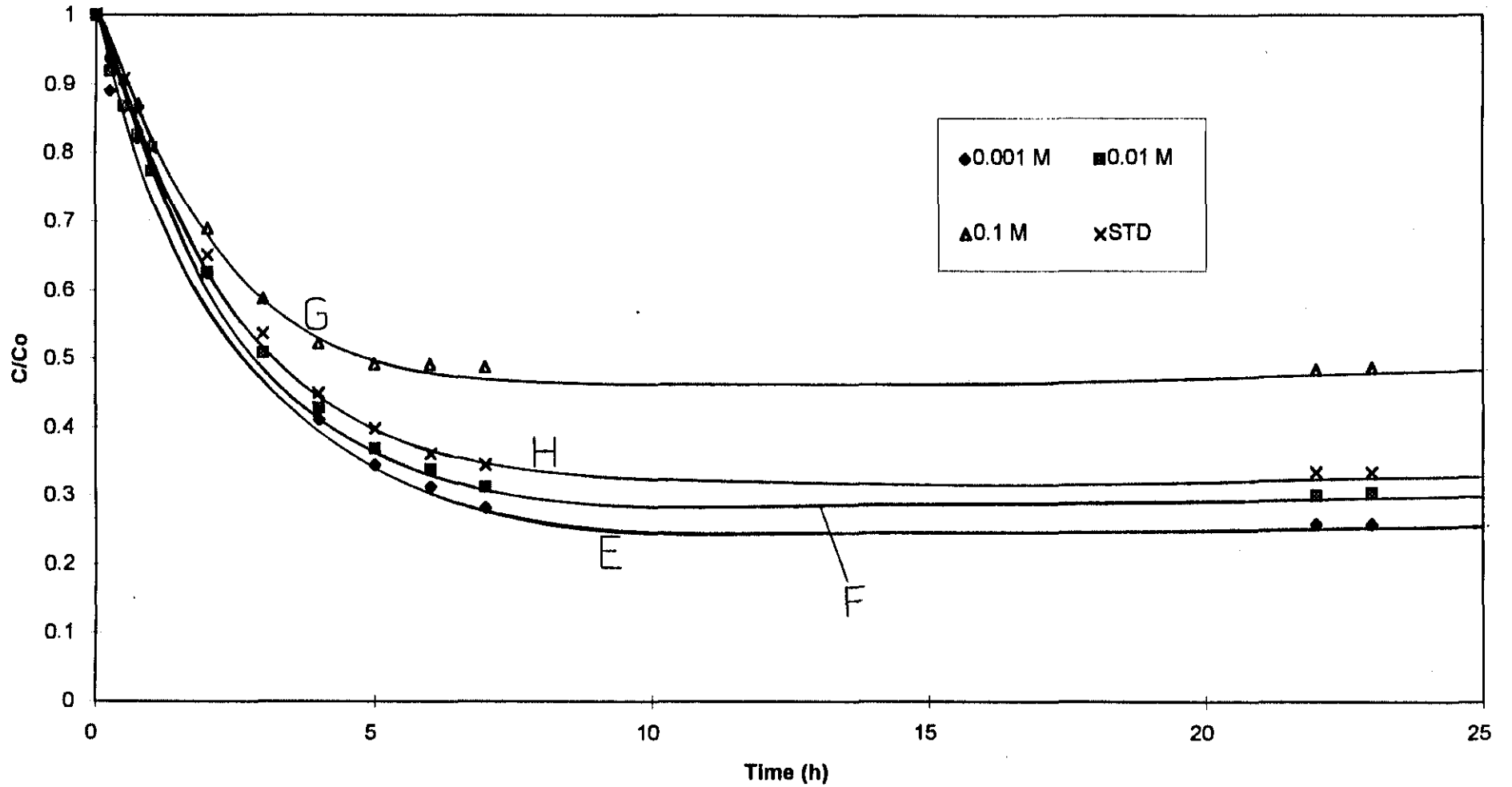


FIGURE 6.14 Adsorption profile of nickel cyanide onto AMBERLITE IRA 900 under different ionic strengths. (  $V = 1.0 \text{ L}$  ;  $m = 0.105\text{g}$  ;  $N = 300\text{rpm}$  )

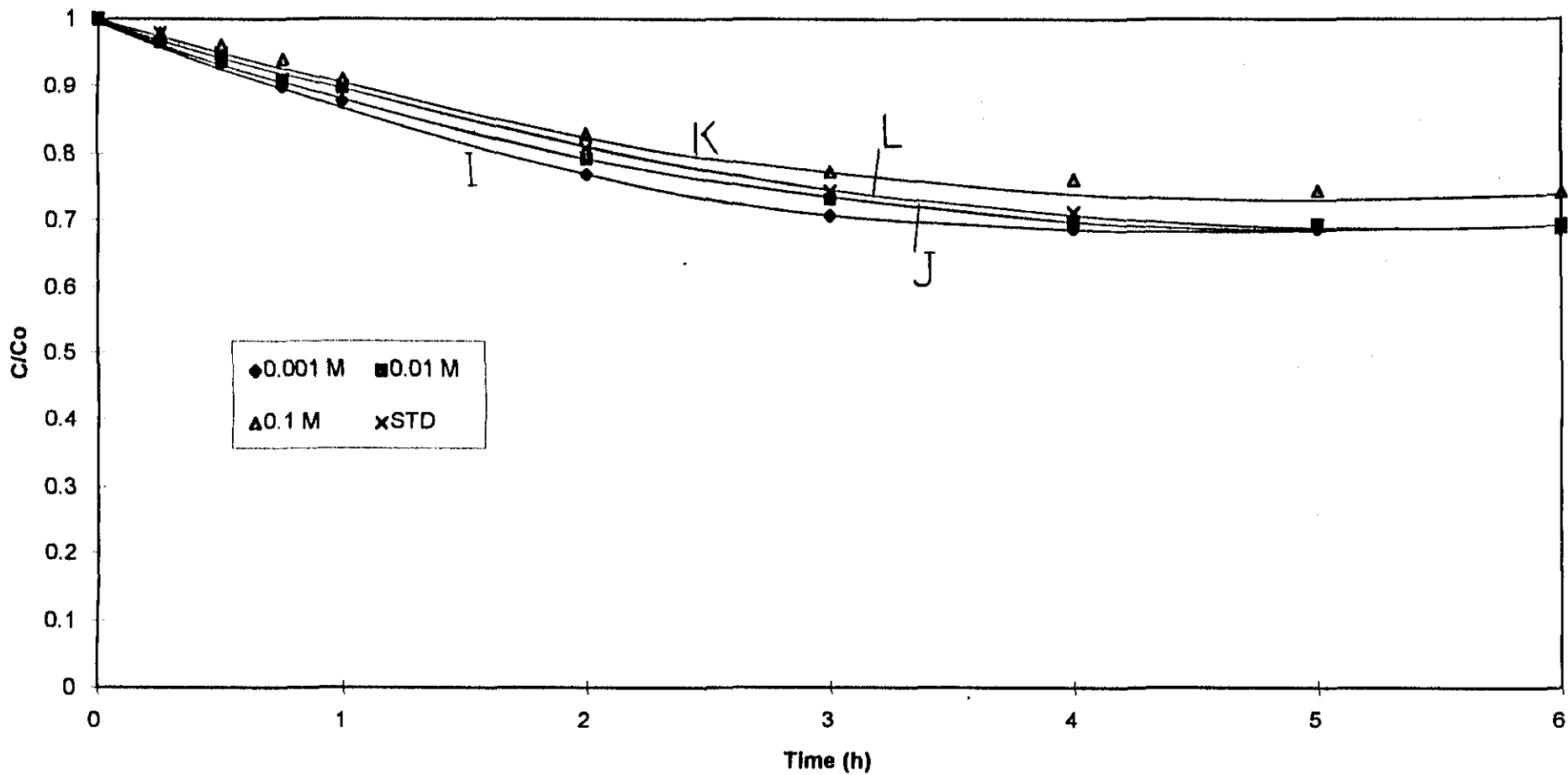


FIGURE 6.15 Adsorption profile of copper cyanide onto AMBERLITE IRA 900 at different ionic strengths. (  $V = 1.0$  L ;  $m = 0.07$ g ;  $N = 300$ rpm )

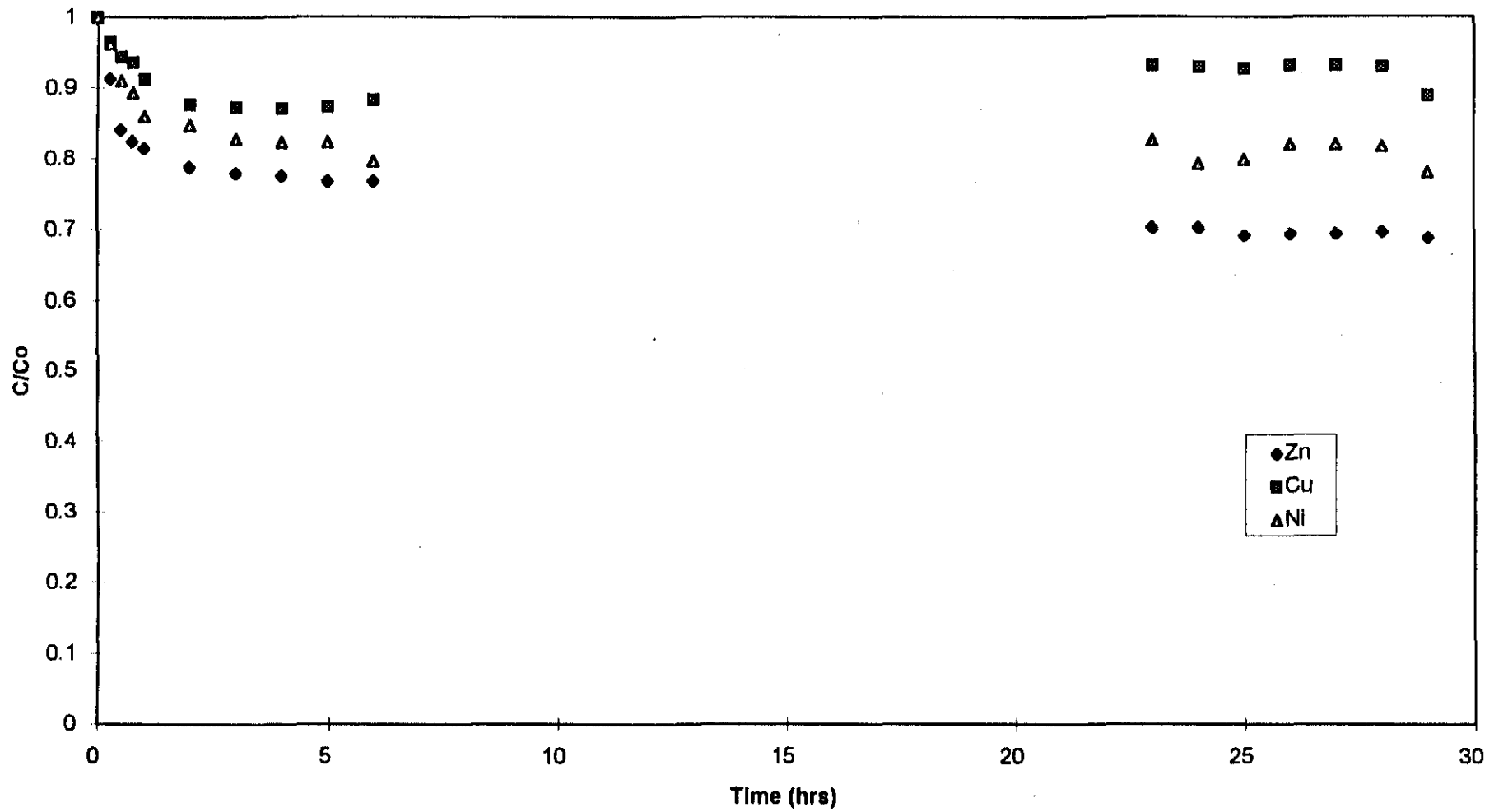


Figure 6.16 The competitive uptake curves of zinc, copper and nickel cyanide adsorption onto AMBERLITE IRA 900

# CHAPTER 7

## COMPARATIVE PERFORMANCE OF CHELATING AND CATION EXCHANGE RESINS

Chelating resins are widely used for the separation and preconcentration of metal ions particularly from complicated matrices, where high amounts of interfering ions are present. By complexation of the metal ions a high level of selectivity is achieved, which makes the use of these resins much more attractive than conventional cation exchange resins. However, in choosing a resin for a particular process, a variety of factors are taken into consideration, such as ion exchange kinetics, loading and resin durability.

In order to evaluate the extraction performance with respect to heavy metals, a comparative study was performed between the resins AMBERLITE IRC 718 and AMBERLITE 252H.

### 7.1 MONOMETALLIC CURVES

Adsorptive tests were performed whereby dilute solutions of cupric sulphate, nickel nitrate and zinc nitrate of no more than 2 ppm initial metal concentration were contacted with the strong acid cation exchange resin AMBERLITE 252H, in batch stirred tank reactors. The uptake curves for all metals are given in Figure 7.1, and the kinetic model data in Table 7.1.

Similar tests were performed on the chelating resin AMBERLITE IRC 718 and the resulting uptake curves are given in Figure 7.2.

The kinetic model, as explained in Chapter 3, could not be applied to the adsorption profiles of the metals on the chelating resin, as this model does not take into account the swelling effects or the effect of internal pH and since swelling is more pronounced at these low concentrations (2ppm initial concentration) and due to the low crosslinking of the resin, (Helfferich 1995), it leads to huge discrepancies between the experimental and the predicted values. At higher initial metal concentrations, however, the model did fit the experimental values.

Analysis of the graphs in Figures 7.1 and 7.2, show that at these low metal concentrations both ion exchange process exhibit similar kinetics. In fact the rate of loading on the chelating resin was slightly higher than the rate of loading on the cation exchange resin, with ion exchange equilibrium reached at 20 and 24 hours respectively. However, independent tests proved that the cation exchange rate improved considerably with an increase in initial metal concentration, while the chelating reaction accompanied-ion exchange process, exhibited slow kinetics even at much higher metal concentrations.

It would thus seem as if the uptake rates of ions on the chelating resin are independent of external solution concentration and that the chelating reactions are solely rate controlling. However, according to Yoshida *et al* (1986), this process is in fact diffusion controlled, although it is influenced by the chelating reaction. Through their experimental work, they found that for chelating resin particles of radius greater than  $10^{-4}$  m, reaction resistance

can be neglected, and reaction retarded intraparticle diffusion is rate controlling.

The reaction retarded diffusion effect is explained by Liberti and Helfferich (1983). Although the chelating reaction occurs faster than diffusion, it is binding ions on whose diffusion ion exchange depends. Such binding of ions to fixed sites inhibits their diffusion and therefore slows the exchange rate. The rate then is controlled by (slow) diffusion which, in turn, is affected by the equilibrium of the (fast) reaction.

In spite of the retarding effects of the chelate reaction, the chelating resin outperformed the cation exchange resin in terms of ion exchange kinetics.

This is probably due to the following factors :

- Due to the low initial metal concentrations, the diffusional driving force is significantly reduced, leading to slow kinetics and rendering the reaction retardation effects to be negligible.
- If it is assumed that reaction retardation is negligible, the ion exchange rate would then be greatly dependent on the structure and particle size of the resin beads.
- AMBERLITE IRC 718 and 252H share a macroreticular styrene-divinylbenzene structure, but the chelating resin is crosslinked to a lower extent, which would aid interdiffusion of ions.
- Both processes are diffusion controlled, and therefore exchange rates would depend on particle size. Although most of the finer sizes were removed from the chelating resin beads, it would still have a smaller effective particle size, which would lead to faster kinetics.

Although similar masses of cation and chelating resin were used, the equilibrium loading values for the cation exchange resin proved to be higher than the values for the chelating resin, except in the case of copper, which proved to have a high affinity for the chelating resin.

## 7.2 MULTIMETALLIC CURVES

### 7.2.1 Competitive ion exchange on AMBERLITE 252H

These experiments were performed with copper, nickel and zinc as competing ions in solution. These metals were made up to a 2mg/L initial concentration and then contacted with the cation exchange resin in a batch stirred tank reactor. The results obtained indicate that there is no significant order of preference for loading of the metals used in this study on cation exchange resin.

Figure 7.3 shows that although nickel and zinc adsorbed at a faster rate, all three metals reached similar loading states. However, a comparison with the monometallic curves is necessary in order to appreciate the extent of the reduction in loading due to the effect of competing ions.

Figures 7.4 to 7.6 show the uptake curves dealt with in section 7.1 in comparison to the multimetallic curves. It can be seen from Table 7.2, where the percentage reduction is representative of the reduction in equilibrium loading of each metal due to the influence of competing ions, that the cation exchange resin prefers zinc, followed by nickel and copper. AMBERLITE 252H is a conventional cation exchange resin and thus the selectivity it exhibits towards the metals, would depend on the properties of the metal

ions, specifically (valencies, activities etc.). However, there is no marked difference in the percentages ( % reduction ranged from 24 to 29 %) and the resin could be seen as being non-selective.

### 7.2.2 Competitive ion exchange on AMBERLITE IRC 718

The curves shown in Figure 7.2 indicate that the chelating resin adsorbs the metals in the order  $\text{Cu} > \text{Ni} > \text{Zn}$ . However, These results are for monometallic solutions, with no interfering cations. From Figure 7.7 it can be seen that this selectivity is greatly enhanced when the metals are present as competing cations. In order to properly illustrate this selectivity, a comparison was made between the monometallic and multimetallic loading. From Table 7.2, it can be seen that the chelating resin, strongly prefers copper followed by nickel and zinc. In competition with nickel and zinc, the loading of copper is reduced by just 31.8 % whereas nickel and zinc loadings are reduced by 62.4 % and 70.9 % respectively. Figures 7.8 to 7.10 graphically show a comparison between the monometallic and multimetallic curves.

The affinity of metal ions to a conventional resin like AMBERLITE 252H depend mainly on factors such as the size of ion, its charge, or other physical properties. The affinity of metal ions for chelating resins however, depend on the complexation characteristics. According to Pesavento *et al* (1993) the affinity of heavy metals for chelating resins and subsequent selectivity exhibited during competitive ion exchange is dependent on the strength of the chelate bond formed with two metal ions.

The strength of the bond formed, gives an indication as to what type of mechanism is followed during sorption. The latter authors determined the complexation constants for the complexes formed between zinc, nickel and copper and a chelating resin. They obtained the following results :

Metal	Log $\beta$
zinc	- 3.60
nickel	- 2.90
copper	- 0.75

They concluded that when metal ions are sorbed on the chelating resin, the chelation mechanism by iminodiacetate clearly prevails if strong complexes are formed, as in the case for copper and nickel, while complexation by carboxylate prevails when metal ions with a lower complexation constant with the iminodiacetate, such as zinc are involved.

### 7.3 DURABILITY TESTS

In order to ascertain whether the degree of crosslinkage of the chelating resin would lead to a marked loss in mechanical strength, the chelating resin was put under extreme physical stress by contact with a coarse, inert sand slurry. These tests were performed in stirred tank reactors at a high stirring speed. After being exposed to the slurry for 72 hours, the resin was separated from the slurry and used in adsorption tests with a solution of cupric sulphate.

The same mass of untreated resin was also contacted with a solution of cupric sulphate of exactly the same concentration as for the above test.

Figure 7.11 shows the uptake curves for copper ions on both the treated and untreated resin. It is clear from the curves that the resin which was contacted with the slurry, slightly lost its ability to adsorb the heavy metal. Moreover, both the kinetics and equilibrium loading were negatively affected. Figures 7.12 and 7.13 are electron micrographs of the external surface of the resin, before and after treatment with the slurry.

Tests were also performed whereby the cation exchange resin was contacted with the slurry by exactly the same procedure. The results for the comparative adsorption test on this resin are given in Figure 7.14. From these curves, it can be seen that the cation exchange resin also slightly lost its ability to adsorb the heavy metal. A likely explanation could be that the effects of the slurry causes a loss in external surface of the resin. The metal ions thus encounter less functional groups on the external surface. From the electron micrographs it can be seen that after treatment with the slurry, the resin surface seems to have deteriorated, which could explain the reduced adsorptive capacity of the resin.

#### 7.4 APPLICATION OF THE KINETIC MODEL

By fitting the kinetic model to the curves in Figure 7.11, the parameters  $\beta$  and  $\delta$ , as introduced in Chapter 3, were evaluated. The curve for the sand treated chelating resin yielded values of 0.99 and 0.93 for  $\beta$  and  $\delta$  respectively, as can be seen from Table 7.3. As explained in Chapter 3, these values indicate a negative effect on both ion exchange kinetics and loading, although the effects on kinetics could be seen as being negligible. It is also clear from a comparison of values obtained for  $k_f$  and  $D$  with the

corresponding values for the untreated resin, that there is indeed no inhibition on the rate of mass transfer.

For the cation exchange resin, the parameters  $\beta$  and  $\delta$  yielded values of 0.99 and 0.88 respectively. From these results it can be seen that the chelating and cation exchange resins are of comparable mechanical strength in spite of the lower degree of crosslinkage of the chelating resin.

## 7.5 REAL MINING LEACHATE

An oxidised mining ore containing the metals, copper, zinc and lead in significant quantities, was leached, in a 1 L batch reactor at a high stirring speed, and with 2 % sulphuric acid as the leaching agent. The solid and liquid phases were separated by the use of vacuum filtration in a Buchner type apparatus. The leaching reaction for an oxidised copper ore may be described as follows : (Habashi, 1980)



Adsorptive tests were then performed on the cation exchange resin, using the clear leachate. In parallel to these tests, tests were performed, using the same mass of resin in a synthetic cupric sulphate solution. It can be seen from Figure 7.15 that the copper from the leachate loaded rapidly onto the resin, but analysis of the equilibrium data revealed that the copper loading from the leachate was all of 66 % less than loading from the synthetic cupric sulphate solution. It is thus clear that competing cations in the leachate, severely inhibited the adsorption of copper ions.

Due to the acidic nature of the leachate, an assessment for the adsorptive performance of the chelating resin could not be made.

Table 7.1 The adsorption of zinc, copper and nickel on AMBERLITE 252 H

no.	Adsorbate	Conditions	$K_f \times 10^5$ (m/s)	$D \times 10^{12}$ (m <sup>2</sup> /s)	P	$K_L$
A	Zn	Co = 2 ppm	4.2	4.8	180.18	2.25
B	Cu	Co = 2 ppm	4.8	3.0	185.57	2.28
C	Ni	Co = 2 ppm	3.6	2.0	79.25	1.00

Table 7.2 Comparison of monometallic and multimetallic loading

## AMBERLITE IRC 718

	Monometallic loading (mg/g)	Multimetallic loading (mg/g)	% Reduction**
Zn	29.87	8.68	70.94
Cu	40.58	27.67	31.83
Ni	30.28	11.38	62.42

$$\text{** \% Reduction} = \frac{\text{monometallic} - \text{multimetallic loading}}{\text{monometallic loading}} \times 100$$

## AMBERLITE 252 H

	Monometallic loading (mg/g)	Multimetallic loading (mg/g)	% Reduction**
Zn	41.56	31.27	24.76
Cu	36.96	26.18	29.17
Ni	36.43	27.17	25.42

Table 7.3 The effect of the sand slurry on AMBERLITE 252 H and AMBERLITE IRC 718.

AMBERLITE IRC 718

No	Adsorbate	Conditions	$k_f \times 10^5$ (m/s)	$D \times 10^{12}$ (m <sup>2</sup> /s)	$\delta$	$\beta$
A	Cu	Untreated	0.78	0.7	1	1
B	Cu	Treated	0.77	0.7	0.99	0.93

AMBERLITE 252 H

No	Adsorbate	Conditions	$k_f \times 10^5$ (m/s)	$D \times 10^{12}$ (m <sup>2</sup> /s)	$\delta$	$\beta$
A	Cu	Untreated	5.0	6.8	1	1
B	Cu	Treated	4.8	6.7	0.99	0.88

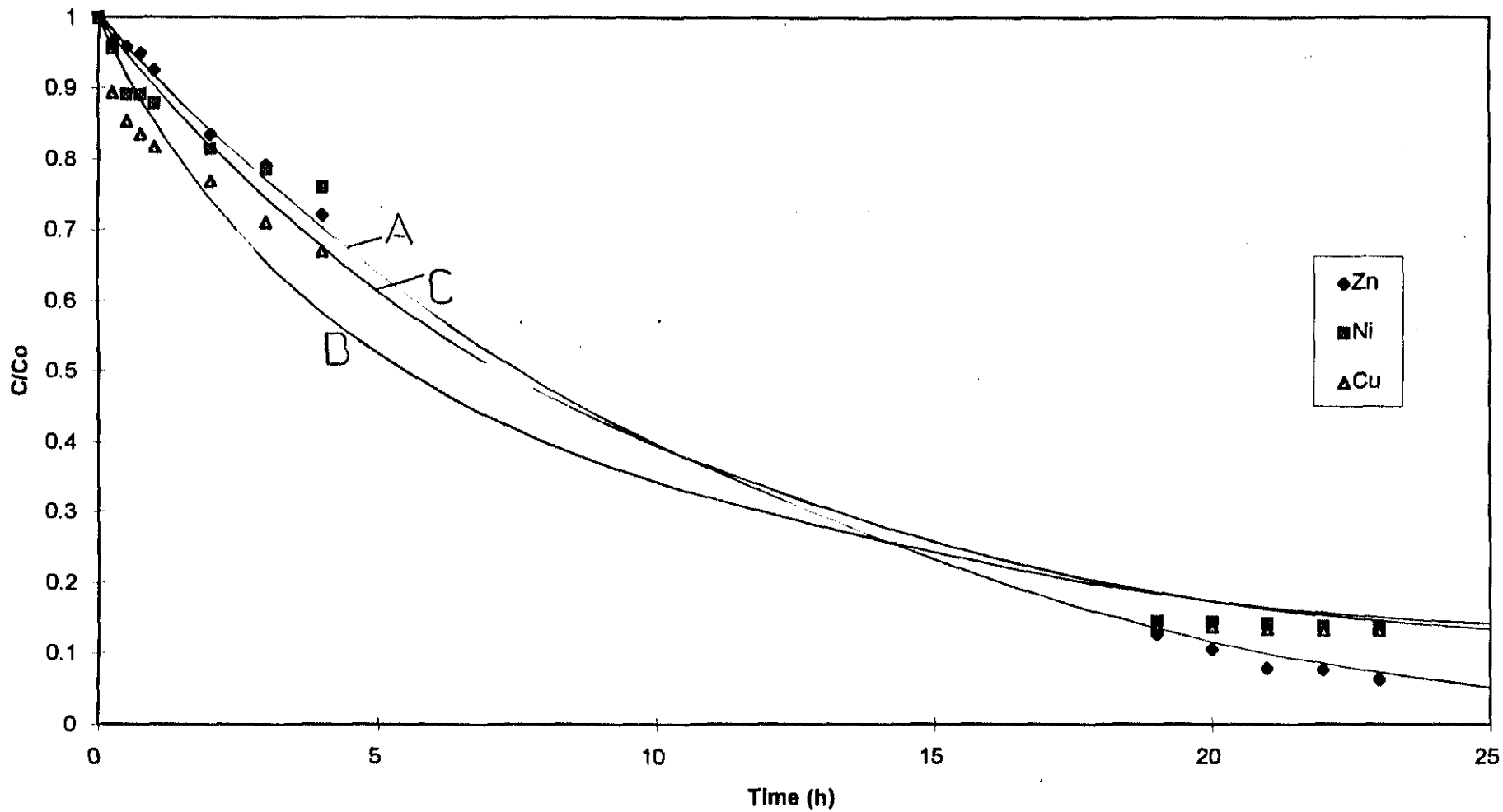
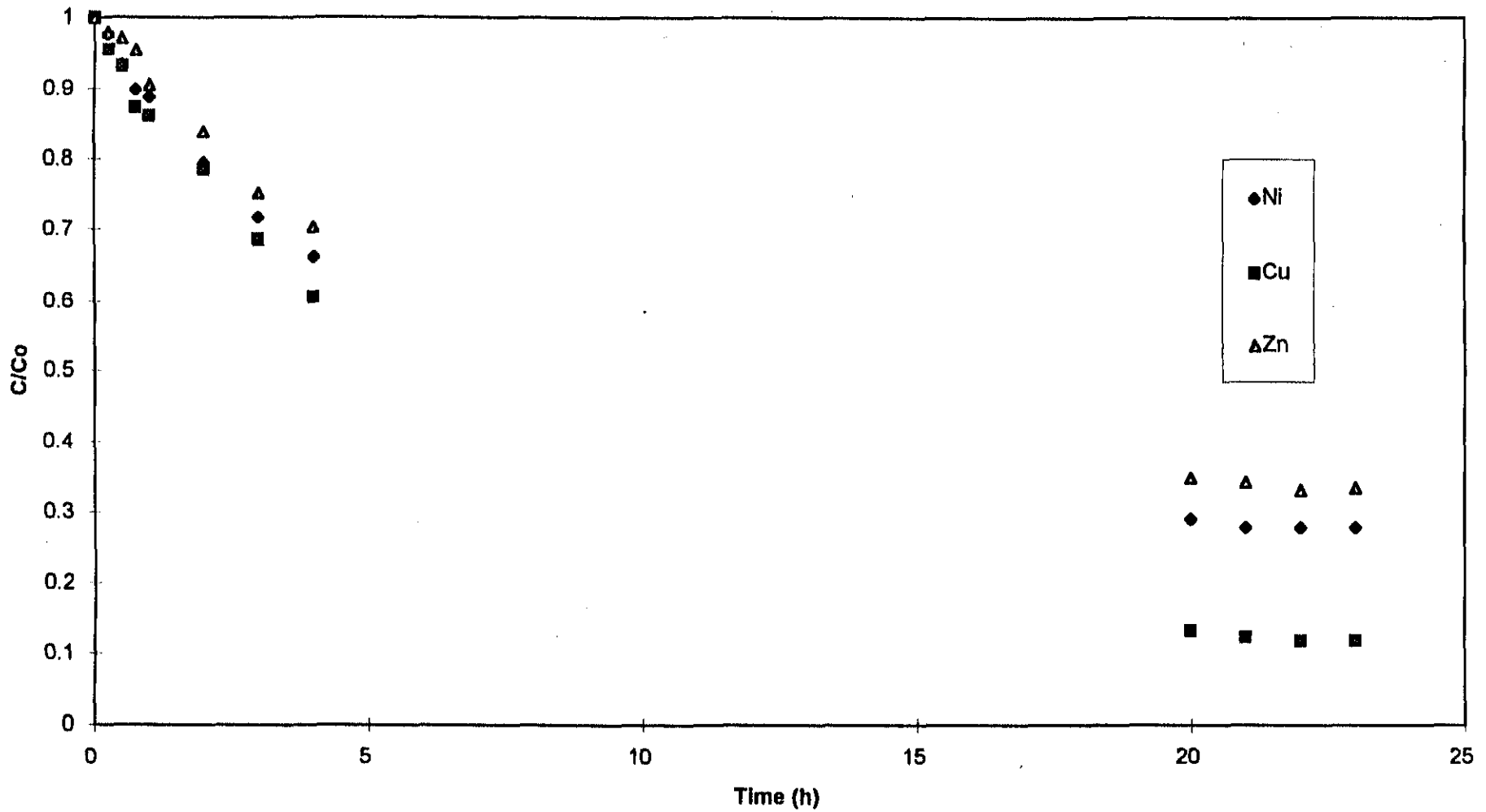
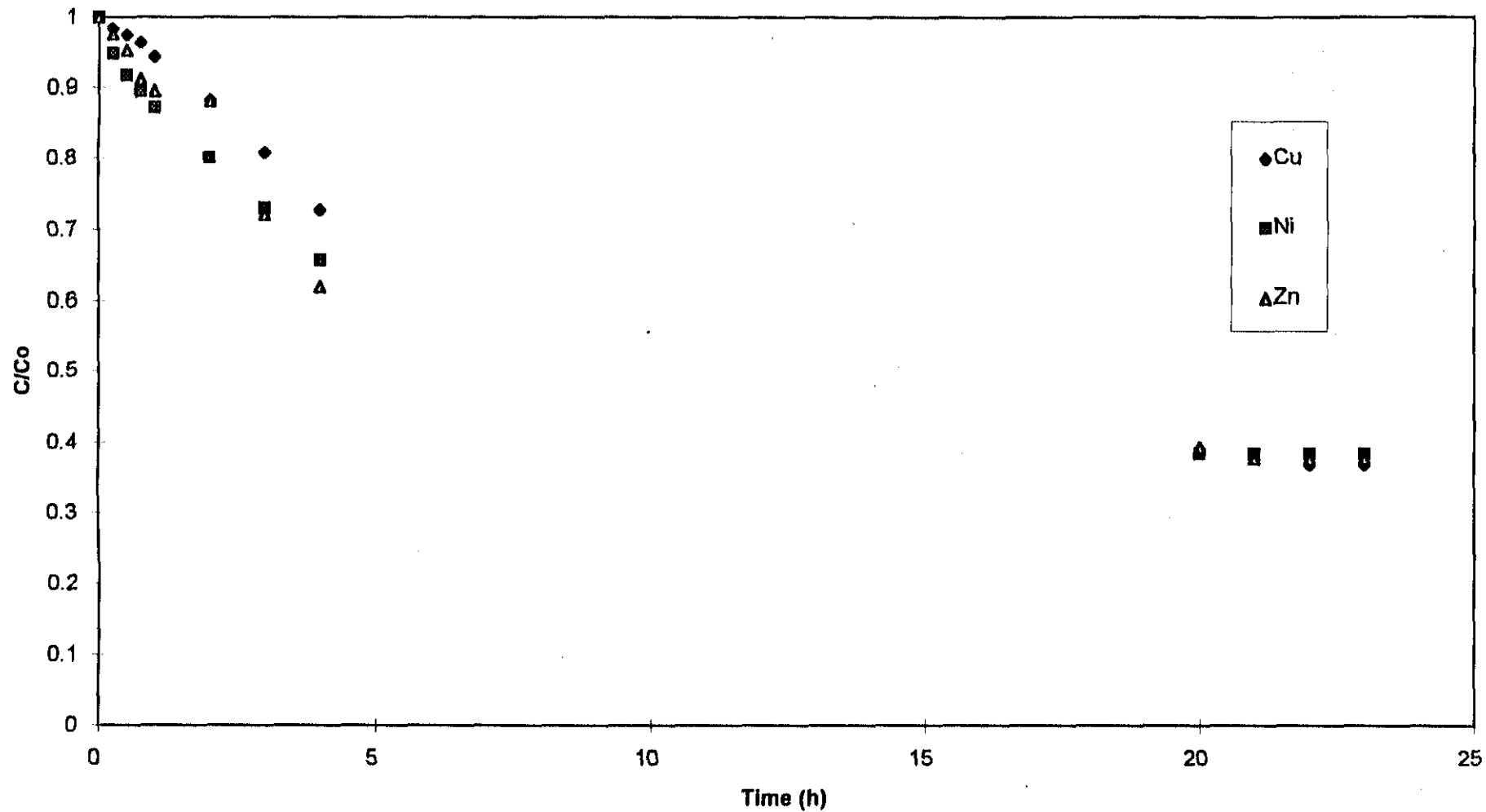


FIGURE 7.1 Monometallic curves of Cu , Ni and Zn adsorption onto AMBERLITE 252 H (  $C_0 = 2\text{ppm}$  ;  $V = 1.0\text{ L}$  ;  $m = 0.046\text{ g}$  ;  $N = 300\text{ rpm}$  )



**FIGURE 7.2 Monometallic curves of Ni , Cu and Zn adsorption onto AMBERLITE IRC 718 (Co = 2ppm ; V = 1.0 L ; m = 0.046 g ; N = 300 rpm )**



**FIGURE 7.3 Competitive adsorption of Ni , Cu and Zn onto AMBERLITE 252 H (C<sub>0</sub> = 2 ppm ; V = 1.0L ; m = 0.046 g ; N = 300 rpm )**

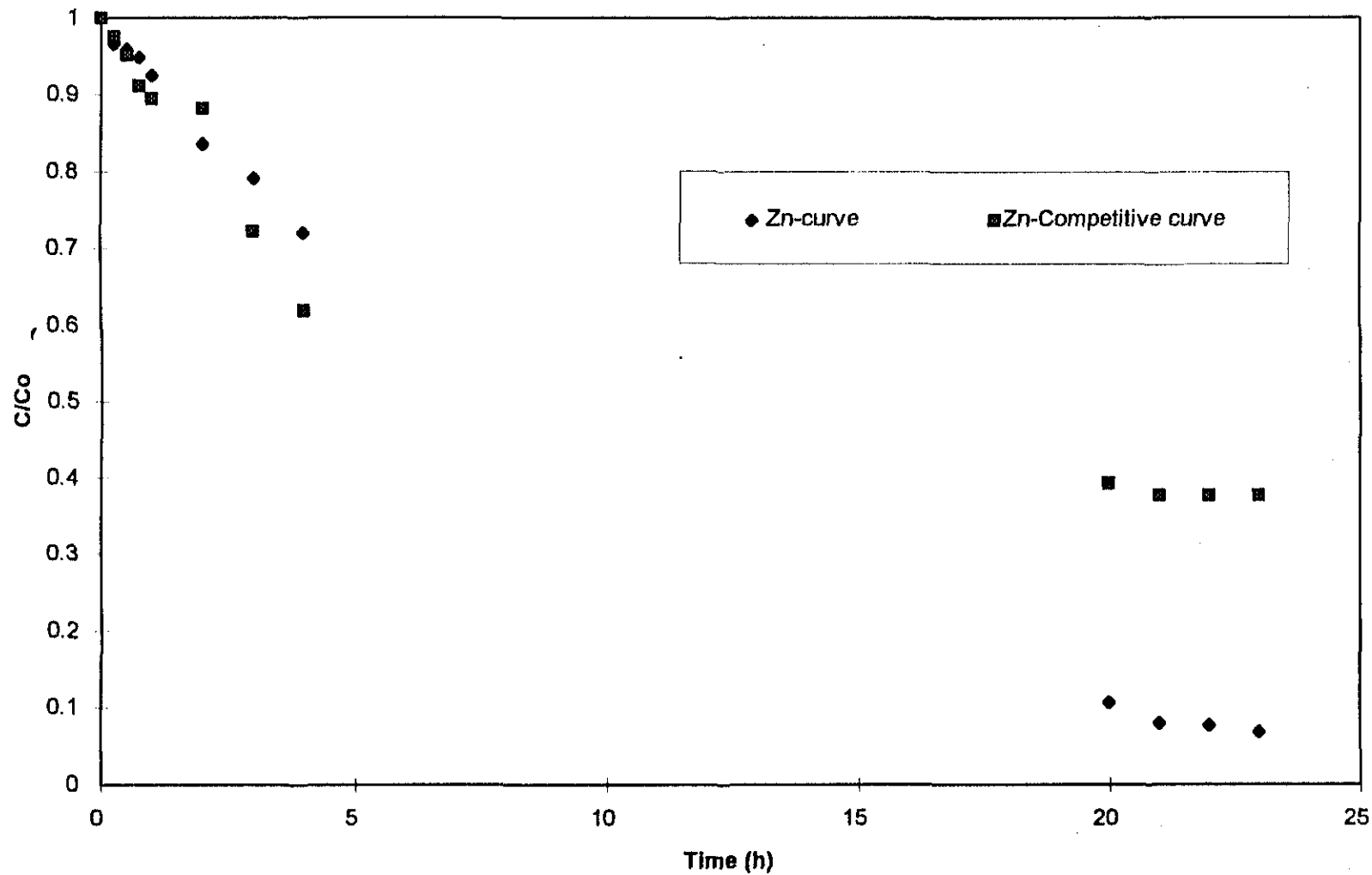


**FIGURE 7.4 Comparison of monometallic and multimetallic curves for Zn adsorption onto AMBERLITE 252 H (  $C_o = 2\text{ppm}$  ;  $V = 1.0\text{ L}$  ;  $m = 0.046\text{ g}$  ;  $N = 300\text{ rpm}$  )**

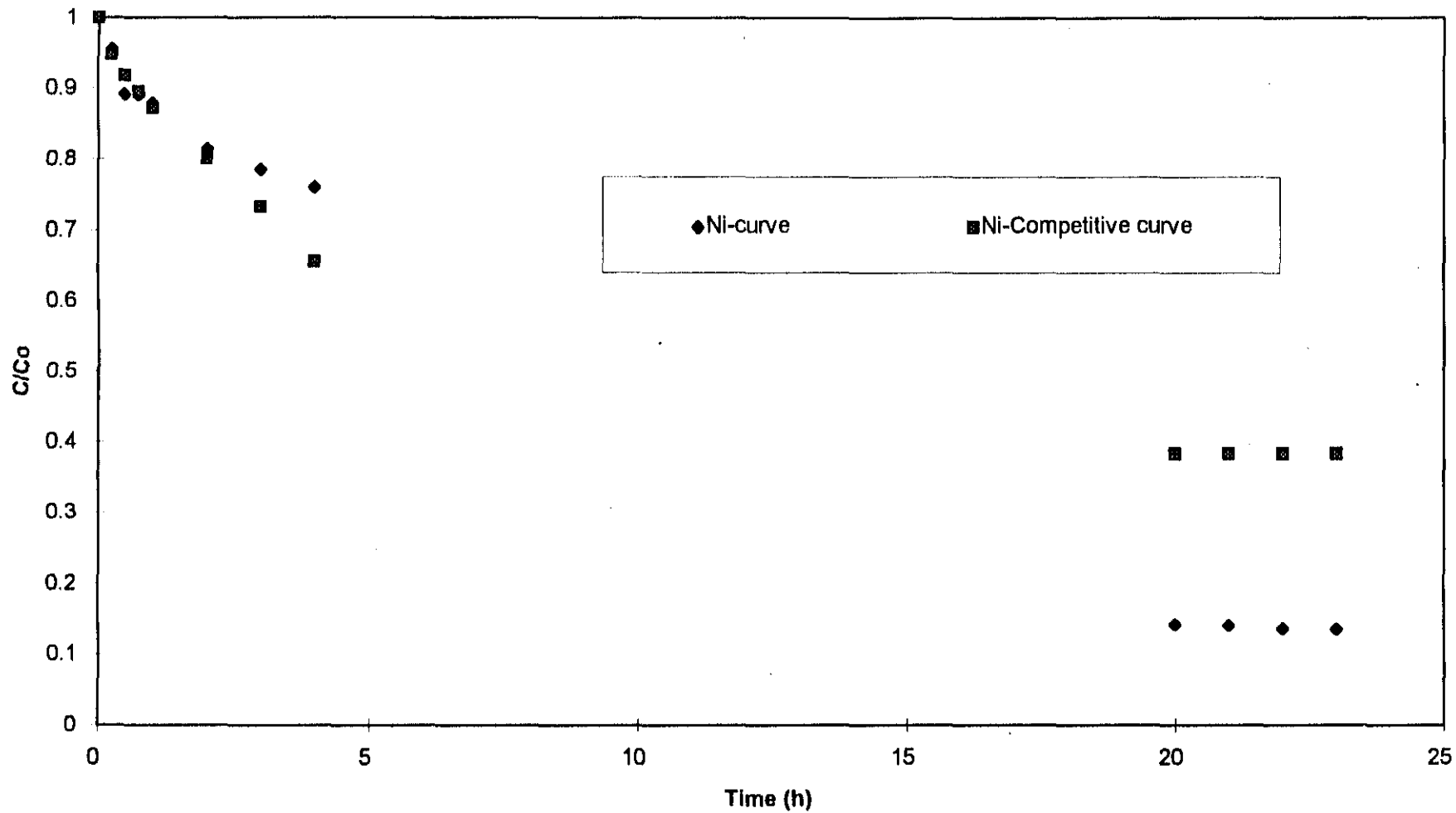


**FIGURE 7.5 Comparison of monometallic and multimetallic curves for Ni adsorption onto AMBERLITE 252 H (  $C_o = 2$  ppm ;  $V = 1.0$  L ;  $m = 0.046$  g ;  $N = 300$  rpm )**

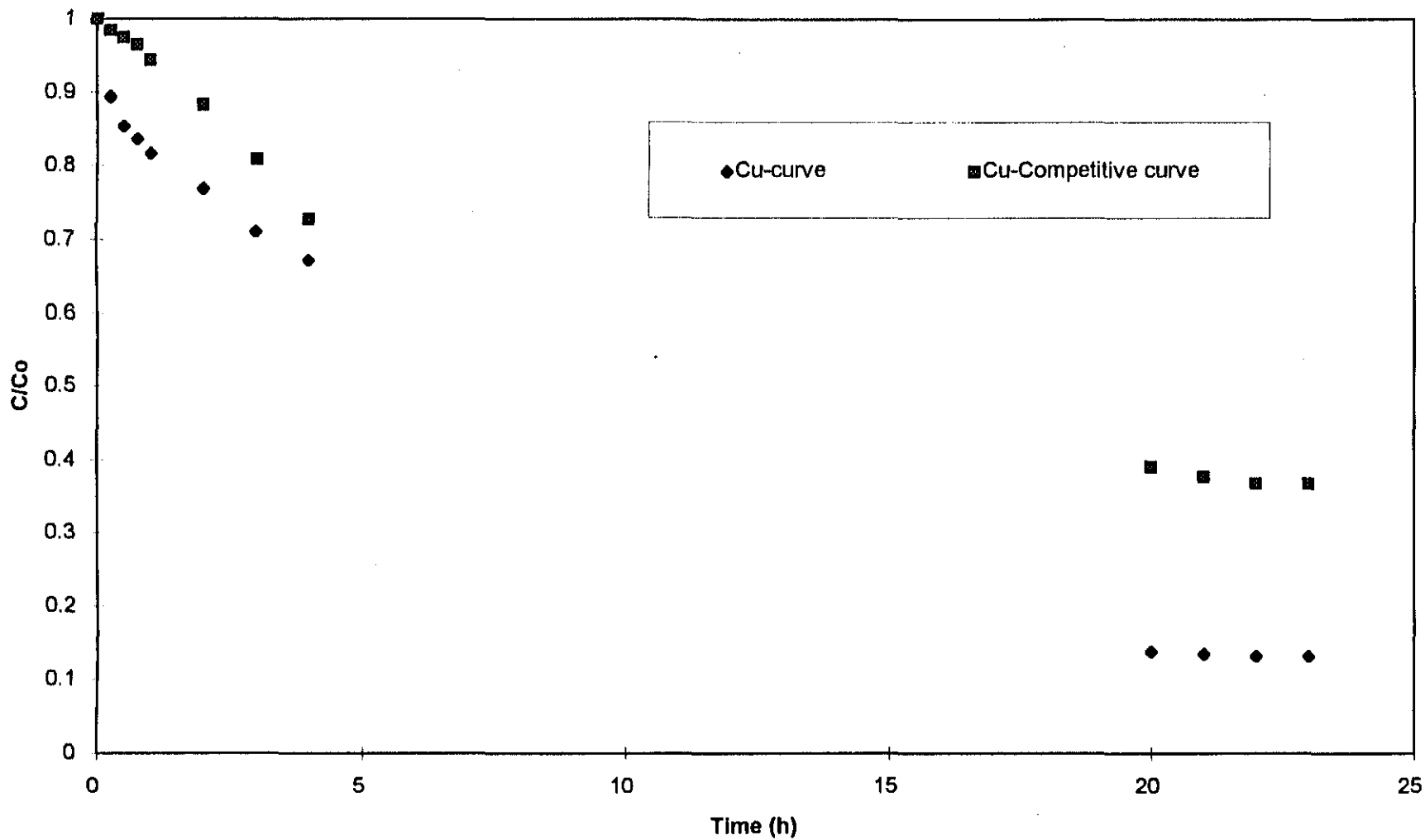


**FIGURE 7.6 Comparison of monometallic and multimetallic curves for Cu adsorption onto AMBERLITE 252 H (  $C_o = 2\text{ppm}$  ;  $V = 1.0\text{ L}$  ;  $m = 0.046\text{ g}$  ;  $N = 300\text{ rpm}$  )**

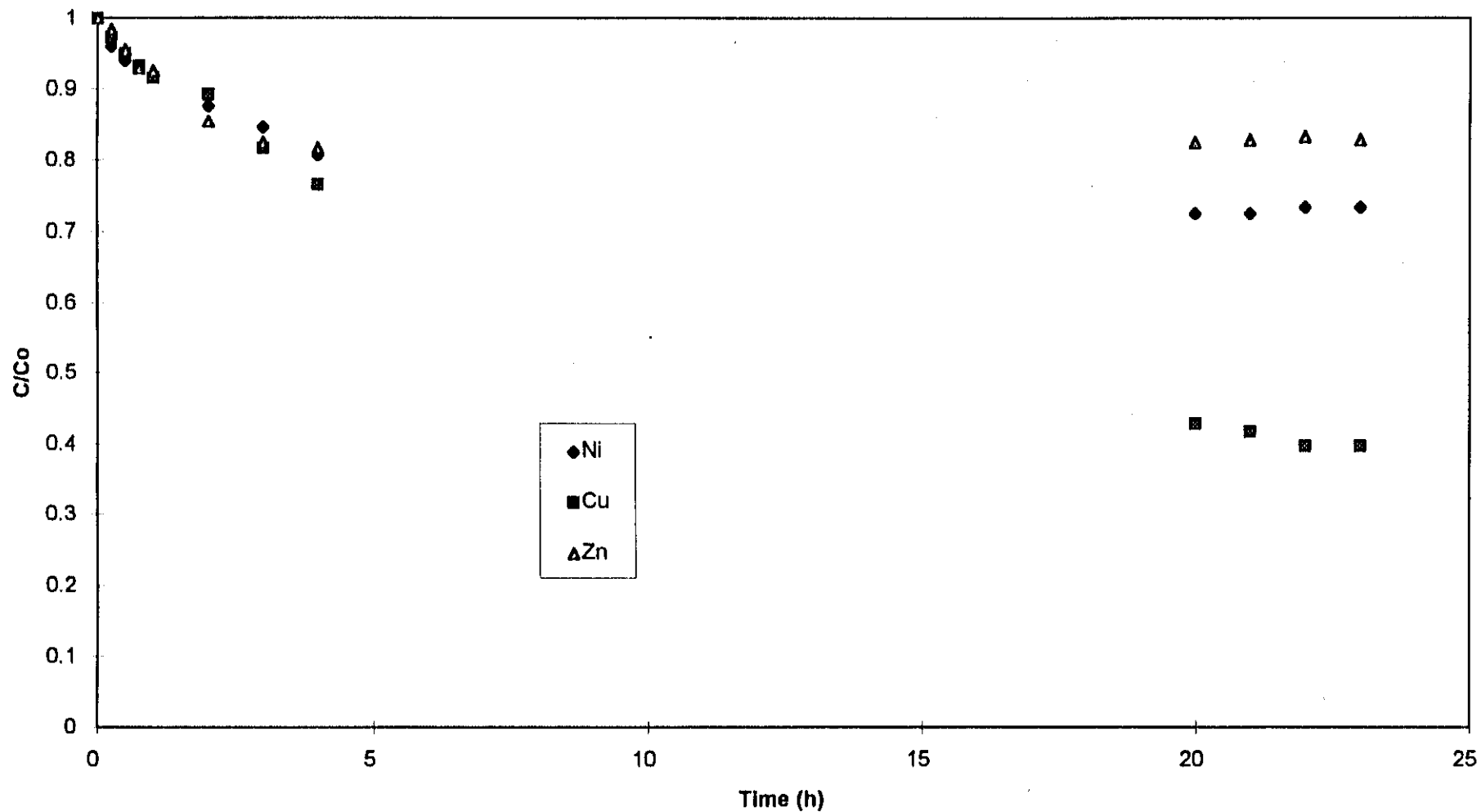


**FIGURE 7.7 Competitive adsorption of Cu , Ni and Zn onto AMBERLITE IRC 718 (Co = 2 ppm ; V = 1.0 L ; m = 0.046 g ; N = 300 rpm )**

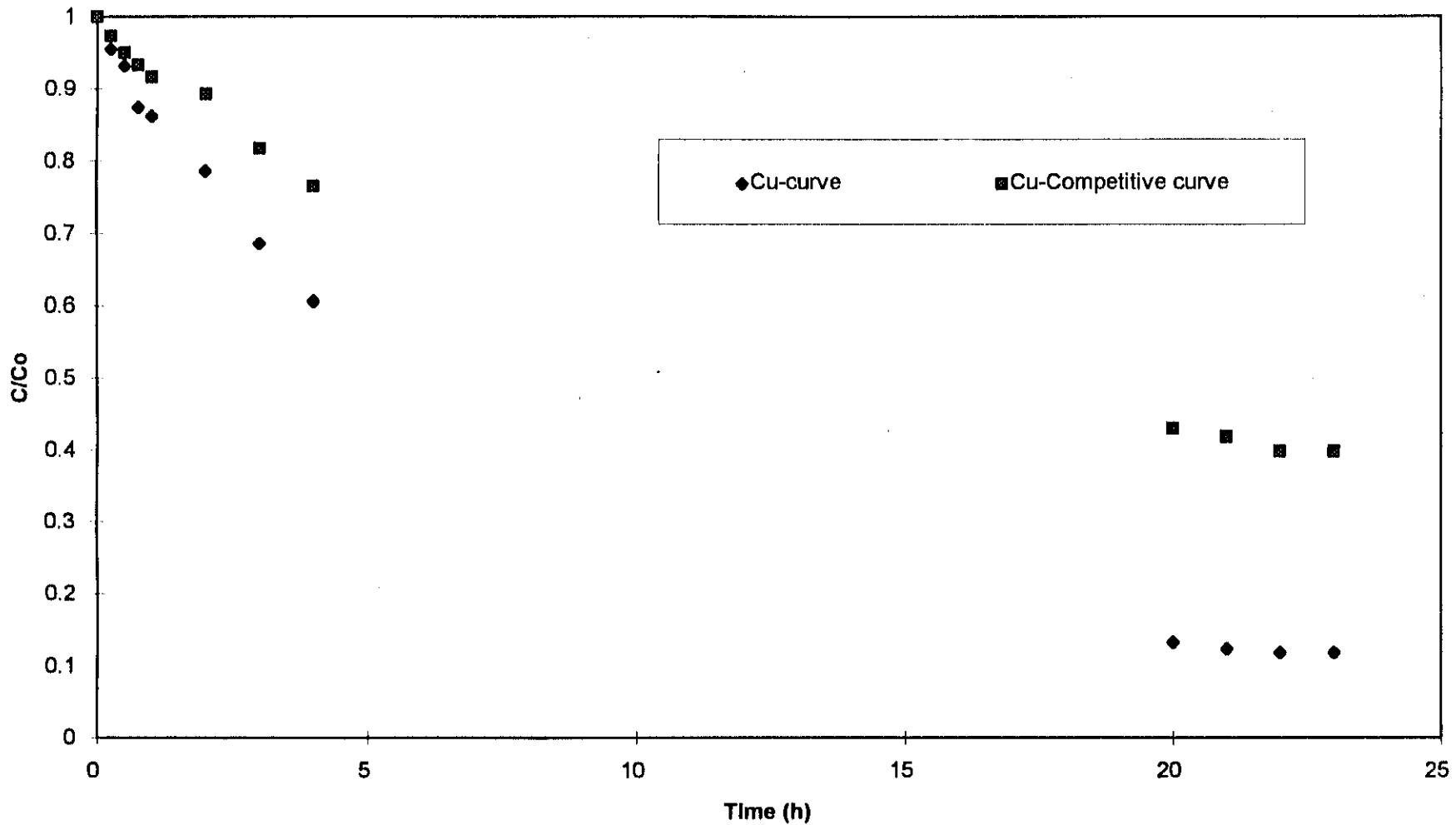


**FIGURE 7.8 Comparison of monometallic and multimetallic curves for Cu adsorption onto AMBERLITE IRC 718 (  $C_o = 2$  ppm ;  $V = 1.0$  L ;  $m = 0.046$  g ;  $N = 300$  rpm )**

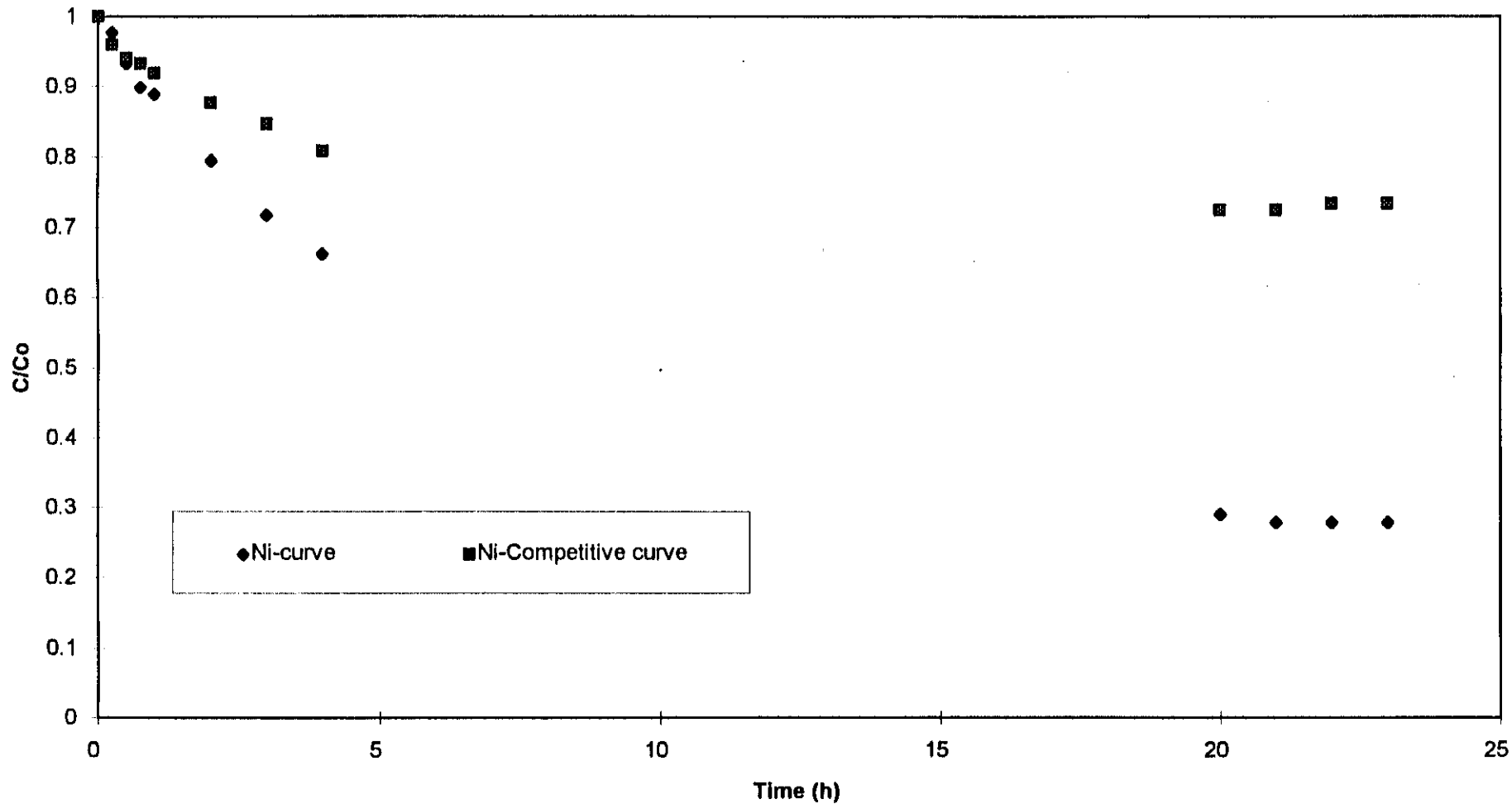


**FIGURE 7.9 Comparison of monometallic and multimetallic curves for Ni adsorption onto AMBERLITE IRC 718 (  $C_o = 2$  ppm ;  $V = 1.0$  L ;  $m = 0.046$  g ;  $N = 300$  rpm )**

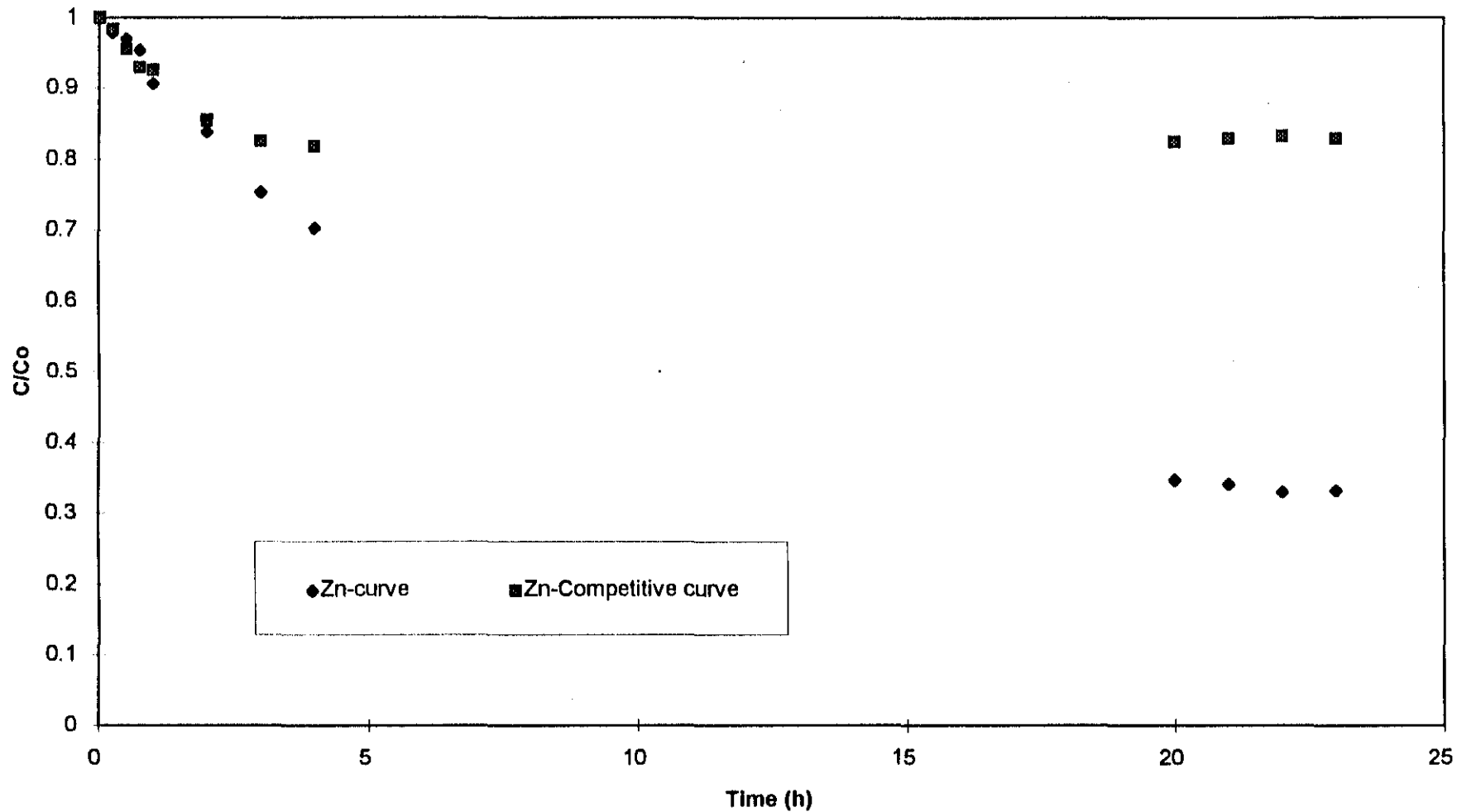


**FIGURE 7.10 Comparison of monometallic and multimetallic curves for Zn adsorption onto AMBERLITE IRC 718 (  $C_o = 2$  ppm ;  $V = 1.0$  L ;  $m = 0.046$  g ;  $N = 300$  rpm )**

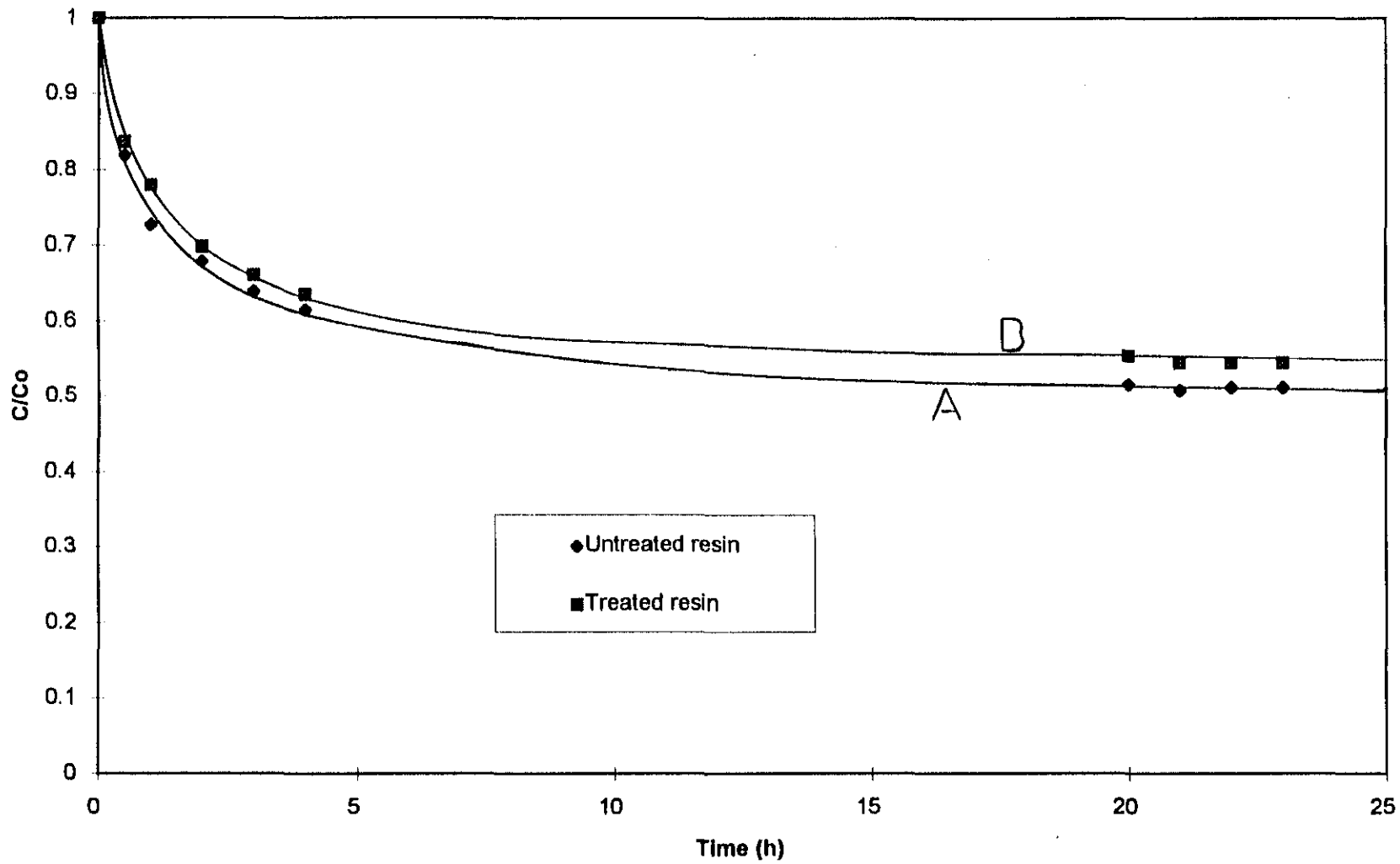


FIGURE 7.11 Effect of the inert sand slurry on the adsorption of Cu onto AMBERLITE IRA 718. (  $C_0 = 100$  ppm ;  $V = 1.0$  L ;  $m = 1.015$  g ;  $N = 550$  rpm )

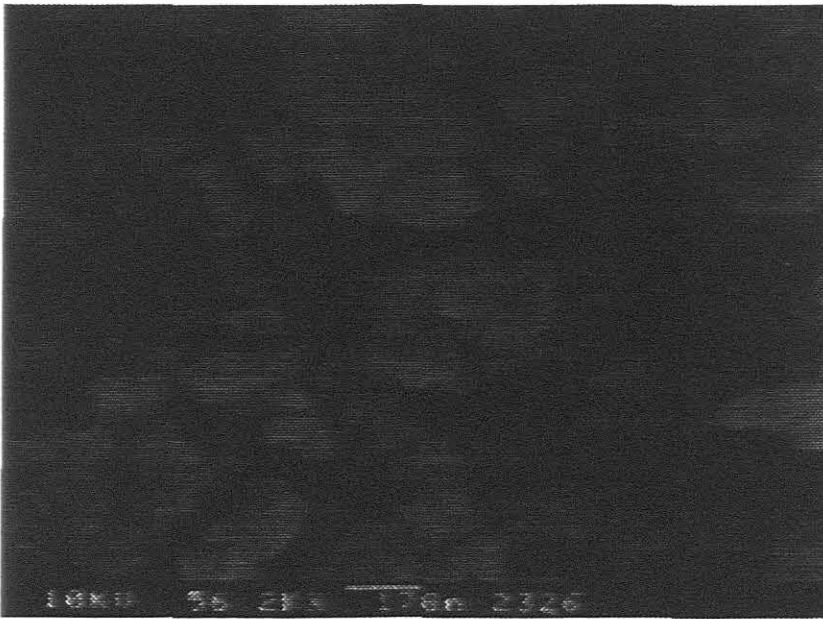


FIGURE 7.12 Electron micrograph of the resin external surface before contact with the sand slurry.



FIGURE 7.13 Electron micrograph of the resin external surface after contact with the sand slurry.

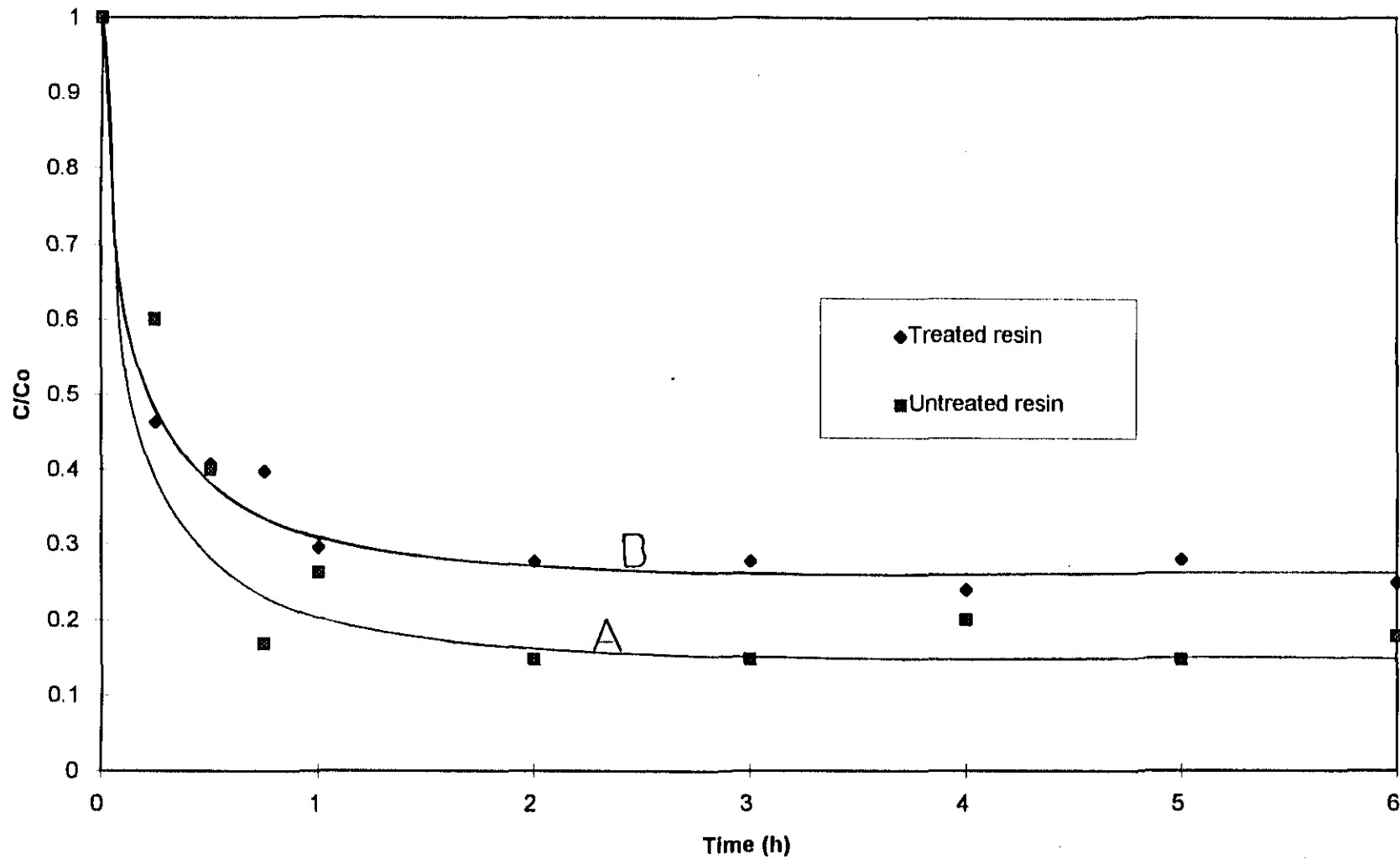
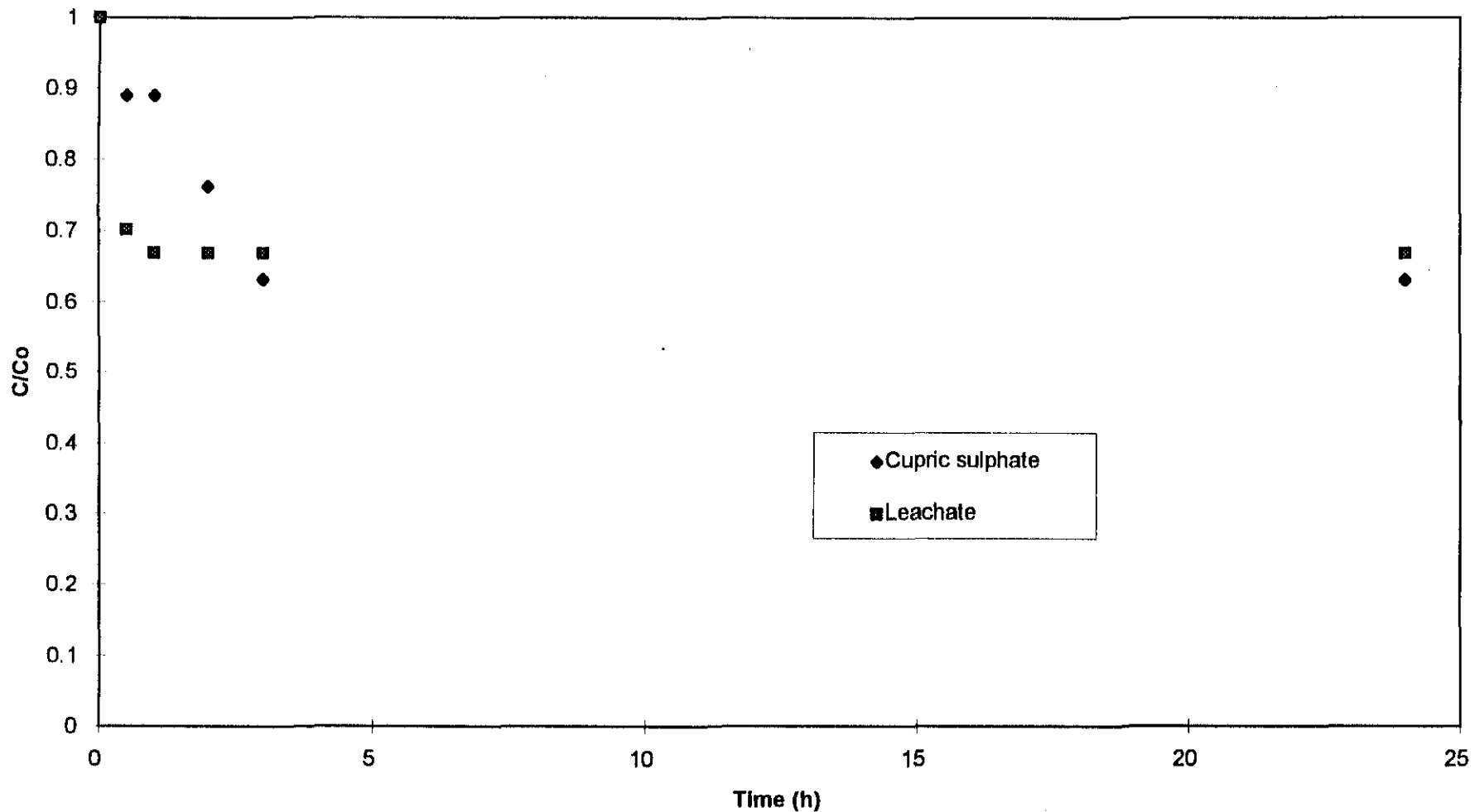


FIGURE 7.14 Effect of the inert sand slurry on the adsorption of Cu onto AMBERLITE 252 H (  $C_0 = 100$  ppm ;  $V = 1.0$  L ;  $m = 1.05$  g ;  $N = 550$  rpm )



**FIGURE 7.15 Comparison of the adsorptive curves of the synthetic solution and the leachate on AMBERLITE 252 H (Co-Synt Soln = 3930 ppm ; Co-Leachate = 1250 ppm ; m = 6.1 g ; V-Synt Soln = 0.85 L ; V-Leachate = 1.0 L )**

## CHAPTER 8

### CONCLUSIONS

The primary aim of this study was to evaluate the interaction of heavy metals and ion exchange resins at trace metal concentrations. It is notable that the metal cyanide complexes all behaved in a similar way when contacted with the anion exchange resin under varying process conditions. Fitting of the dual resistance model showed that  $k_f$  and  $D$  improved with an increase in temperature and  $k_f$  improved with an increase in stirring speed. A high ionic strength negatively affected the equilibrium parameter  $P$  as well as the kinetic parameters  $k_f$  and  $D$ . It was found that at these low concentrations the rate of loading improves with a decrease in external metal concentration.

The macroporous nature of all the resins used in this study coupled with a small particle size leads to favourable ion exchange kinetics. At trace metal concentrations, the retarding effects induced by the chelate reaction in the chelating resin, is virtually negated. It is only at higher metal concentrations that this rate inhibiting effect becomes significant.

The cation and anion exchange resins exhibited a high equilibrium loading capacity (60 - 80 kg/t) but the metals zinc and nickel loaded on the chelating resin to a much smaller extent. It was found that only the copper loading values on the chelating resin was comparable to those of the cation and anion exchange resins. Whereas the cation exchange resin, exhibited little

selectivity in adsorbing the metals, it was found that the chelating resin prefers the metals in the order  $\text{Cu} > \text{Ni} > \text{Zn}$ .

The chelating resin proved to be no less durable than the cation exchange resin, and both slightly lost their ability to adsorb the metal cations as a result of the effects of an inert coarse sand slurry.

The kinetic model provided a good fit for all monometallic curves except for the curves representing adsorption on the chelating resin at 2 ppm initial concentration, where the predictive curves could not adequately describe the true equilibrium conditions.

It is interesting to note that at high initial concentrations (100 ppm), the value for  $k_f$  and  $D$  for the chelating resin are significantly smaller than at trace concentrations. This was however not the case for the cation exchange resin.

Due to the low pH of the leachate, the performance of the chelating resin could not be evaluated in a real situation. However, copper loading from the leachate onto the cation exchange resin was found to be 66 % less than loading from a synthetic sulphate solution.

## RECOMMENDATIONS FOR FUTURE RESEARCH

This study was essentially an investigation into the interaction of heavy metals and ion exchange resins at dilute metal concentration. Although a firm basis has been laid, it is necessary to expand this database by giving special attention to the following aspects :

- (a) Column tests need to be done to compliment the batch reactor tests.
- (b) A more specialised kinetic model should be developed to account for metal adsorption onto the chelating resin, especially at trace concentrations.
- (c) Attention need to be given to ion exchange phenomenon such as swelling, and the effect of internal pH.

## **REFERENCES**

## CHAPTER 9

### REFERENCES

Chapra, S.C. , and Canale, R.P. , Numerical methods for Engineers, Second Edition, McGraw Hill Book co. Singapore, 1989.

Diaz, M. , and Mijangos, F. , “ Metal recovery from hydrometallurgical wastes” *Journal of metals*, 1987, pp. 42 - 44.

Fleming, C.A. , and Cromberge, G. , “ The extraction of Gold from cyanide solutions by strong and weak base anion exchange resins” *Journal of the SAIMM*, vol. 84, no.5, 1984 , pp. 125 - 137.

Green, B.R. , “ Mechanisms of loading of metal cyanides by weak - base resins” *Reactive polymers*, 8 , 1988, pp.221 - 234.

Grosse, D.W. , “Metal Bearing Hazardous Waste Streams.” *Journal of the Air Pollution Control Association*, Volume 36, no. 5, 1986, pp. 603 - 613.

Gupta, A. , Johnson, E.F. , and Schlossel, R.H. , “ Investigation into the ion exchange of cyanide complexes of zinc (2+), cadmium (2+), and copper (1+) ions.” *Ind.Eng.Chem.Res.* , vol. 26, no.3, 1987, pp 588 - 594.

Habashi, F. , Principles of Extractive Metallurgy, Volume 2 ; *Hydrometallurgy*, Gordon and Breach science publishers, 1980.

Hall, K. , Eagleton, L.C. , Acrivos, A. , and Vermeulen, T. , “ Pore-and solid-diffusion kinetics in fixed-bed adsorption under constant-pattern conditions” *Industrial and Engineering chemistry fundamentals*, vol. 5, no.2, 1966, pp. 212 - 223.

Helfferich, T. , *Ion exchange*, McGraw-Hill Book Company, Inc, 1995.

Liberti, L. , and Helfferich F.G. , “Mass transfer and kinetics of ion exchange.” Martinus Nijhoff Publishers, no. 71, 1983.

Lopez, M. , Coca, J. , and Sastre, H. , “Anion exchange in Amberlite IRA-400 and Amberlite IRA-410 Ion exchange resins.” *J Chem Eng Data*, vol 37, no. 2, 1992.

Loureiro, J.M. , Costa, C.A. , and Rodrigues, A.E. , “Recovery of copper, zinc and lead from liquid streams by chelating ion exchange resins” *Chemical Engineering Science*, vol. 43, no. 5, pp. 1115 - 1123, 1988.

Mijangos, F. , and Diaz, M. , “ Metal-proton Equilibrium relations in a chelating Iminodiacetic resin” *Ind.Eng.Chem.Res.* , vol. 31, no.11, 1992, pp. 2524 - 2530.

Morris, J.C. , Weber, W.J.Jr. , “ Removal of boilologically-resistant pollutants from waste waters by adsorption .” *Proceedings of first International conference on water pollution research*, Pergamon press, Ltd. Oxford England, 1962.

Murray, K.A. , *Wastewater treatment and pollution control*, Heer Printing Co. 1987.

Neretnieks, I. , “ Analysis of some adsorption experiments with activated carbon” *Chem.Eng.Sci.* , 31 1029, 1976.

Nestle, N.F.E.I. , and Kimmich, R. , “ Concentration - dependent diffusion coefficients and sorption isotherms. Application to Ion exchange processes as an example.” *J.Phys.Chem.* , vol. 100, no.30, 1996, pp. 12569 - 12573.

Pesavento, M. , Biesuz, R. , Gallorini, M. , and Profumo, A. , “ Sorption mechanism of trace amounts of divalent metal ions on a chelating resin containing iminodiacetate groups.” *Analytical chemistry*, vol. 65, no.18, 1993, pp. 2522 - 2527.

Petersen, F.W. , Inhibition of mass transfer to porous adsorbents by fine particles and organic compounds, *M Eng Thesis*, 1991, University of Stellenboch.

Petruzzelli, D. , Kalinitchev, A. , Soldatov, V.S. , and Tiravanti, G. , “ Chloride / sulfate Ion exchange kinetics on fibrous resins. Two independent models for film diffusion control.” *Ind.Eng.Chem.Res.* , vol. 34, no.8, 1995, pp. 2618 - 2624.

Reed, B.E. , Arunachalam, S. , and Thomas, B. , “Removal of lead and cadmium from aqueous waste streams using granular activated carbon (G.A.C.) columns.” *Environmental Progress*, vol. 13, no. 1, 1994,pp. 60 - 64.

Schmuckler, G. , “ Chelating resins - Their analytical properties and applications.” *Talanta*, vol. 12, 1965, pp. 281 - 290.

Sengupta, A.K. , and Zhu, Y. , “ Metal sorption by chelating polymers : a unique role of Ionic strength” *AIChE Journal*, vol. 38, no.1, 1992, pp. 153 - 157.

Sengupta, A.K. , Zhu, Y. , and Hanze, D. , “ Metal (II) Ion Binding onto Chelating exchangers with nitrogen donor atoms : some new observations and related implications” *Environ.Sci.Technol.* , vol. 25, no. 3, 1991, pp. 481 - 488.

Shallcross, D.C. , Herrmann, C.C. , and McCoy, B.J. , “An improved model for the prediction of multicomponent ion exchange equilibria” *Chemical Engineering Science*, vol. 43, no. 2, pp. 279 - 288, 1988.

Tan, T.C. , and Teo, W.K. , “ Combined effect of carbon dosage and initial adsorbate concentration on the adsorption isotherm of heavy metals on activated carbon.” *Wat.Res.* , vol. 21, no.10, 1987, pp. 1183 - 1188.

Treybal, R.E. , *Mass Transfer Operations*, second edition, McGraw-Hill book company, 1968.

Valenti, M. , “Recovering heavy metals” *Mechanical Engineering*, vol 114, 1992, pp. 54 - 58.

Van Deventer, J.S.J. , *Kinetic model for the adsorption of metal cyanides on activated carbon*, Ph.D.Thesis 1984, University of Stellenbosch.

Van Lier, W.C. , “ On the kinetics of adsorption on activated carbon from the aqueous phase. Activated carbon .... a fascinating material,” *Norit* , 129 (1983).

Van Vliet, B. , Weber JR W.J. and Hozumi, H. , “ Modelling and prediction of specific compound adsorption by activated carbon

and synthetic adsorbents" *Water Research*, vol. 14, 1980, pp. 1719 - 1728.

Vermeulen, T., "Separation by adsorption methods", *Advances in Chemical Engineering*, vol. 2, 1958, pp. 147- 208.

Yoshida, H. , Kataška, T. , and Fujikawa, S. , "Kinetics in a chelate ion exchanger - II Experimental" *Chemical Engineering Science*, vol. 41, no. 10 pp. 2525 - 2530, 1986.

Young, B.D. ,Bryson, A.W. , and Glover, M.R.L. , "A study of the kinetics of adsorption of gold and zinc cyanide onto a strong base anion exchange resin using a minicolumn technique." , *Hydrometallurgy* no. 26, 1991, pp. 151 - 162.

Zheng, Z. , Gu, D. , Anthony, R.G. , and Klavetter, E. , "Estimation of Cesium Ion Exchange distribution coefficients for concentrated electrolytic solutions when using crystalline silicotitanates." *Ind.Eng.Chem.Res.* , vol. 34, no.6, 1995, pp. 2142 - 2147.

Zhu, Y. , Millan, E. , and Sengupta, A.K. , "Towards separation of toxic metal (II) cations by chelating polymers : some noteworthy observations." *Reactive polymers*, no. 13, 1990, pp. 241 -253.

## **APPENDIX A**

**COMPUTER PROGRAM FOR THE ADSORPTION OF A  
SINGLE METAL SPECIES ONTO ION EXCHANGE RESIN IN  
A BATCH REACTOR**

{Model for adsorption of heavy metals in batch reactors}

```

program pars;
uses crt, graph, grafiek;
const
  k=5;
  delt=20;
var
  cred,ckm,ckb,p,vol,cmass,dp,dens,kl,co,fkf,qo,qs,csb,qt,
  hours,ta,pa,ka,ca,q,r,s,v,w,x,delr,delta,m:double;
  ds,qm,qb,qmo,qbo:array[0..k] of double;
  time,c:array[0..1] of double;
  cs:array[-1..1] of double;
  d:array[0..k,0..k] of double;
  e:array[0..k] of double;
  t,u:array[1..k] of double;
  answ,chg,ver,on;n;
  mde,her:integer;
  lr:string[24];
  st:text;
  xx,yy:punte;
  nxy:array[1..8] of integer;
label
  nuut;

procedure defaults;
begin
  default;
  opskrf[5]='Time [hr]'; opskrf[6]='C/Co';
  grte:=4; fnt:=2; fntsize:=7; stlsize:=6; mde:=3; answ='N'; lr='';
  co:=2; qo:=0; cmass:=0.101e-3; vol:=0.001; p:=185.57; kl:=2.279;

  fkf:=0.0001374; ckm:=4.25e-12; delta:=0.999; ckb:=0; dp:=700e-6;
  dens:=700;
end;

procedure Model;

begin
time[0]:=0;
cs[0]:=0; cs[-1]:=0;
c[0]:=co;
delr:=dp/(2*k);
for j:=0 to k do
  begin
  qm[j]:=qmo[j];
  qb[j]:=qbo[j];
  for i:=0 to k do d[j,i]:=0;
  end;
q:=(delt*ckb);
r:=(6*delt*fkf*cmass)/(dens*dp*vol);
s:=-ckm*delt/(delr*delr);
v:=(ckb*delt)/((1+q));
w:=1-(6*s)+(ckb*delt)-(v*q);
for j:=1 to k do
  begin
  m:=j*delr;
  t[j]:=1+((2*ckm*delt)/(m*delr))-(2*s)+(ckb*delt)-(v*q);
  u[j]:=-ckm*delt*((2/m)+(1/delr))/delr;

```

```

end;
d[0,0]:=w; d[0,1]:=6*s;
for j:=1 to (k-1) do
  begin
  d[j,j-1]:=s;
  d[j,j]:=t[j];
  d[j,j+1]:=u[j];
  end;
d[k,k-1]:=s; d[k,k]:=t[k]+u[k];
for j:=0 to k do d[0,j]:=d[0,j]/w;
for i:=1 to k do for j:=0 to k do d[i,j]:=d[i,j]/s;
for i:=1 to k do
  begin
  for j:=0 to k do d[i,j]:=d[i,j]-d[i-1,j];
  ds[i]:=d[i,i];
  for j:=0 to k do d[i,j]:=d[i,j]/ds[i];
  end;
case mde of 1: cred:=1;
           2: cred:=0;
           3: cred:=co;
           end;
moveto(xscr(time[0]),yscr(cred));
repeat
  time[1]:=time[0]+delt;
  if time[0]=0 then cs[1]:=0.05      {0.005}
    else cs[1]:=2*cs[0]-cs[-1];
  csb:=cs[1];
  repeat
    cs[1]:=csb;
    c[1]:=(c[0]+r*cs[1])/(1+r);
    x:=delr*fkf*(((c[0]+r*cs[1])/(1+r))-cs[1])/(dens*ckm);
    for i:=0 to (k-1) do e[i]:=qm[i]+v*qb[i];
    e[k]:=qm[k]+v*qb[k]-u[k]*x;
    e[0]:=e[0]/w;
    for i:=1 to k do e[i]:=e[i]/s;
    for i:=1 to k do
      begin
        e[i]:=e[i]-e[i-1];
        e[i]:=e[i]/ds[i];
      end;
    csb:=qm[k]/(delta*P-qm[k]*k);
  until abs(csb-cs[1])<0.0000001;
  qm[k]:=e[k];
  for i:=(k-1) downto 0 do qm[i]:=e[i]-d[i,i+1]*qm[i+1];
  for i:=0 to k do qb[i]:=(qb[i]+(q*qm[i]))/(1+q);
  hours:=time[1]/3600;
  qt:=qo+(((co-c[1])*vol)/cmass);
  case mde of 2: cred:=(qo-qt)/qo;
               1: cred:=c[1]/co;
               3: cred:=c[1];
               end;
  lineto(xscr(hours),yscr(cred));
  cs[-1]:=cs[0];
  cs[0]:=cs[1];
  c[0]:=c[1];
  time[0]:=time[1];
until (keypressed) or (time[0]>=(xmks*3600));
end;

```

```

procedure data;

procedure sup(var other:double);
begin
writeLn;
write('Give the new value : ');
readLn(other);
end;

begin
repeat
  clrscr;
  writeLn('Parametersystem');
  writeLn('-----');
  writeLn;
  chg:='J';
  writeLn('C : Co [mg/l]      = ',co:4:1);
  writeLn('Q : Qo (total) [mg/l] = ',qo:4:1);
  writeLn('K : Mass of resin [kg] = ',cmass:6:4);
  writeLn('V : Volume [m3] = ',vol:6:4);
  writeLn('P : p = ',p:6:3);
  writeLn('Kl: kl = ',kl:5:3);
  writeLn('L : Film diffusion coeff. (fkf) = ',fkf:9:7);
  writeLn('M : Macro pore diff. (ckm) = ',ckm:6);
  writeLn('F : delta = ',delta:4:2);
  {writeLn('B : Micro pore diff. (ckb) = ',ckb:6);}
  writeLn('P : Particle size [m] = ',dp:7:5);
  writeLn('D : Density [kg/m3] = ',dens:4:0);
  write('T : Draw ');
  case mde of 1: writeLn('C/Co');
                2: writeLn('(Qo-Q)/Qo');
                3: writeLn('C [mg/l]');
            end;
  writeLn('S : Write answers to file ? = ',answ);
  writeLn('G : No corrections');
  writeLn;
  write('Key in the number of correction : ');
  repeat
    chg:=upcase(readkey);
  until (chg='C') or (chg='Q') or (chg='K') or (chg='V') or (chg='A') or
        (chg='N') or (chg='L') or (chg='M') or (chg='F') or (chg='P') or
        (chg='D') or (chg='G') or (chg='B') or (chg='S') or (chg='T');
  writeLn(chg);
  if chg='C' then sup(co);
  if chg='Q' then sup(qo);
  if chg='K' then sup(cmass);
  if chg='V' then sup(vol);
  if chg='A' then sup(p);
  if chg='N' then sup(kl);
  if chg='L' then sup(fkf);
  if chg='M' then sup(ckm);
  if chg='F' then sup(delta);
  if chg='B' then sup(ckb);
  if chg='P' then sup(dp);
  if chg='D' then sup(dens);
  if (chg='T') then case mde of 1: mde:=2;
                        2: mde:=3;
                        3: mde:=1;
                    end;
  if chg='S' then

```

```

begin
writeln;
write('Want to write answers to file? (y/n) ');
vraag(answ);
if answ='Y' then
begin
write('Give the name of file : ');
readln(lr);
end;
end;
until (chg='G');
end;

procedure Stoor;
begin
clrscr;
gotoxy(1,8);
write('Give name of file (bv. prent.pic) : b:');
readln(Inaam[13]);
writeln;
writeln('Put the graph disc in B and press [CR]');
readln;
Inaam[13]:='b:'+Inaam[13];
assign(st,Inaam[13]);
rewrite(st);
for i:=1 to 4 do writeln(st,opskrf[i]);
writeln(st,fkf);
writeln(st,ckm);
writeln(st,delta);
writeln(st,ckb);
writeln(st,co);
writeln(st,qo);
writeln(st,cmass);
writeln(st,vol);
writeln(st,p);
writeln(st,kl);
writeln(st,dp);
writeln(st,dens);
writeln(st,opskrf[5]);
writeln(st,opskrf[6]);
writeln(st,xmn);
writeln(st,xmks);
writeln(st,ymn);
writeln(st,ymks);
writeln(st,nx);
writeln(st,ny);
writeln(st,np);
for i:=1 to np do
begin
writeln(st,Inaam[i]);
writeln(st,plt[i]);
writeln(st,verb[i]);
writeln(st,ltp[i]);
end;
writeln(st,stl);
if stl='J' then
begin
writeln(st,nv,' ',xv,' ',yv);
for i:=1 to (np+nv) do writeln(st,sl[i]);
end;

```

```

writeln(st,eks);
if eks='J' then
  begin
    writeln(st,ni);
    for i:=1 to ni do
      begin
        writeln(st,ins[i]);
        writeln(st,xi[i], ' ',yi[i]);
      end;
    end;
  if mde=1 then for j:=0 to k do writeln(st,qm[j]:6:3,qb[j]:10:3)
    else for j:=0 to k do writeln(st,qmof[j]:6:3,qbo[j]:10:3);
  close(st);
end;

```

```

procedure Lees;
begin
  write('Give the name of file (bv. prent.pic) : b:');
  readln(Inaam[13]);
  Inaam[13]:=b'+Inaam[13];
  writeln;
  writeln('Put the graph disc in B');
  wag;
  assign(st,Inaam[13]);
  reset(st);
  for i:=1 to 4 do readln(st,opskrf[i]);
  readln(st,fkf);
  readln(st,ckm);
  readln(st,delta);
  readln(st,ckb);
  readln(st,co);
  readln(st,qo);
  readln(st,cmass);
  readln(st,vol);
  readln(st,p);
  readln(st,kl);
  readln(st,dp);
  readln(st,dens);
  readln(st,opskrf[5]);
  readln(st,opskrf[6]);
  readln(st,xmn);
  readln(st,xmks);
  readln(st,ymn);
  readln(st,ymks);
  readln(st,nx);
  readln(st,ny);
  readln(st,np);
  for i:=1 to np do
    begin
      readln(st,Inaam[i]);
      readln(st,plt[i]);
      plt[i]:=upcase(plt[i]);
      readln(st,verb[i]);
      verb[i]:=upcase(verb[i]);
      readln(st,ltp[i]);
    end;
  readln(st,stl);
  stl:=upcase(stl);
  if stl='J' then
    begin

```

```
readln(st,nv,xv,yv);
for i:=1 to (np+nv) do readln(st,sl[i]);
end;
readln(st,eks);
eks:=uppercase(eks);
if eks='J' then
begin
readln(st,ni);
for i:=1 to ni do
begin
readln(st,ins[i]);
readln(st,xi[i],yi[i]);
end;
end;
for j:=0 to k do readln(st,qmo[j],qbo[j]);
ver:='1';
xl:=xmks-xmn;
yl:=ymks-ymn;
if nx>0 then xin:=xl/nx else xin:=xl;
if ny>0 then yin:=yl/ny else yin:=yl;
end;
```

## **APPENDIX B**

### **TABULATION OF EXPERIMENTAL RESULTS**

Experiment no.1

Equilibrium adsorption of zinc on AMBERLITE IRA 900.

Volume of solution = 1.0 L

Mass of resin = 0.02 g

$C_o$ (mg / L)	$C_e$ (mg / L)	$q_e$ (g metal / kg resin)
1.026	0.549	23.866
2.809	1.759	52.465
5.198	3.992	60.273
7.439	6.252	59.399
9.514	8.332	59.141
12.296	11.070	61.291
19.773	18.852	46.048

Experiment no.2

Equilibrium adsorption of nickel on AMBERLITE IRA 900.

Volume of solution = 1.0 L

Mass of resin = 0.02 g

$C_o$ (mg / L)	$C_e$ (mg / L)	$q_e$ (g metal / kg resin)
2.118	1.044	53.668
6.821	5.594	61.335
8.916	7.536	69.002
12.545	11.012	76.669
19.479	18.052	71.359
29.887	28.441	72.266
39.539	37.948	79.587

Experiment no.3

Equilibrium adsorption of copper on AMBERLITE IRA 900.

Volume of solution = 1.0 L

Mass of resin = 0.02 g

$C_o$ (mg / L)	$C_e$ (mg / L)	$q_e$ (g metal / kg resin)
5.576	4.848	36.362
7.360	6.442	45.911
13.903	12.749	57.665
20.401	19.148	62.638
32.665	31.316	67.447

Experiment no.4

Equilibrium adsorption of zinc on AMBERLITE 252H.

Volume of solution = 1.0 L

Mass of resin = 0.375 g

$C_o$ (mg / L)	$C_e$ (mg / L)	$q_e$ (g metal / kg resin)
17.586	0.580	45.349
29.141	2.817	70.195
37.782	11.247	70.761
48.710	21.769	71.842
64.397	32.226	85.789
73.588	41.183	86.415

Experiment no.5

Equilibrium adsorption of nickel on AMBERLITE 252H

Volume of solution = 1.0 L

Mass of resin = 0.375 g

$C_o$ (mg / L)	$C_e$ (mg / L)	$q_e$ (g metal / kg resin)
17.532	1.190	43.577
28.126	5.177	61.198
40.333	11.962	75.656
51.071	22.751	75.516
59.383	30.046	78.232
68.692	38.730	79.898

Experiment no.6

Equilibrium adsorption of copper on AMBERLITE 252H.

Volume of solution = 1.0 L

Mass of resin = 0.375 g

$C_o$ (mg / L)	$C_e$ (mg / L)	$q_e$ (g metal / kg resin)
20.328	0.762	52.174
30.136	4.918	67.246
44.135	13.644	81.307
55.296	23.536	84.691
64.278	33.700	81.541
71.192	40.848	80.914

Experiment no.7

Equilibrium adsorption of zinc on AMBERLITE IRC 718.

Volume of solution = 1.0 L

Mass of resin = 0.7 g

$C_o$ (mg / L)	$C_e$ (mg / L)	$q_e$ (g metal / kg resin)
12.286	3.264	12.889
21.215	12.377	12.626
30.804	20.629	14.535
40.348	29.799	15.068
52.804	39.110	19.563
62.104	48.368	19.623
63.526	49.987	19.355

Experiment no.8

Equilibrium adsorption of nickel on AMBERLITE IRC 718.

Volume of solution = 1.0 L

Mass of resin = 0.7 g

$C_o$ (mg / L)	$C_e$ (mg / L)	$q_e$ ( g metal / kg resin)
9.601	1.649	11.361
16.875	7.878	12.854
25.911	14.284	16.609
34.372	21.971	17.716
44.407	29.385	21.461
52.549	38.876	19.532
73.034	56.172	24.088
92.544	74.761	25.405
114.375	84.318	42.937

Experiment no.9

Equilibrium adsorption of copper on AMBERLITE IRC 718.

Volume of solution = 1.0 L

Mass of resin = 0.7 g

$C_o$ (mg / L)	$C_e$ (mg / L)	$q_e$ (g metal / kg resin)
20.235	1.182	27.218
29.911	3.718	37.419
43.520	12.527	44.275
51.227	19.727	45.001
77.237	43.173	48.662
136.072	99.466	52.292
160.275	124.679	50.849

Experiment no.10

The effect of stirring speed on the adsorption of zinc cyanide on AMBERLITE IRA 900.

Conditions :

$C_0 = 10$  ppm

Volume of solution = 1.0 L

Mass of resin = 0.101 g

	C/C <sub>0</sub>	C/C <sub>0</sub>	C/C <sub>0</sub>	C/C <sub>0</sub>
Time (hrs)	180 rpm	300 rpm	440 rpm	standard
0	1	1	1	1
0.25	0.996	0.937	0.933	0.978
0.5	0.950	0.933	0.873	0.882
0.75	0.904	0.887	0.800	0.874
1	0.863	0.836	0.768	0.827
2	0.756	0.679	0.608	0.733
3	0.639	0.581	0.505	0.583
4	0.567	0.502	0.479	0.511
5	0.515	0.485	0.468	0.477
6	0.504	0.481	0.466	0.466
22	0.500	0.483	0.466	0.466
23	0.502	0.483	0.468	0.466

Experiment no.11

The effect of stirring speed on the adsorption of nickel cyanide on AMBERLITE IRA 900.

Conditions :

$C_0 = 10$  ppm

Volume of the solution = 1.0 L

Mass of resin = 0.1 g

	C/C <sub>0</sub>	C/C <sub>0</sub>	C/C <sub>0</sub>	C/C <sub>0</sub>
Time (hrs)	180 rpm	300 rpm	440 rpm	standard
0	1	1	1	1
0.25	0.975	0.929	0.900	0.929
0.5	0.943	0.909	0.886	0.909
0.75	0.919	0.861	0.793	0.861
1	0.864	0.808	0.761	0.808
2	0.738	0.652	0.593	0.652
3	0.647	0.537	0.472	0.537
4	0.552	0.450	0.410	0.450
5	0.489	0.398	0.365	0.398
6	0.434	0.360	0.346	0.360
7	0.406	0.345	0.336	0.345
22	0.345	0.334	0.336	0.334
23	0.345	0.334	0.336	0.334

Experiment no.12

The effect of stirring speed on the adsorption of copper on AMBERLITE IRA 900.

Conditions :

$C_0 = 10$  ppm

Volume of solution = 1.0 L

Mass of resin = 0.07 g

	C/Co	C/Co	C/Co	C/Co
Time (hrs)	180 rpm	300 rpm	440 rpm	standard
0	1	1	1	1
0.25	0.977	0.959	0.975	0.980
0.5	0.953	0.933	0.933	0.951
0.75	0.926	0.895	0.890	0.911
1	0.912	0.872	0.872	0.900
2	0.833	0.762	0.759	0.801
3	0.757	0.694	0.695	0.743
4	0.709	0.668	0.678	0.712
5	0.677	0.668	0.674	0.692
6	0.675	0.668	0.681	0.690

Experiment no.13

The effect of initial metal concentration on the adsorption of zinc cyanide on AMBERLITE IRA 900.

Conditions :

Volume of solution = 1.0 L

Mass of resin = 0.054 g

Stirring speed = 300 rpm

	C/Co	C/Co	C/Co	C/Co
Time (hrs)	5 ppm	8 ppm	10 ppm	standard
0	1	1	1	1
1	0.927	0.980	0.938	0.827
2	0.839	0.901	0.893	0.733
3	0.781	0.863	0.854	0.583
4	0.705	0.804	0.833	0.511
5	0.649	0.769	0.821	0.477
6	0.576	0.769	0.821	0.466
7	0.560	0.769	0.821	0.466

Experiment no.14

The effect of initial metal concentration on the adsorption of nickel cyanide on AMBERLITE IRA 900.

Conditions :

Volume of solution = 1.0 L

Mass of resin = 0.04 g

Stirring speed = 300 rpm

	C/Co	C/Co	C/Co	C/Co
Time (hrs)	5 ppm	8 ppm	10 ppm	standard
0	1	1	1	1
0.25	0.977	0.973	0.989	0.929
0.5	0.948	0.951	0.935	0.909
0.75	0.933	0.941	0.930	0.861
1	0.925	0.920	0.925	0.808
2	0.852	0.867	0.852	0.652
3	0.801	0.816	0.801	0.537
4	0.751	0.765	0.760	0.450
5	0.700	0.730	0.760	0.398
6	0.650	0.710	0.746	0.360
21	0.508	0.700	0.746	0.334
22	0.508	0.700	0.746	0.334

Experiment no.15

The effect of initial metal concentration on the adsorption of copper cyanide on AMBERLITE IRA 900.

Conditions :

Volume of solution = 1.0 L

Mass of resin = 0.045 g

Stirring speed = 300 rpm

	C/Co	C/Co	C/Co	C/Co
Time (hrs)	5 ppm	8 ppm	10 ppm	standard
0	1	1	1	1
0.25	0.938	0.967	0.981	0.981
0.5	0.907	0.947	0.972	0.951
0.75	0.868	0.927	0.935	0.911
1	0.829	0.899	0.914	0.900
2	0.725	0.801	0.785	0.809
3	0.593	0.695	0.717	0.743
4	0.512	0.645	0.715	0.712
5	0.442	0.617	0.698	0.692
6	0.396	0.607	0.673	0.689

Experiment no.16

The effect of pH on the adsorption of zinc cyanide on AMBERLITE IRA 900.

Conditions :

Volume of solution = 1.0 L

Mass of resin = 0.101 g

Co = 10 ppm

Stirring speed = 300 rpm

	C/Co	C/Co	C/Co	C/Co
Time (hrs)	pH 8	pH 10	pH 12	standard
0	1	1	1	1
0.25	0.995	0.942	0.939	0.978
0.5	0.954	0.927	0.849	0.882
0.75	0.833	0.864	0.837	0.874
1	0.797	0.758	0.789	0.827
2	0.716	0.632	0.648	0.733
3	0.625	0.590	0.591	0.584
4	0.589	0.527	0.519	0.511
5	0.562	0.505	0.481	0.477
6	0.506	0.494	0.472	0.466
23	0.420	0.494	0.473	0.466

Experiment no.17

The effect of pH on the adsorption of nickel cyanide on AMBERLITE IRA 900.

Conditions :

$C_0 = 10$  ppm

Volume of solution = 1.0 L

Mass of resin = 0.101 g

Stirring speed = 300 rpm

	C/Co	C/Co	C/Co	C/Co
Time (hrs)	pH 8	pH 10	pH 12	standard
0	1	1	1	1
0.25	0.920	0.970	0.963	0.929
0.5	0.915	0.949	0.947	0.909
0.75	0.867	0.897	0.916	0.861
1	0.811	0.875	0.877	0.808
2	0.689	0.729	0.748	0.652
3	0.566	0.611	0.622	0.537
4	0.468	0.515	0.518	0.450
5	0.409	0.441	0.452	0.398
6	0.366	0.393	0.391	0.361
22	0.318	0.326	0.338	0.335
23	0.319	0.326	0.338	0.335

Experiment no.18

The effect of pH on the adsorption of copper cyanide on AMBERLITE IRA 900.

Conditions :

$C_0 = 10$  ppm

Volume of solution = 1.0 L

Mass of resin = 0.07 g

Stirring speed = 300 rpm

	C/C <sub>0</sub>	C/C <sub>0</sub>	C/C <sub>0</sub>	C/C <sub>0</sub>
Time (hrs)	pH 8	pH 10	pH 12	standard
0	1	1	1	1
0.25	0.960	0.966	0.961	0.980
0.5	0.939	0.940	0.947	0.951
0.75	0.918	0.914	0.918	0.912
1	0.908	0.910	0.912	0.900
2	0.794	0.801	0.805	0.809
3	0.729	0.738	0.742	0.743
4	0.708	0.721	0.721	0.712
5	0.696	0.710	0.708	0.692
6	0.696	0.710	0.708	0.689

Experiment no. 19

The effect of temperature on the adsorption of zinc cyanide on AMBERLITE IRA 900.

Conditions :

$C_0 = 10$  ppm

Volume of solution = 1.0 L

Mass of resin = 0.1 g

stirring speed = 300 rpm

	C/C <sub>0</sub>	C/C <sub>0</sub>	C/C <sub>0</sub>	C/C <sub>0</sub>
Time (hrs)	20°C	40°C	60°C	standard
0	1	1	1	1
0.25	0.978	0.909	0.902	0.978
0.5	0.882	0.838	0.835	0.882
0.75	0.874	0.792	0.766	0.874
1	0.827	0.746	0.658	0.827
2	0.733	0.558	0.519	0.733
3	0.583	0.503	0.507	0.583
4	0.511	0.503	0.502	0.511
5	0.478	0.503	0.502	0.478
6	0.466	0.501	0.500	0.466
7	0.466	0.503	0.502	0.466

Experiment no.20

The effect of temperature on the adsorption of nickel cyanide on AMBERLITE IRA 900.

Conditions :

$C_0 = 10$  ppm

Volume of solution = 1.0 L

Mass of resin = 0.1 g

Stirring speed = 300 rpm

	$C/C_0$	$C/C_0$	$C/C_0$	$C/C_0$
Time (hrs)	20°C	40°C	60°C	standard
0	1	1	1	1
0.25	0.925	0.887	0.967	0.929
0.5	0.908	0.857	0.892	0.909
0.75	0.858	0.773	0.783	0.861
1	0.821	0.708	0.709	0.808
2	0.684	0.531	0.496	0.652
3	0.578	0.438	0.426	0.537
4	0.505	0.402	0.407	0.450
5	0.456	0.384	0.407	0.398
6	0.418	0.375	0.412	0.361
7	0.399	0.383	0.412	0.345
8	0.394	0.383	0.412	0.334
9	0.394	0.383	0.406	0.334

Experiment no.21

The effect of temperature on the adsorption of copper cyanide on AMBERLITE IRA 900.

Conditions :

$C_0 = 10$  ppm

Volume of solution = 1.0 L

Mass of resin = 0.07 g

Stirring speed = 300 rpm

	C/Co	C/Co	C/Co	C/Co
Time (hrs)	20°C	40°C	60°C	standard
0	1	1	1	1
0.25	0.980	0.952	0.937	0.980
0.5	0.952	0.907	0.877	0.952
0.75	0.911	0.848	0.803	0.911
1	0.900	0.753	0.729	0.900
2	0.809	0.705	0.658	0.809
3	0.744	0.671	0.656	0.744
4	0.713	0.668	0.653	0.713
5	0.692	0.671	0.656	0.692
6	0.689	0.671	0.656	0.689

Experiment no.22

The effect of ionic strength on the adsorption of zinc cyanide on AMBERLITE IRA 900.

Conditions :

$C_0 = 10$  ppm

Volume of solution = 1.0 L

Mass of resin = 0.101 g

Stirring speed = 300 rpm

	C/Co	C/Co	C/Co	C/Co
Time (hrs)	0.001 M	0.01 M	0.1 M	standard
0	1	1	1	1
0.25	0.930	0.927	0.950	0.978
0.5	0.904	0.907	0.924	0.882
0.75	0.851	0.860	0.875	0.874
1	0.815	0.844	0.832	0.827
2	0.678	0.695	0.706	0.733
3	0.545	0.567	0.625	0.583
4	0.498	0.514	0.596	0.511
5	0.465	0.463	0.582	0.477
6	0.455	0.444	0.563	0.466
7	0.453	0.446	0.563	0.466
24	0.451	0.446	0.554	0.466
25	0.451	0.446	0.557	0.466

Experiment no.23

The effect of ionic strength on the adsorption of nickel cyanide on AMBERLITE IRA 900.

Conditions :

$C_0 = 10$  ppm

Volume of solution = 1.0 L

Mass of resin = 0.105 g

Stirring speed = 300 rpm

	$C/C_0$	$C/C_0$	$C/C_0$	$C/C_0$
Time (hrs)	0.001 M	0.01 M	0.1 M	standard
0	1	1	1	1
0.25	0.891	0.919	0.945	0.929
0.5	0.866	0.868	0.907	0.909
0.75	0.822	0.826	0.871	0.861
1	0.811	0.774	0.816	0.808
2	0.626	0.627	0.689	0.652
3	0.508	0.508	0.588	0.537
4	0.410	0.428	0.522	0.450
5	0.345	0.368	0.493	0.398
6	0.313	0.338	0.493	0.361
7	0.282	0.312	0.488	0.345
22	0.259	0.302	0.485	0.335
23	0.259	0.305	0.488	0.335

Experiment no.24

The effect of ionic strength on the adsorption of copper cyanide on AMBERLITE 900.

Conditions :

$C_0 = 10 \text{ ppm}$

Volume of solution = 1.0 L

Mass of resin = 0.07 g

Stirring speed = 300 rpm

	C/C <sub>0</sub>	C/C <sub>0</sub>	C/C <sub>0</sub>	C/C <sub>0</sub>
Time (hrs)	0.001 M	0.01 M	0.1 M	standard
0	1	1	1	1
0.25	0.968	0.967	0.979	0.980
0.5	0.937	0.949	0.962	0.951
0.75	0.899	0.911	0.942	0.911
1	0.877	0.897	0.911	0.900
2	0.768	0.792	0.828	0.809
3	0.707	0.731	0.772	0.743
4	0.688	0.699	0.762	0.712
5	0.688	0.693	0.744	0.693
6	0.688	0.693	0.742	0.689

Experiment no. 25

Monometallic curves of copper , nickel and zinc adsorption onto AMBERLITE 252 H.

Conditions :

Co = 2 ppm

Volume of solution = 1.0 L

Mass of resin = 0.046 g

Stirring speed = 300 rpm

	C/Co	C/Co	C/Co
Time (hrs)	Zn	Ni	Cu
0	1	1	1
0.25	0.966	0.956	0.894
0.5	0.959	0.891	0.854
0.75	0.949	0.891	0.836
1	0.925	0.879	0.817
2	0.836	0.815	0.769
3	0.792	0.786	0.711
4	0.721	0.76	0.67
19	0.128	0.146	0.139
20	0.107	0.145	0.138
21	0.08	0.143	0.135
22	0.077	0.138	0.133
23	0.063	0.135	0.133

Experiment no. 26

Monometallic curves of Nickel , Copper and Zinc adsorption onto AMBERLITE IRC 718.

Conditions :

Co = 2 ppm

Volume of solution = 1.0 L

Mass of resin = 0.046 g

Stirring speed = 300 rpm

	C/Co	C/Co	C/Co
Time (hrs)	Zn	Ni	Cu
0	1	1	1
0.25	0.966	0.956	0.894
0.5	0.959	0.891	0.854
0.75	0.949	0.891	0.836
1	0.925	0.879	0.817
2	0.836	0.815	0.769
3	0.792	0.786	0.711
4	0.721	0.76	0.67
19	0.128	0.146	0.139
20	0.107	0.145	0.138
21	0.08	0.143	0.135
22	0.077	0.138	0.133
23	0.063	0.135	0.133

Experiment no. 27

Competitive adsorption of nickel , copper and zinc onto AMBERLITE 252 H

Conditions :

Co = 2 ppm

Volume of solution = 1.0 L

Mass of resin = 0.046 g

Stirring speed = 300 rpm

	C/Co	C/Co	C/Co
Time (hrs)	Cu	Ni	Zn
0	1	1	1
0.25	0.984	0.947	0.975
0.5	0.974	0.917	0.952
0.75	0.963	0.895	0.912
1	0.943	0.873	0.895
2	0.883	0.801	0.882
3	0.809	0.732	0.722
4	0.729	0.656	0.62
20	0.392	0.385	0.394
21	0.378	0.385	0.378
22	0.369	0.385	0.378
23	0.369	0.385	0.378

Experiment no. 28

Comparison of monometallic and multimetallic curves for zinc adsorption onto AMBERLITE 252 H.

Conditions :

$C_0 = 2$  ppm

Volume of solution = 1.0 L

Mass of resin = 0.046 g

Stirring speed = 300 rpm

	C/Co	C/Co
Time (hrs)	Monometallic profile	Multimetallic profile
0	1	1
0.25	0.966	0.975
0.5	0.959	0.952
0.75	0.949	0.912
1	0.925	0.895
2	0.836	0.882
3	0.792	0.722
4	0.721	0.62
20	0.107	0.394
21	0.08	0.378
22	0.077	0.378
23	0.068	0.378

Experiment no. 29

Comparison of monometallic and multimetallic curves for nickel adsorption onto AMBERLITE 252 H.

Conditions :

$C_0 = 2$  ppm

Volume of solution = 1.0 L

Mass of resin = 0.046 g

Stirring speed = 300 rpm

	C/Co	C/Co
Time (hrs)	Monometallic profile	Multimetallic profile
0	1	1
0.25	0.956	0.947
0.5	0.892	0.917
0.75	0.891	0.895
1	0.879	0.872
2	0.815	0.801
3	0.786	0.732
4	0.76	0.656
20	0.143	0.385
21	0.141	0.385
22	0.137	0.385
23	0.136	0.385

Experiment no. 30

Comparison of monometallic and multimetallic curves for copper adsorption onto AMBERLITE 252 H.

Conditions :

$C_0 = 2$  ppm

Volume of solution = 1.0 L

Mass of resin = 0.046 g

Stirring speed = 300 rpm

	C/Co	C/Co
Time (hrs)	Monometallic profile	Multimetallic profile
0	1	1
0.25	0.894	0.984
0.5	0.854	0.974
0.75	0.836	0.964
1	0.817	0.943
2	0.769	0.883
3	0.711	0.809
4	0.671	0.729
20	0.139	0.392
21	0.136	0.378
22	0.133	0.369
23	0.133	0.369

Experiment no. 31

Competitive adsorption of copper , nickel and zinc onto AMBERLITE IRC 718.

Conditions :

Co = 2 ppm

Volume of solution = 1.0 L

Mass of resin = 0.046 g

Stirring speed = 300 rpm

	C/Co	C/Co	C/Co
Time (hrs)	Cu	Ni	Zn
0	1	1	1
0.25	0.984	0.947	0.975
0.5	0.974	0.917	0.952
0.75	0.963	0.895	0.912
1	0.943	0.873	0.895
2	0.883	0.801	0.882
3	0.809	0.732	0.722
4	0.729	0.656	0.62
20	0.392	0.385	0.394
21	0.378	0.385	0.378
22	0.369	0.385	0.378
23	0.369	0.385	0.378

Experiment no. 32

Comparison of monometallic and multimetallic curves for copper adsorption onto AMBERLITE IRC 718.

Conditions :

Co = 2 ppm

Volume of solution = 1.0 L

Mass of resin = 0.046 g

Stirring speed = 300 rpm

	C/Co	C/Co
Time (hrs)	Monometallic profile	Multimetallic profile
0	1	1
0.25	0.955	0.973
0.5	0.932	0.95
0.75	0.874	0.933
1	0.862	0.916
2	0.787	0.893
3	0.686	0.818
4	0.606	0.766
20	0.133	0.43
21	0.124	0.419
22	0.119	0.399
23	0.119	0.399

Experiment no. 33

Comparison of monometallic and multimetallic curves for nickel adsorption onto AMBERLITE IRC 718.

Conditions :

$C_0 = 2$  ppm

Volume of solution = 1.0 L

Mass of resin = 0.046 g

Stirring speed = 300 rpm

	$C/C_0$	$C/C_0$
Time (hrs)	Monometallic profile	Multimetallic profile
0	1	1
0.25	0.977	0.96
0.5	0.933	0.94
0.75	0.899	0.933
1	0.889	0.919
2	0.795	0.877
3	0.718	0.847
4	0.662	0.808
20	0.291	0.726
21	0.28	0.726
22	0.28	0.735
23	0.28	0.735

Experiment no. 34

Comparison of monometallic and multimetallic curves for zinc adsorption onto AMBERLITE IRC 718.

Conditions :

$C_0 = 2$  ppm

Volume of solution = 1.0 L

Mass of resin = 0.046 g

Stirring speed = 300 rpm

	$C/C_0$	$C/C_0$
Time (hrs)	Monometallic profile	Multimetallic profile
0	1	1
0.25	0.979	0.984
0.5	0.97	0.955
0.75	0.954	0.929
1	0.906	0.925
2	0.839	0.855
3	0.753	0.826
4	0.703	0.818
20	0.349	0.826
21	0.343	0.83
22	0.332	0.834
23	0.334	0.83

Experiment no. 35

Effect of the inert sand slurry on the adsorption of copper onto AMBERLITE IRC 718.

Conditions :

$C_0 = 100$  ppm

Volume of solution = 1.0 L

Mass of resin = 1.015 g

Stirring speed = 550 rpm

	C/Co	C/Co
Time (hrs)	Untreated resin	Treated resin
0	1	1
0.5	0.82	0.837
1	0.727	0.779
2	0.679	0.698
3	0.639	0.66
4	0.615	0.635
20	0.517	0.555
21	0.509	0.546
22	0.513	0.546
23	0.513	0.546

Experiment no. 36

Effect of the inert sand slurry on the adsorption of copper onto AMBERLITE 252 H.

Conditions :

$C_0 = 100$  ppm

Volume of solution = 1.0 L

Mass of resin = 1.05 g

Stirring speed = 550 rpm

	C/C <sub>0</sub>	C/C <sub>0</sub>
Time (hrs)	Treated resin	Untreated resin
0	1	1
0.25	0.463	0.6
0.5	0.407	0.4
0.75	0.398	0.168
1	0.296	0.263
2	0.277	0.147
3	0.277	0.147
4	0.24	0.2
5	0.28	0.147
6	0.25	0.178

Experiment no. 37

Comparison of the adsorptive curves of the synthetic cupric sulphate solution and the leachate on AMBERLITE 252 H.

Conditions :

Cu in synthetic soln. = 3930 ppm (Co)

Cu in leachate = 1250 ppm (Co)

Volume - synthetic soln. = 0.85 L

Volume - leachate = 1.0 L

Mass of resin = 6.1 g

	C/Co	C/Co
Time (hrs)	Cu - synthetic soln.	Cu - leachate
0	1	1
0.5	0.89	0.701
1	0.89	0.668
2	0.762	0.668
3	0.631	0.668
24	0.631	0.668

## NOMENCLATURE

C	solution phase concentration (mg/l)
C <sub>e</sub>	equilibrium solution concentration (mg/l)
C <sub>0</sub>	initial solution concentration (mg/l)
D	surface diffusivity (m <sup>2</sup> /s)
$\bar{D}$	combined surface diffusivity defined in Eq. (3.5 b) (m <sup>2</sup> /s)
K <sub>f</sub>	external film transfer coefficient (m/s)
N	rotational speed of impeller (r.p.m.)
Q	metal loading on resin (g/kg resin)
r	radial variable (m)
t	time variable (s)
V	volume of liquid in reactor (m <sup>3</sup> )

### *Greek letters*

$\beta$	change in rate of adsorption due to effects of the sand slurry.
$\delta$	change in capacity for solute to the resin due to effects of the sand slurry.
$\phi$	phase conversion factor (m <sup>3</sup> of resin/m <sup>3</sup> of wet settled resin)
$\epsilon$	volumetric fraction of wet - settled resin occupied by resin (m <sup>3</sup> of resin / m <sup>3</sup> of wet - settled resin)

- $\rho$       apparent density of resin ( $\text{g/m}^3$ )
- $\psi$       correction factor in quadratic expression

*Subscripts*

- e      equilibrium
- R      resin
- s      liquid - adsorbent interface